

Improving the operability of planing monohulls using proactive control

From idea to proof of concept



A.F.J. van Deyzen

**IMPROVING THE
OPERABILITY OF PLANING
MONOHULLS USING
PROACTIVE CONTROL**
*FROM IDEA TO PROOF OF
CONCEPT*

Alex F.J. van Deyzen

**HET VERBETEREN VAN DE
INZETBAARHEID VAN
PLANERENDE SCHEPEN
MIDDELS PROACTIEF
REGELEN**

***VAN IDEE TOT BEWIJS VAN HET
CONCEPT***

PROEFSCHRIFT

ter verkrijging van de graad van doctor
aan de Technische Universiteit Delft,
op gezag van de Rector Magnificus prof. ir. K.C.A.M. Luyben,
voorzitter van het College voor Promoties,
in het openbaar te verdedigen op donderdag 18 september 2014 om 12:30 uur

door Alexander Franciscus Johannes van DEYZEN

scheepsbouwkundig ingenieur
geboren te Roosendaal en Nispen.

Dit proefschrift is goedgekeurd door de promotor:

Prof. dr. ir. R.H.M. Huijsmans

Copromotor: Dr. ir. J.A. Keuning

Samenstelling promotiecommissie:

Rector Magnificus	voorzitter
Prof. dr. ir. R.H.M. Huijsmans	Technische Universiteit Delft, promotor
Dr. ir. J.A. Keuning	Technische Universiteit Delft, copromotor
Prof. ir. D. Stapersma	Technische Universiteit Delft
Prof. dr. J.E. Bos	Vrije Universiteit Amsterdam
Dr. ir. F. van Walree	Maritime Research Institute (Marin), Wageningen
Prof. dr. M. Renilson	Higher Colleges of Technology, United Arab Emirates
Prof. dr. P.A. Wilson	University of Southampton, United Kingdom

Dit onderzoek was ondersteund door:

Maritieme Fondsen

Agentschap NL

Koninklijke Nederlandse Redding Maatschappij (KNRM)

Damen Shipyards Group

Technische Universiteit Delft

ISBN **978-94-6108-777-5**

Copyright © 2014 by Alex F.J. van Deyzen. All rights reserved.

Cover illustrations

Front: Dutch Search and Rescue vessel of the Arie Visser class in rough seas (Photo KNRM - Arie van Dijk)

Back: Scale model of the Arie Visser in the towing tank at the Delft University of Technology

Cover artwork: Michiel Katgert

Printed by Gildeprint drukkerijen, Enschede, the Netherlands

In dedication to Monique & Juliette

Nomenclature

Latin Letters

$a_{\theta x}$	Added mass moment of inertia due to surge motion in θ -dir	$[kgm]$	
$a_{\theta z}$	Added mass moment of inertia due to heave motion in θ -dir	$[kgm]$	
$a_{\theta\theta}$	Added mass moment of inertia in θ -dir	$[kgm^2]$	
$a_{z\theta}$	Added mass due to pitch motion in z -dir	$[kgm]$	
A_{z_p}	Vertical accelerations at a certain point on the ship	$[m/s^2]$	$\ddot{z} - \xi_P \cdot \ddot{\theta}$
$A_{z_{bow}}$	Vertical accelerations at the bow	$[m/s^2]$	$\ddot{z} - \xi_{bow} \cdot \ddot{\theta}$
$A_{z_{bridge}}$	Vertical accelerations at the bridge	$[m/s^2]$	$\ddot{z} - \xi_{bridge} \cdot \ddot{\theta}$
$A_{z_{CG}}$	Vertical accelerations at CG	$[m/s^2]$	
a_{zx}	Added mass due to surge motion in z -dir	$[kgm]$	
a_{zz}	Added mass in z -dir	$[kg]$	
$b_{\theta x}$	Damping coefficient due to surge motion in θ -dir	$[Nms/m]$	
$b_{\theta z}$	Damping coefficient due to heave motion in θ -dir	$[Nms/m]$	
$b_{\theta\theta}$	Damping coefficient in θ -dir	$[Nms]$	
B_{oa}	Breadth over all	$[m]$	
B_{wl}	Breadth waterline	$[m]$	
$b_{z\theta}$	Damping coefficient due to pitch motion in z -dir	$[N/s]$	
b_{zx}	Damping coefficient due to surge motion in z -dir	$[Ns/m]$	
b_{zz}	Damping coefficient in z -dir	$[Ns/m]$	
c	Phase velocity	$[m/s]$	$\frac{\lambda}{T} = \frac{\omega}{k}$
c_g	Group velocity	$[m/s]$	
$c_{\theta z}$	Spring coefficient due to heave motion in θ -dir	$[Nm/m]$	
$c_{\theta\theta}$	Spring coefficient in θ -dir	$[Nm]$	
$c_{z\theta}$	Spring coefficient due to pitch motion in z -dir	$[N]$	
c_{zz}	Spring coefficient in z -dir	$[N/m]$	
D	Propeller diameter	$[m]$	
dt	Calculation time step	$[s]$	
$f_{\theta}(\dot{\theta})$	Nonlinear damping in θ -dir	$[Nms]$	
$f_{\theta}(\dot{x})$	Nonlinear damping due to surge motion in θ -dir	$[Nms/m]$	
$f_{\theta}(\theta)$	Nonlinear restoring force in θ -dir	$[Nm]$	
f_b	Sectional buoyancy force	$[N/m]$	
F_{dyn}	Total hydrodynamic force	$[kN]$	
f_l	Sectional hydrodynamic lift force	$[N/m]$	
$F_{N\triangleright}$	Froude number over displacement	$[-]$	$\left(\frac{V_s}{\sqrt{g \cdot \nabla^{1/3}}} \right)$

F_{sta}	Total hydrostatic force	[kN]
F_{wz}	Wave exciting force in z -dir	[N]
$f_x(\dot{x})$	Nonlinear damping in x -dir (resistance)	[Nms]
$f_z(\dot{x})$	Nonlinear damping due to surge motion in z -dir	[Ns/m]
$f_z(z)$	Nonlinear restoring force in z -dir	[N/m]
g	Acceleration due to gravity	[m/s ²]
H_s	Significant wave height	[m]
I	Mass moment of inertia for pitch	[kgm ²]
k	Radius of gyration for pitch	[m]
k	Wave number	[rad/m]
L_{bow}	Distance between Centre of Gravity and bow of the ship	[m]
L_{oa}	Length over all	[m]
L_{probe}	Distance between wave probe and model	[m]
L_{wl}	Length waterline	[m]
$LCCG$	Longitudinal Centre of Gravity	[m]
M	Mass of the ship	[kg]
m	Mass	[kg]
M_B	Break torque engine	[kNm]
M_{prop}	Torque propeller	[kNm]
M_{shaft}	Shaft torque	[kNm]
$M_{w\theta}$	Wave exciting moment in θ -dir	[Nm]
Q	Open water torque propeller	[kNm]
n_e	Speed engine	[1/s]
n_p	Speed propeller	[1/s]
P_e	Effective power	[kW]
r	Measured water elevation	[cm]
r_a	Wave amplitude	[cm]
Rt	Calm water resistance	[kN]
Rt_o	Total calm water resistance at design speed	[N]
Rt_o	Total steady-state resistance	[kN]
T	Thrust force	[kN]
T_p	Peak period wave spectrum	[s]
T_1	Initial thrust before ac-/deceleration	[m/s]
T_2	Final thrust after ac-/deceleration	[m/s]
T_{dw}	Net available time interval for speed reduction	[s]
T_{max}	Maximum thrust force	[kN]
T_{pw}	Duration prediction window	[s]
t_p	Time interval between two predictions	[s]
T_s	Sample time during run	[s]
V_a	Entrance velocity propeller	[m/s]
V_1	Initial speed before ac-/deceleration	[m/s]
V_2	Final speed after ac-/deceleration	[m/s]
V_o	Design speed ship	[m/s]
V_{s_o}	Initial speed during model tests	[m/s]
$V_{s_{des}}$	Desired forward speed	[m/s]
V_s	Forward speed	[m/s]
VCG	Vertical Centre of Gravity	[m]
W	Weight of the ship	[kN]
w	Vertical orbital velocity at the undisturbed water level	[m/s]
\dot{x}_o	Steady-state forward speed	[m/s]
x	Fuel rack	[g/cycle]
x,y,z	Earth fixed coordinate system	

x, \dot{x}, \ddot{x}	Displacement, velocity and acceleration relative to equilibrium in x -dir	
x_a	Moment arm of hydrodynamic lift force	[m]
x_b	Moment arm of hydrostatic lift force	[m]
$x_{CG}, \dot{x}_{CG}, \ddot{x}_{CG}$	Displacement, velocity and acceleration of CG in x -dir in earth fixed axes system	
z, \dot{z}, \ddot{z}	Displacement, velocity and acceleration relative to equilibrium in z -dir	
z_o	Steady-state sinkage/rise	[m]
$z_{CG}, \dot{z}_{CG}, \ddot{z}_{CG}$	Displacement, velocity and acceleration of CG in z -dir in earth fixed axes system	

Greek Letters

β	Angle of attack propeller blade	[deg]
Δt_c	Calculation time	[s]
Δt_{tc}	Reaction time towing carriage	[s]
η_{TRM}	Transmission efficiency	[-]
γ	Bridge handle position	[-]
λ	Wave length	[m]
∇	Displacement	[m ³]
ω	Wave frequency	[rad/s]
ω_e	Wave encounter frequency	[rad/s]
ρ	Density of the water	[kg/m ³]
θ	Propeller pitch angle	[deg]
$\theta, \dot{\theta}, \ddot{\theta}$	Pitch angle, velocity and acceleration	
θ_o	Steady-state pitch angle	[°]
ξ, χ, ζ	Body fixed coordinate system	

Contents

Nomenclature	i
1 Introduction	1
1.1 Seakeeping behaviour of planing monohulls	1
1.2 Improve the operability using proactive control	2
1.3 Research objective	4
2 Manual versus automated thrust control	7
2.1 Full scale trials	7
2.2 Lessons learned	17
2.3 Proposed control system	40
2.4 Important issues concerning automated proactive thrust control	43
3 Conceptual model of automated proactive thrust control	45
3.1 Setup conceptual model	45
3.2 Elementary response model	47
3.3 Calculation input	54
3.4 Applicability conceptual model	57
3.5 Expected influence automated proactive thrust control	60
3.6 Conclusions	63
4 Idealised model of automated proactive thrust control	65
4.1 Setup idealised model	65
4.2 Used computational model	68
4.3 Calculation input	72
4.4 Applicability idealised model	77
4.5 Influence of automated proactive thrust control in ideal situation	79
4.6 Influence of inaccurate response predictions	90

4.7	Conclusions	95
5	Proof of concept	99
5.1	Limitations experimental setup	99
5.2	Implementation control scheme	101
5.3	Experimental setup	105
5.4	Results	109
5.5	Conclusions	115
6	Conclusions and recommendations	117
6.1	Conclusions	117
6.2	Recommendations	119
Appendices		
A	Coefficients in elementary response model	123
B	Repetition intervals	129
	Bibliography	133
	Summary	137
	Samenvatting	141
	Dankwoord	145
	Curriculum Vitae	147

Chapter 1

Introduction

1.1 Seakeeping behaviour of planing monohulls

The demand to sail at high forward speeds in both calm water and in a seaway remains high. Fast transportation of personnel, passengers or goods may give ship-owners an economical advantage. For various patrol, search, rescue or military operations attaining high forward speeds is essential.

Ship-owners and operators still tend to favour the planing monohull, in particular in various military, rescue and patrol applications. The planing monohull is well-established and can be considered a proven concept (one of the first fast monohulls appeared in the late 1800s). It is a relatively uncomplicated design. Monohulls are easy to build and the operational costs are low.

Sailing in heavy weather conditions at a high forward speed on a monohull is very demanding for both crew and ship. In head and bow quartering seas, the main factor for voluntary speed reduction is the occurrence of large vertical peak accelerations (Keuning 1994). Results of full scale measurements showed that a professional crew rather reacts to these extremes than to significant or 'average' values (Keuning 2006, Keuning and van Walree 2006). Large vertical accelerations may cause discomfort, fatigue or even serious injuries. The forces acting on the hull may become large; structural failure may occur. Large vertical accelerations are therefore experienced as dangerous. In many cases the crew reduces the speed and/or alters the heading in order to avoid unacceptably large vertical peak accelerations. Furthermore, the motion and acceleration levels increase with decreasing ship size.

The occurrence of large vertical accelerations while sailing in head and bow quartering seas imposes limits to the operability. The operability is defined as the percentage of time a ship can operate at its design speed given the scatter diagram of the area of operation. In calm water, fast monohulls can attain high forward speeds, but in seaway the occurrence of large vertical peak accelerations impose a limit to the

maximum attainable forward speed.

The challenge for designers of fast monohulls is to explore different possibilities to increase the operability for planing monohulls sailing in head and bow quartering seas. To improve the operability a reduction of the vertical accelerations is required.

A possible solution for increasing the operability of fast monohulls is found by increasing the ship's length, whilst the other dimensions, the design speed and the functionality are kept the same. This change made it possible to optimise the hull shape forward with emphasis on reduced accelerations sailing in head waves. The length to beam ratio of the ship is increased, as well as the length to displacement ratio, the longitudinal radius of gyration in pitch is reduced and the flare at the bow is decreased. This concept, called the Enlarged Ship Concept (ESC) (Keuning and Pinkster 1995; 1997), was later evolved into the Axe Bow Concept (ABC) with more radical bow sections and a significantly improved operability (Keuning et al. 2001; 2002, Keuning 2006) (see Figure 1.1).



(a) Dutch coast guard patrol vessel Visarend, Damen Stan Patrol 4207



(b) Offshore crew supplier Silni, Damen Fast Crew Supplier 3507

Figure 1.1: Photos of an Enlarged Ship (left) & Axe Bow Concept (right)

Active motion control is another possible method for improving the operability. This is in particular useful due to the high efficiency of the various control devices. A possibility to increase the operability is to use active controlled stern flaps or interceptors (see for example Wang 1985, Rijkens et al. 2011, Rijkens 2013b). Active controlled stern flaps or interceptors used to reduce the vertical acceleration level are not applied on full scale yet.

1.2 Improve the operability using proactive control

A solution for increasing the operability of planing monohulls sailing in head and bow quartering seas may also be found in proactive control. Vertical peak accelerations

have a very short duration. Unacceptably large vertical peak accelerations have a low frequency of occurrence; not all wave encounters result in large vertical peak accelerations. The occurrence of an unacceptably large vertical peak acceleration is a result of the complex interplay between the ship's geometry, the incoming wave, the motions of the ship before impact and the forward speed at impact. The response of a planing monohull sailing in head seas can be considered to be nonlinear to the amplitude of the incoming wave (Troesch 1992, Keuning 1994). These aspects are the incentive for proactive control.

The purpose of a proactive control system is to intervene before the ship encounters a wave that leads to an unacceptably large vertical peak acceleration. An example of proactive control is thrust control. Thrust control can be very effective for smaller high speed ships with a high power to weight ratio (specific power). Operators on board of small, planing boats apply thrust control manually. They temporarily reduce the forward speed before impact (proactive control) if they anticipate that the next vertical peak acceleration might be unacceptably large. By doing so, they try to avoid unacceptably large vertical peak accelerations during a trip. Results of full scale measurements showed that if helmsmen are free to influence the thrust, a higher average forward speed is attained during the trial compared to a trial where the operator had to choose a constant throttle opening before the start of the trial (Nieuwenhuis 2005). This shows that thrust control may be an effective way of increasing the operability of small, planing monohulls.

As a first step proactive control for one variable, the forward speed, is considered. This has been termed automated proactive thrust control. The forward speed is controlled by the thrust; the actual controlling variable is the bridge handle. The response of a planing monohull in head seas is considered (response in 3 Degrees of Freedom: surge, heave and pitch motion) The influence of the roll motion on the vertical accelerations in bow quartering seas has not been taken into account. Proactive control of the forward speed has been explored first, because thrust control is applied in practice already. Proactive control of stern flaps or interceptors has not been considered first, because this requires a preliminary study into the hydrodynamics of these devices and into their interaction with the ship (Wang 1985, Rijkens et al. 2011, Rijkens 2013b).

What makes automated proactive thrust control unique is the fact that control, effectuated before impact, is based on **predicted vertical peak accelerations**. For this, the response needs to be predicted real-time while sailing. The magnitude of the predicted vertical peak acceleration determines the amount of thrust reduction. It is therefore essential that the vertical peak accelerations are predicted with a sufficient degree of accuracy. In essence, this is equal to what the operators do when they apply thrust control. They also estimate ('predict') the magnitude of the next vertical peak acceleration and decide if thrust reduction is required. The ship has a high forward speed. In combination with a large wave celerity this leads to a time interval for effectuating control that is quite short. These aspects imply that the response needs to be predicted much faster than real-time.

Automated proactive thrust control is expected to be more effective than thrust control applied manually. One of the disadvantages of applying thrust control manually is that the operators need to rely on their intuition and experience. They cannot predict the magnitude of the slam, nor the time instant it occurs. Consequently, it is difficult for them to apply the optimal thrust reduction with exact the right timing. Large vertical accelerations may still occur when applying thrust control manually. The reasons for this can be due to the operator's misjudgement, loss of concentration or fatigue. Their judgement also depends on visibility: Reduced visibility at night, in case of excessive amounts of spray or in foggy conditions make it difficult to apply thrust control. These issues do not play a role anymore when thrust control has been automated. Automation of thrust control means that thrust reductions will be applied more consistently and more accurately. Moreover, it is also possible to apply automated proactive thrust control having poor visibility (e.g. at night or in case of excessive spray).

Moreover, on unmanned fast ships proactive control may be a necessity. An unmanned fast ship is still a new concept. Since there is no crew present on board the acceleration level needs to be monitored and controlled. If high forward speeds are desired, the forward speed needs to be controlled proactively in order to avoid unacceptably large vertical peak accelerations that may cause structural damage or damage to the computer hardware or sensors on board.

1.3 Research objective

The main research question of this dissertation is:

What is the level of reduction of the vertical accelerations possible with automated proactive thrust control?

A reduction of the vertical accelerations implies that it is possible to sail faster without increasing the discomfort on board. This means an improvement of the operability.

This study proofs the feasibility of the concept of proactive control in five stages.

In the first stage thrust control applied manually by helmsmen has been explored. Chapter 2 presents and discusses the results of a limited number of full scale trials carried out on board of SAR boats. The relevant physics associated with thrust control are discussed. Applying the lessons learned a setup for a proactive control system for the thrust has been derived.

To show the level of reduction of the vertical accelerations possible with automated proactive thrust control in an early stage of this study a conceptual simulation model has been setup. It consists of an elementary response model, which mimics the motions of a planing monohull sailing in head seas, and a proactive control system, that determines the desired thrust force continuously. The results of simulations presented in Chapter 3 are used to show that a reduction of the vertical acceleration

level may be expected when automated proactive thrust control would be applied on board of a planing monohull sailing in head seas.

In the third stage automated proactive thrust control has been simulated in more realistic conditions on board. The elementary model is replaced by a more adequate computational model, that describes the nonlinear seakeeping behaviour of a planing monohull sailing in head seas more accurately. The results presented in Chapter 4 should give insight to what extent the vertical accelerations can be reduced when automated proactive thrust control is applied on board of a planing boat.

In the fourth stage a proof of concept of proactive control is presented. Chapter 5 presents the results of model experiments employing proactive control. During a run, the forward speed is determined continuously based on the outcome of real-time response predictions. Results of the model tests proof that it is possible to control the vertical acceleration level by means of proactive control of the forward speed.

In the last stage the presented results are evaluated and generalised. Chapter 6 finalises this dissertation by presenting conclusions and recommendations for further research.

Automated proactive thrust control is the first step towards a proactive control system for more than one control variable, based on predicted vertical peak accelerations, that may increase the operability of a planing monohull sailing in head seas. This study can be followed up by a study where the effectiveness of proactive control of two control variables, for example the thrust in combination with stern flaps or interceptors, for a planing monohull sailing in head and bow quartering seas is analysed.

Chapter 2

Manual versus automated thrust control

In the Introduction it was stated that the average forward speed of a planing monohull sailing in head seas may be increased using thrust control. Full scale trials where operators use thrust control provide more insight in how operators typically carry out thrust control. In this chapter the current application of thrust control is explored and applying the lessons learned a setup for automated proactive thrust control has been derived.

Section 2.1 presents the results of the full scale trials carried out on two SAR boats. Section 2.2 addresses the relevant physics, learned from the full scale trials, important for automated proactive thrust control. Section 2.3 presents the proposed setup for the proactive control system for the thrust. Important issues related to the real-time response predictions required for automated proactive thrust control that need further elaboration are pointed out in Section 2.4.

2.1 Full scale trials

2.1.1 Setup full scale trials

The Royal Dutch Lifeboat Association (KNRM) provided the Delft University of Technology with the opportunity to carry out full scale trials on two SAR boats (including crew). The ships used were the 'Jeanine Parqui' from rescue station Hoek van Holland and the 'Koos van Messel' from rescue station IJmuiden. The 'Jeanine Parqui' and the 'Koos van Messel' belong to the Arie Visser class (28 *t*, 18.8 *m*) (see Figure 2.1). They have two engines, each having a power of 736 *kW*. The engines drive two waterjets.

The trials were carried out on the North Sea and the relative wave direction was head seas. Table 2.1 presents an overview of the trials, sorted by sea state. As depicted in Table 2.1 each trial day one helmsman operated the ship.



Figure 2.1: Dutch SAR boat of Arie Visser class (Photo KNRM - Arie van Dijk)

Table 2.1: Full scale trials with SAR boat of Arie Visser class

Trial number	Trial date	Ship	Operator	Sea state	H_s [m]	T_p [s]	Duration [min]
1	3 May 2011	Jeanine Parqui	1	calm	1.00	3.90	13
2	3 May 2011	Jeanine Parqui	1	calm	1.00	3.90	14
3	3 May 2011	Jeanine Parqui	1	calm	1.00	3.90	14
4	9 March 2011	Jeanine Parqui	2	moderate	2.00	5.30	13
5	22 Feb 2012	Koos van Messel	3	moderate	1.95	4.60	13
6	26 April 2012	Koos van Messel	3	moderate	1.80	5.80	20
7	7 Sept 2011	Jeanine Parqui	1	rough	2.40	5.20	14
8	15 Dec 2011	Koos van Messel	4	rough	2.65	5.70	20

Both ships were instrumented equally. The forward speed was measured using a GPS. Unfortunately, the sample frequency of the GPS was 1 Hz. For the time scale we are interested in, the axial deceleration over a few seconds, a sample rate of 1 Hz is quite coarse. Accelerometers to measure the vertical accelerations were positioned at 40 and 65% of the total length, measured from the transom stern. The first position corresponds with the lengthwise position of the bridge ($A_{z_{bridge}}$ in the following figures), the second is assumed to be the bow ($A_{z_{bow}}$). The vertical accelerations were measured body fixed. Body fixed vertical accelerations are easier to relate to what a

person on board experiences. The sample frequency of the accelerometers was 500 Hz . The position of the bridge handle (100% is full speed ahead) and the pitch angle were also measured (sample frequency equal to 50 Hz). All signals were filtered with a frequency of 10 Hz , except the forward speed, which remained unfiltered.

The results of these trials (except trial 1) are used to find out how these operators typically apply thrust control. A number of time-traces of the bridge handle position, the forward speed and the vertical acceleration at the bow are depicted. This is to show the relation between a reduced bridge handle and the corresponding deceleration, speed reduction and vertical peak acceleration in more detail. The number of thrust reductions were also counted to get an idea of how often they apply thrust control. The average forward speed and level of accelerations are given to show the variation in order of magnitude, even between four operators who sail the same SAR boat in the same area.

The results of trials 1, 2 and 3 (all operator 1) are used to illustrate the effect of thrust control by comparing the distributions of the vertical accelerations and the average forward speed during these trials. During trial 1 the operator had to choose a desired speed before the start of the run and was not allowed to make any changes to the bridge handle afterwards. These three trials provide an estimate to what extent operator 1 was able to increase the average forward speed using thrust control.

2.1.2 Illustration of the current application of thrust control

The operators continuously observed the incoming waves. If they believed that the next encounter would result in an unacceptably large vertical peak acceleration, they reduced the thrust. The experience of the operator and his intuition play an important role here.

Figure 2.2 shows the typical sequence of events. It displays a part of trial 3. Operator 1 steered the boat. The bridge handle position, the forward speed and the vertical acceleration at the bow are depicted. For a consistent convention with the rest of this dissertation the z -axis is pointed downwards, yielding negative values for a vertical peak acceleration upwards. The operator probably estimated that the next incoming wave would yield an unacceptably large vertical peak acceleration. hence, he decided to reduce the thrust. In this case the speed decreased nearly 10 kts within a approximately 5 seconds. When comparing the position of the bridge handle to the forward speed it seems that the time lag between the adjustment of the handle and the moment the speeds starts to diminish is small, not perceivable. It is at least an order of magnitude smaller than the time scale we are interested in (the axial deceleration over a few seconds, in this 4 seconds).

It cannot directly be concluded if the vertical accelerations were diminished by the speed reduction since we do not know what would have happened if the speed was not reduced. The vertical peak accelerations, however, do not show extraordinary large values. 20% of the vertical peaks accelerations measured at the 65% of the ship's

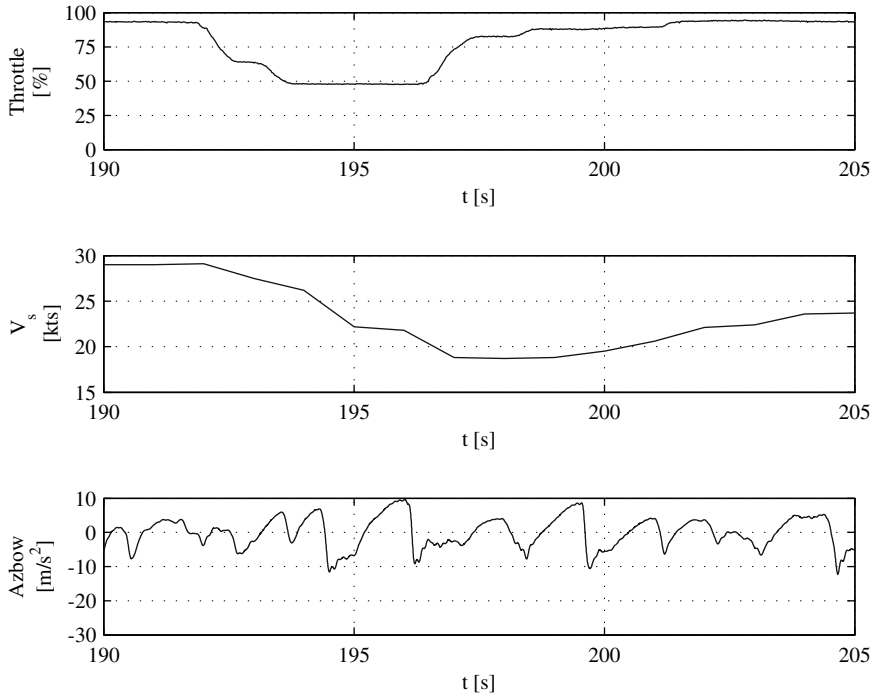


Figure 2.2: Typical time-traces, obtained during trial 3

length exceeded 10 m/s^2 throughout this trial (see Figure 2.5 or 2.6). It may therefore be concluded that a vertical peak acceleration of 10 m/s^2 was acceptable for the crew.

Figure 2.3 shows a part of the same trial, where the first vertical peak acceleration is much larger than the following two. When relating the bridge handle position with the vertical acceleration it seems that the operator was too late with reducing the thrust. Perhaps he misjudged the incoming wave and thought that he could maintain the current speed or perhaps he was not paying attention and the first impact alerted him. This sequence of a large vertical acceleration followed by a thrust reduction was observed more often during trials 2 and 3. He was probably alarmed by the first large vertical peak acceleration and judged by looking at the incoming wave that the next one or two might also be unacceptable. Hence, he still decided to reduce speed.

Operator 2, a less experienced operator than the other three, carried out thrust control in a similar way as operator 1. The main difference was that he chose a more conservative forward speed, probably to reduce the probability of having unacceptably large vertical peak accelerations. The forward speed during his trial was 23 kts , while operator 3 was able to maintain an average forward speed of 26 kts during his trials

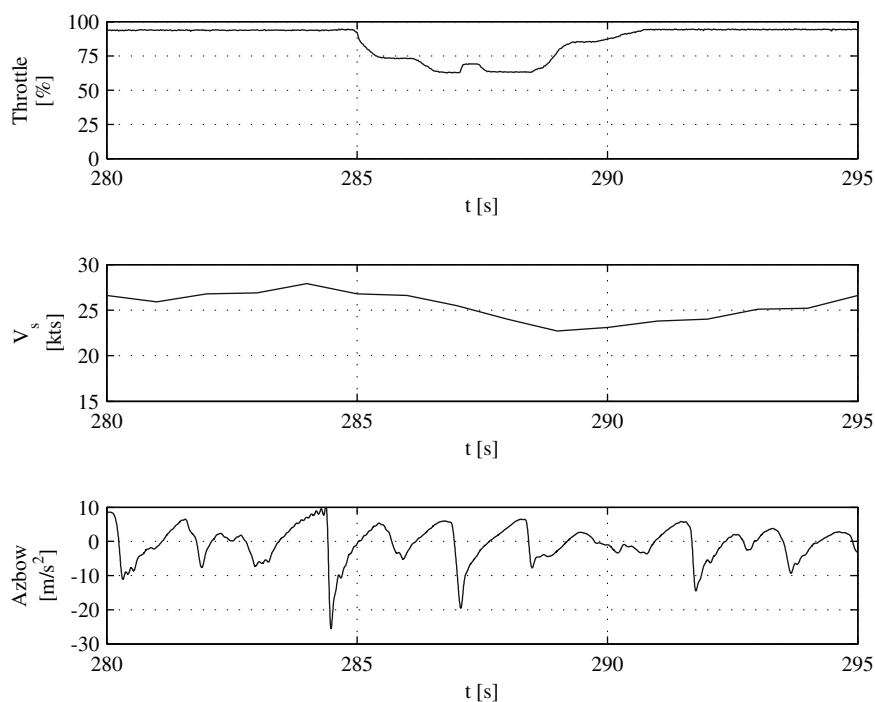


Figure 2.3: Typical time-traces, obtained during trial 3 (operator 1)

in similar sea states. Still, operator 2 had to reduce the thrust a few times during his trial.

Operator 3 applied thrust control more often than operator 1 or 2, nearly each 20 to 30 s. He reduced the thrust a little bit and quite briefly. He also restored the thrust before impact had taken place (see Figure 2.4). The time-trace of the vertical acceleration clearly shows the short duration of the peaks (more than in Figures 2.2 or 2.3).

Operator 4 had a significantly different way of carrying out thrust control. He constantly changed the thrust. A clear distinction for which individual peak he had reduced the thrust could not be made. The main difference with operator 1 in a similar sea state (trial 7) was that he was able to maintain a higher average forward speed (19 versus 13 kts).

Figure 2.5 shows the measured distributions of the vertical peak accelerations at both the bridge and bow. All the minima and maxima during the trip are counted. These figures, the so-called Rayleigh plots, indicate the probability of exceedance that a peak is larger than a certain value. The probability is given on the horizontal axis, which

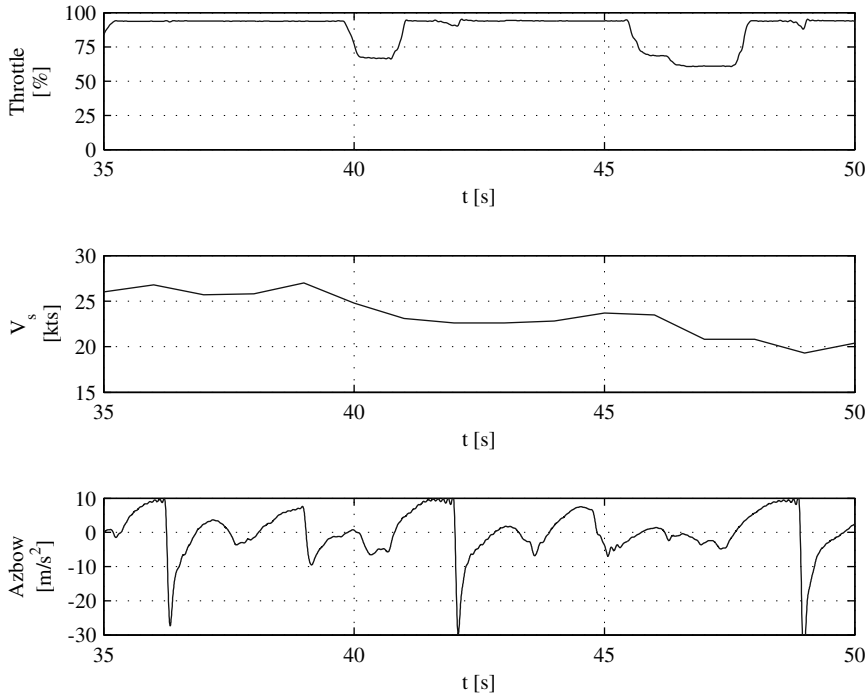


Figure 2.4: Typical time-traces, obtained during trial 6 (operator 3)

is deformed in such way that the probability of exceedance of Rayleigh distributed maxima and minima appear as a straight line in the Rayleigh plot. For this it is required that the wave crests and troughs are Rayleigh distributed. Between a downward and upward zero-crossing of the vertical acceleration one minimum is considered (z -axis is orientated downwards). If more troughs exist between these two zero-crossings the minimum trough value is considered as the vertical peak acceleration of interest. In other words, for each wave encounter one vertical peak acceleration is counted.

Figure 2.5 shows that there is a significant spreading in the level of accelerations. There even is a difference between trial 2 and 3 which were carried out on the same day by the same operator. During the second trial with thrust control, trial 3, the operator remembered trial 2, so he probably pushed the boundaries a bit further. More thrust reductions were observed and a higher level of accelerations was found. The level of accelerations measured during the trials strongly depended on the motivation and experience of the operator.

Table 2.2 summarises the results of the limited number of full scale trials. To indicate the level of accelerations the magnitude of the vertical acceleration at the bow at a

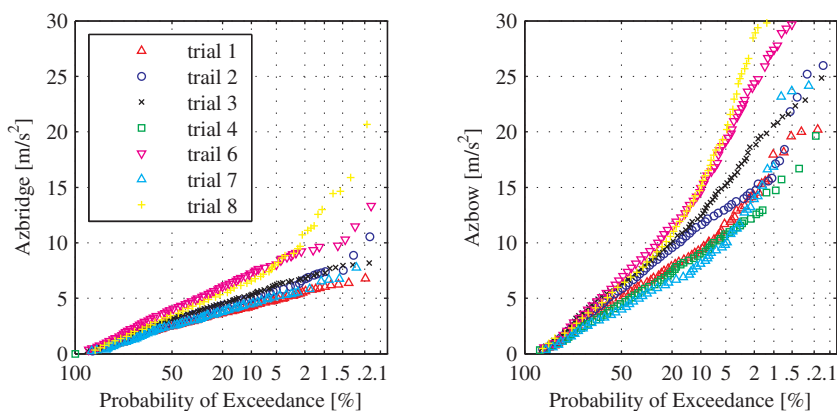


Figure 2.5: Rayleigh plots of the vertical peak accelerations obtained during trials

probability of 2% is also given.

Three out of four of these operators chose a desired speed that he would like to maintain during the trial beforehand. If he anticipated an unacceptably large vertical peak acceleration he temporarily reduced the speed. Choosing a higher desired forward speed implied that it is more likely that unacceptably large vertical peak accelerations would occur. The average forward speed, an indication for the speed the operator wanted to maintain during the trial, varied, even for similar sea states (see Table 2.2). The variation can be explained by the different acceptance levels for the vertical accelerations and by the different level of experience of the operators.

Based on trials 2, 3, 4 and 7 the speed reduction, when the thrust was reduced, was in the range of 2 to 10 *kts*. The average speed reduction was approximately 5 *kts*. The individual speed reductions measured during trial 5, 6 and 8 were not as clearly distinguishable. The (axial) deceleration after a thrust reduction varied between -0.3 m/s^2 and -1.5 m/s^2 .

The minimum observed position of the handle during these trials was around 50%. The bridge handle was never set in neutral position during the trials. The operators stated that on this boat they required thrust to maintain manoeuvrability. If they reduced the thrust to idle, the incoming wave may push the ship out of course. The time interval the operators sustained a reduced thrust varied between 1 to 5 s. The number of thrust reductions showed a large variation (see Table 2.2).

The minimum speed that can be realised before impact is an important parameter concerning thrust control. When the speed at impact is low, it is more likely that the vertical peak accelerations has been diminished. The minimum speed that can be realised before impact is largely dependent on the current forward speed when the thrust is reduced. The deceleration of the ship and the time available to decelerate are

Table 2.2: Summary results full scale trials with SAR boat of Arie Visser class

Trial number	Operator	Sea state	H_s [m]	T_p [s]	Duration [min]	\bar{V}_s [kts]	No. of reductions	$A_{z_{bow}}$ [m/s ²]
1	1	calm	1.00	3.90	13	23	0	14
2	1	calm	1.00	3.90	14	27	11	15
3	1	calm	1.00	3.90	14	≈27	27	19
4	2	moderate	2.00	5.30	13	23	7	13
5	3	moderate	1.95	4.60	13	26	35	–
6	3	moderate	1.80	5.80	20	26	≈70	25
7	1	rough	2.40	5.20	14	13	>15	≈20
8	4	rough	2.65	5.70	20	19	–	28

also relevant. These two parameters determine the maximum possible speed reduction before impact. The deceleration depends on the amount of thrust reduction and on the wave force acting on the ship. The specific power of the ship is also important. The specific power is the ratio between effective power and the weight of the ship. A large specific power implies a large deceleration. For larger fast ships with a small specific power the thrust control may become ineffective and impractical to employ. For example, during full scale trials on board of an English coast guard patrol vessel of 42 m thrust control was not observed (Keuning and van Walree 2006).

The relation between bridge handle, engine, waterjet, thrust force and forward speed is and especially the time lag between them is also relevant for thrust control. The dynamic effects in the propulsive system should be taken into account to determine the time lag. On this ship the time lag was not perceivable, but on other ships it may be larger, perhaps in the same order of magnitude to the time required to decelerate (a few seconds). This may jeopardise the effectiveness and applicability of thrust control.

2.1.3 The effect of thrust control

Rayleigh plots are a powerful tool to compare the reduction of the level of accelerations using thrust control. For a fair comparison the forward speed during a trip without thrust control should be equal to the average forward speed using thrust control. The distributions of the vertical peak accelerations at both the bridge and bow, measured during trials 1, 2 and 3, are given in Figure 2.6. The average forward speed during trial 1 (constant thrust) was 23 kts. During trial 2 it was equal to 27 kts, but during trial 3 the GPS failed halfway. The measured forward speed for that part was also equal to 27 kts.

The operator was able to attain a higher average forward speed using thrust control.

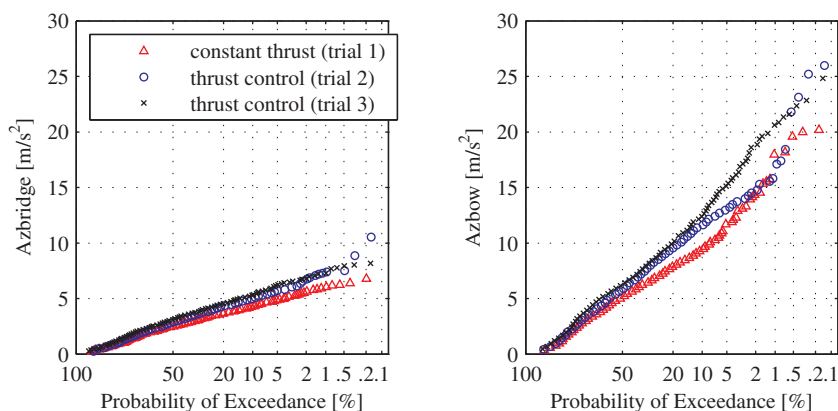


Figure 2.6: Rayleigh plots of the vertical accelerations at the bow obtained during trials 1, 2 and 3

The level of accelerations, however, were also higher when he was allowed to use thrust control. A possible explanation for this could be that when he was not allowed to reduce the speed in case of a possible high, steep incoming wave, he rather chose his desired forward speed more conservatively, yielding a relatively low level of accelerations and less extreme impacts. The level of accelerations (despite a few large peaks) measured during the trials with thrust control seemed to be acceptable for the crew. During trials 2 and 3 the crew sometimes mentioned that a slam was too severe (they could be ascribed to misjudgements or loss of concentration), but they generally did not complain about the accelerations they experienced.

The results obtained during trial 1, 2 and 3 are similar to the results Nieuwenhuis obtained during her experiments (Nieuwenhuis 2005). The boat she used was a Dutch SAR boat of the Johannes Frederik class, called 'Kapiteins Hazewinkel'. The Johannes Frederik class is the predecessor of the Arie Visser class. It is smaller boat (14.6 t, 14.4 m). The trials were carried out on the North Sea near the Dutch village Hoek van Holland. The sea state during the trials had a significant wave height of 2.0 m and a peak period of 4.6 s. The operator was operator 1, the same one as on the 'Jeanine Parqui' during trials 1, 2, 3 and 7.

Figure 2.7 shows the distributions of the vertical peak accelerations at both the bridge and bow measured during two trials. During one trial the operator was free to use thrust control, during the other he had to choose a desired speed before the start of the run. The average forward speed during the trial with a constant thrust was equal to 18 *kts*. During the trial with thrust control it was equal to 22 *kts*.

Based on the limited number of full scale trials it cannot explicitly be concluded

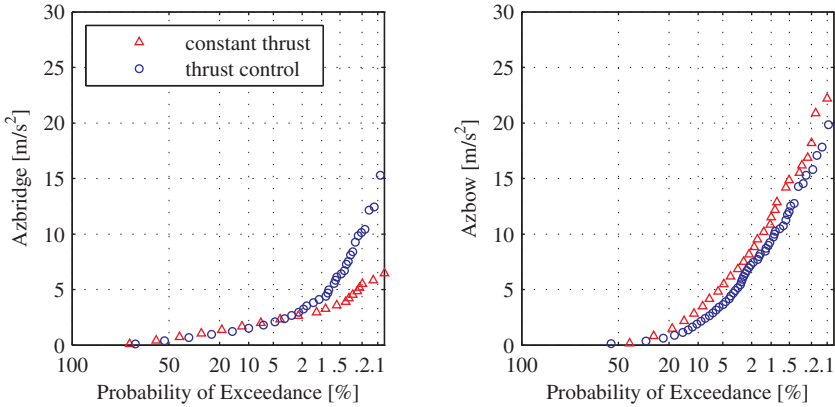


Figure 2.7: Rayleigh plots of the vertical accelerations obtained during full scale trials with SAR boat of the Johannes Frederik class (Nieuwenhuis 2005)

whether it was possible to sail at a higher forward speed without increasing the discomfort on board. It is difficult to conclude whether the operator could sail at a higher average forward speed, because he was able to avoid (most of the) unacceptably large vertical peak accelerations using thrust control or because he dared to sail at a higher forward speed when he was allowed to apply thrust control.

For a fair comparison either the distributions of the vertical accelerations should be compared at an equal average forward speed or the average forward speed should be compared at an equal level of the vertical accelerations. During these full scale trials both the vertical accelerations and the forward speed were the variables to be measured. None of the two was controlled. Both the distribution of the vertical accelerations and the average forward speed were the outcome of the trials.

Moreover, there are many human factors involved that affect the outcome of these trials, such as the motivation of the operator to show his capability of applying thrust control or the fact that he perhaps chose a conservative constant forward speed to avoid severe impacts during the trials where he was not allowed to apply thrust control. The fact that these measurements were not taken during an actual rescue operation, where the behaviour and motivation of the crew is probably different, may also be an important issue.

The results, however, do suggest that thrust control (applied manually) has a beneficial effect. The average forward speed was higher during the trials with thrust control, while the level of accelerations remained acceptable for the crew. The increase of average forward speed that the operator could realise was approximately 20%, based on five trials (23 *kts* versus 27 *kts* and 18 *kts* versus 22 *kts*).

2.2 Lessons learned

Based on the presented full scale trials on board of a SAR boat the following issues can be considered important for automated proactive thrust control:

1. The relation between bridge handle and thrust force (time lag propulsive system);
2. The ability to decelerate before impact and to accelerate afterwards (the minimum speed that can be realised before impact);
3. The nonlinear seakeeping behaviour of a planing monohull sailing in head seas (see also Section 1.2);
4. The acceptance level for the vertical accelerations;

These four issues are discussed in this section.

2.2.1 Relation between bridge handle and thrust force

The variable that affects the magnitude of the next vertical peak acceleration is the actual forward speed at impact. The forward speed is defined as the controlled variable. The speed is controlled by the thrust. The controlling variable is the bridge handle.

A time delay and/or lag between the bridge handle, thrust force and ultimately the forward speed most likely exists. A time delay in a dynamic system is in fact equal to transport of information. When the command to change the speed has been given it takes time before it is processed. A time delay can be caused by many factors, either electrical or mechanical (eg. processing time computer or other instrumentation, sample time (speed) measurement, the time it takes to turn a switch or open a valve, etc.). The thrust force does not respond immediately to speed setting changes. A time lag between them most likely exists. The time it takes to reduce the forward speed once the thrust has been reduced is also a time lag. The latter one will be discussed in the next section.

A significant time delay and/or lag between a change of the position of the bridge handle and the corresponding thrust force may jeopardise the feasibility of automated proactive thrust control. A significant time delay reduces the available time to decelerate. A time lag may reduce the deceleration. Both issues reduce the maximum possible speed reduction before impact.

An analysis of the possible order of magnitude of a time delay between bridge handle and thrust on board of a planing monohull is considered to be beyond the scope of this dissertation. The time delay is most often less than the time lag of a propulsive system. At this stage of the study the effect of a time delay on the performance of automated proactive thrust control is more relevant than the exact cause of the time it takes to process the command to change the speed. The effect of the time available to decelerate before impact will be analysed in this dissertation.

To determine the time lag between bridge handle and thrust force the dynamic response of the entire propulsion system should be considered. The main machinery on board of a planing monohull consists of:

- One or more diesel engines;
- Gearbox(es);
- Shafts;
- Propulsors;

Planing monohulls are often equipped with one or two diesel engines and two, sometimes even four propulsors. This is done for redundancy and manoeuvrability but also to provide sufficient propulsive power to attain high forward speeds.

The operator controls the speed of the engine using the bridge handle. When he alters the position of the bridge handle a speed governor determines the required amount of fuel injection in the cylinders (fuel rack). This alters the torque provided to the drive shafts. A gearbox transfers the power from the drive shafts to the driven shafts. The driven shafts rotate the propulsors, which can be either propellers or waterjets. The propulsors provide the required thrust force to overcome the resistance of the ship. This equilibrium determines the speed.

Figure 2.8 depicts a block diagram of the ship propulsion dynamics in the most general form (Grimmelius et al. 2007):

The right hand side shows the force balance between ship resistance and thrust force (to be elaborated in the next section). On the left hand side the torque balance between engine output torque and propeller torque provides the shaft speed. The ship's speed, after correction for the wake factor, provides the entrance velocity of the propeller. With the shaft speed this results in the effective propeller blade angle of attack. Propeller thrust coefficient and torque coefficient are a function of the blade angle of attack, the propeller pitch and the shaft speed. The propeller pitch is set by a pitch control and an actuating system that gets its set point from the ship propulsion control system. The propulsion system also provides a set point to the prime mover control block that normally contains the engine governor. For diesel engines the governor actuates the fuel rack.

This block diagram shows that between the bridge handle (propulsion control system) and a change of thrust at the propeller four time lags exist:

1. Governor to fuel rack;
2. Fuel rack to engine torque;
3. Engine torque to shaft speed (shaft speed loop);
4. Shaft speed to thrust;

The first two time lags can be assumed small compared to the last two. Not much dynamics are involved in between the governor and the fuel rack. The second time lag is in the order of magnitude of a few engine cycles (it takes time to fill all cylinders with the new desired fuel rack; ideally it takes one engine revolution). The last one involves the dynamics of the gearbox, shaft and propeller. Their inertia may be large enough to cause a perceivable time lag in the order of magnitude of one second (or more). The last one is is the dynamics of the the propeller (adjusting of the circulation around the blades, normally ignored) or the waterjet (changing the water velocity in the duct, also normally ignored).

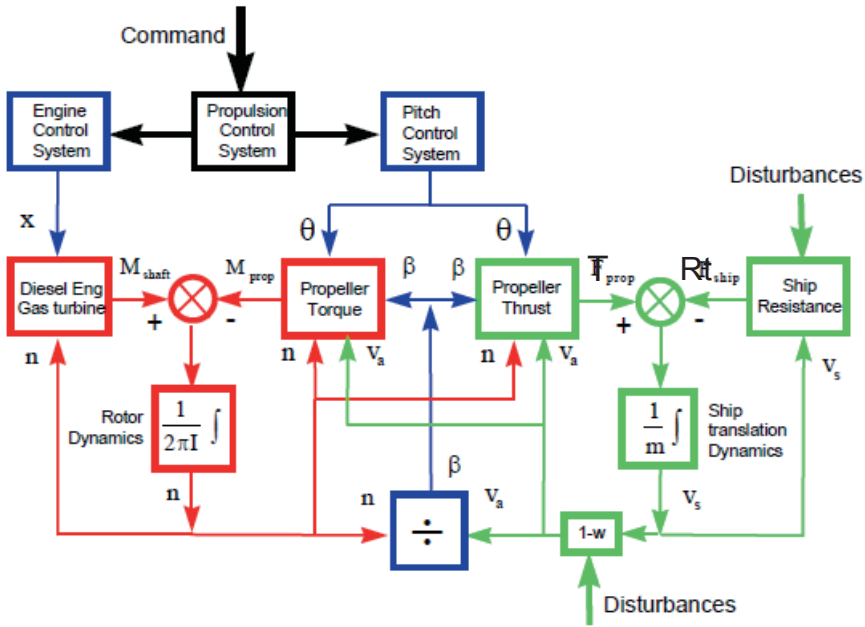


Figure 2.8: General block diagram ship propulsion dynamics (Grimmelius et al. 2007)

A diesel engine model as defined in the overall model ultimately generates the shaft torque M_{shaft} , given a certain fuel rack (dependent on position of the bridge handle and the quick action of the governor) and shaft speed n_e :

$$M_{shaft} = \eta_{TRM} \cdot M_B(x, n_e) \quad (2.1)$$

in which η_{TRM} is the transmission efficiency between engine power and power delivered to the propeller.

The torque absorbed by the propeller is defined by the relation of the torque of the propeller in open water and the relative rotative efficiency:

$$M_{prop} = \frac{Q(n_p, V_a, D, \theta)}{\eta_R} \quad (2.2)$$

where the open water torque of the propeller depends on the propeller speed, diameter and pitch and on the instream velocity. The dynamics of the water surrounding the propeller is normally been neglected.

To describe the dynamic behaviour of the entire propulsion installation the following equation of motion for the shaft can be setup:

$$I \cdot 2\pi\dot{n} = M_{shaft} - M_{prop} = \eta_{TRM} \cdot M_B(\gamma, n_e) - \frac{Q(n_p, V_a, D, \theta)}{\eta_R} \quad (2.3)$$

in which the inertia of the engine should be corrected for the speed of the propeller (when the speed of the engine differs from the speed of the propeller). The inertia should include an allowance for the inertia of the water surrounding the propeller.

When the position of the bridge handle has been changed the time lag of the entire propulsion installation can be determined if all terms in Equation 2.3 are known. For this the relation between bridge handle, fuel rack, engine speed and the brake torque should be known. The relation between the speed, instream velocity and torque of the propeller should also be known.

What has been omitted in Figure 2.8 and what has not been taken to account is the dynamics of the water surrounding the propeller or, in case of a waterjet, the water in the tube. This water also needs to be accelerated, both axial and rotational. The amount of water that needs to be accelerated axially in the tube of waterjet may introduce a significant time lag. The amount of water surrounding a propeller that needs to be accelerated axially may be less. The rotational component, however, may be larger than for a waterjet.

Equation of motion 2.3 may be difficult to solve analytically. When the bridge handle is pulled back the fuel rack reduces. This reduces the torque provided by the engine. The propeller decelerates, meaning not only a reduction of torque absorbed the propeller but a reduction of the torque delivered to the propeller (shaft torque) as well. Furthermore, the relation between torque and thrust is defined by the torque and thrust coefficient. Both have a nonlinear relation with the instream and propeller velocity. The dynamics of the water surrounding the propeller complicate the dynamics even more.

To proof the feasibility of automated proactive thrust control it is sufficient to assume a relation in time between bridge handle and thrust. It has been assumed that the time delay or lag in the system is smaller than the assumed slower action of the bridge

handle. Each propulsion system on a planing monohull has its own time delay and lag. Their order of magnitude may become significant for some ships, which may jeopardise the feasibility of the concept of automated proactive thrust control for that particular ship. For other ships the time delay may be negligible and the time lag may be insignificantly small. It is not the purpose of this study to analyse the applicability of automated proactive thrust control for a range of ships and propulsions systems. This is saved for a later stage, when this study has proven that automated proactive thrust control reduces the vertical accelerations on board of a planing monohull sailing in head seas.

It has been assumed that the time delay and lag between the bridge handle and thrust are zero and that thrust is changed gradually. The thrust reacts directly to the handle: $\gamma(t) \cdot T_{max} = T(t)$. It has been assumed that a 100% change (in-/decrease) can be realised in 1 second ($d\gamma/dt = dT/dt = 1 \text{ 1/s}$). This is similar to what was observed during the full scale trials on the SAR boat of the Arie Visser class; the operator gradually reduced the bridge handle. When a temporary speed reduction is required, the thrust will be reduced using a continuous function, yielding a continuous function for the forward speed. The same applies for when the bridge handle position is restored again. Figure 2.9) shows the relation between bridge handle position and thrust force. On the left it shows the most likely relation including a time lag and delay and including the increase of thrust when the instream velocity decreases; on the right the assumed relation for this study.

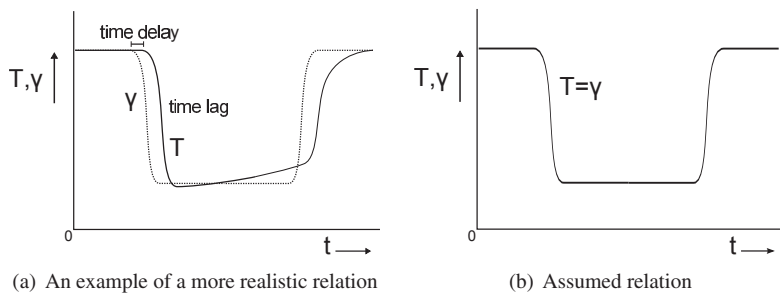


Figure 2.9: Relation between position bridge handle and thrust force

2.2.2 Ac- and deceleration capacity

The actual variable that influences the vertical peak acceleration is the forward speed of the ship. The reduction of the speed over time and consequently its increase for a certain ship when thrust control has been applied is a function of:

- Specific power of the ship: P_e/m [kW/t], in which:
 - $P_e = Rt_o \cdot V_o$: Effective power at the propulsor at the design speed V_o ;

- m : Mass of the ship;
- The relation between resistance and speed;
- The initial speed before deceleration (V_1);

The minimum speed that can be realised before impact largely determines the extent of the reduction of the level of accelerations using thrust control. For ships having a high deceleration capacity it is more likely that the vertical accelerations can be reduced effectively using thrust control than for ships that decelerate slowly. For these ships the unacceptably large vertical peak accelerations should be anticipated far ahead, something that may become impractical. The time it takes to restore the forward speed, however, is also relevant with respect to the average forward speed that can be maintained throughout a trip using thrust control.

The equation of motion for ac- and deceleration of a ship after a change of thrust can be written as (see also Figure 2.8):

$$m \cdot \dot{V} = T - Rt \quad (2.4)$$

To determine the ac- or deceleration over time a 5 to 10% allowance for the added mass of the water may be taken into account, but this has been neglected (5% to 10% extra mass does not significantly change the values presented in this section).

While sailing in head waves the resistance force is a time variant force. Trim (pitch angle) and sinkage (heave motion) change constantly, introducing time variations in the resistance force. Furthermore, wave action exists. These effects influence the actual ac- and deceleration after a change of thrust force. For example, it may cause a larger deceleration when the ship encounters an incoming wave. It may also cause a higher acceleration when the ship surfs down the back of the wave.

For this study it has been assumed that the calm water resistance curve suffices to determine the ac- and deceleration when thrust control has been applied. The effect of trim and sinkage variations and wave action on the ac- and deceleration have been neglected in this study. At this stage it is more relevant to use a good estimate of the speed reduction over a few seconds after the thrust has been reduced than to model the exact speed oscillations due to trim and sinkage variations and wave action. For the time it takes to restore the forward speed these effects are less relevant. The time it takes to restore the speed is not directly relevant for thrust control except that it affects the overall average forward speed.

The calm water resistance curve of a planing monohull shows a nonlinear relation with the forward speed. The shape of the resistance curve is dependent on the the length of the ship, the hull geometry (deadrise angle and ratio between length and width), the displacement and the lengthwise position of the centre of gravity. The resistance curve of a planing monohull in calm water is characterised by a local maximum in the semi-planing range. For smaller vessels this local maximum is more profound than

for larger vessels. This is also related to the length over width ratio. Smaller planing boats often have a higher length over width ratio than larger planing monohulls. Much about the calm water planing of monohulls is known based on the extensive number of model tests that have been carried out at the Ship Hydromechanics Laboratory at the Delft University of Technology (see for example the Delft Systematic Deadrise Series (DSDS): Keuning and Gerritsma 1982, Keuning et al. 1993).

Figure 2.10 shows examples of the typical resistance curves of planing monohulls in calm water. The figure depicts the calm water resistance for the SAR boat of the Arie Visser class (Visch and Keuning 2011), for a much larger Enlarged Ship Concept of 50 m (Keuning and van Walree 2006) and for a pilot boat of 20 m (Visch 2007). The speed has been normalised. The graph is actually for a maximum speed of 5 *kts* (V_o). The resistance at 35 *kts* (Rt_o) has been used to normalise the total calm water resistance.

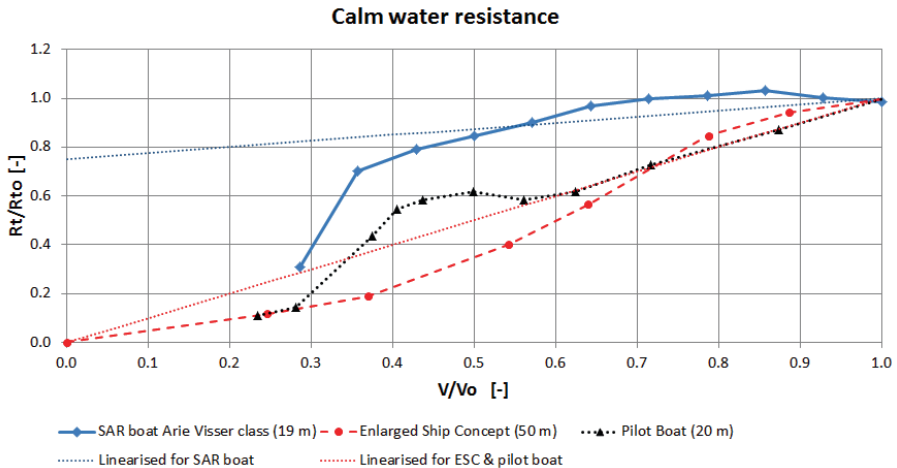


Figure 2.10: Example of typical calm water resistance curves for planing monohulls

The specific power of the ship, the initial forward speed and the gradient of the resistance curve around the initial forward speed determine the time it takes to ac- or decelerate to a new desired forward speed. Figure 2.10 also shows the linearised approximation of the calm water resistance for the Arie Visser and for the other two vessels. Both linearisations represent two typical relations between resistance and forward speed. One represents a high resistance in the high speed range (low gradient), while the other represents a quicker decrease of the resistance (higher gradient).

The normalised, linearised resistance can be written as:

$$\frac{Rt}{Rt_o} = a \cdot \frac{V}{V_o} + b, \quad a + b = 1 \quad (2.5)$$

The linearised resistance for the SAR boat of the Arie Visser class can be written as:

$$\frac{Rt}{Rt_o} = 0.25 \cdot \frac{V}{V_o} + 0.75 \quad (2.6)$$

The linearised resistance for the Enlarged Ship Concept and the pilot boat can be written as:

$$\frac{Rt}{Rt_o} = \frac{V}{V_o} \quad (2.7)$$

Equation 2.4 can now be rewritten in non-dimensional form:

$$\begin{aligned} \frac{mV_o}{T_o} \cdot \frac{dV/V_o}{dt} &= \frac{T}{T_o} - \frac{Rt}{Rt_o} \Rightarrow \\ \frac{mV_o}{T_o} \cdot \frac{dV/V_o}{dt} + a \cdot \frac{V}{V_o} &= \frac{T}{T_o} - b \end{aligned} \quad (2.8)$$

in which $T_o = Rt_o$ (resistance at V_o). The term $\frac{mV_o}{T_o}$ can also be written as $\frac{mV_o^2}{T_o \cdot V_o} = \frac{mV_o^2}{P_e}$, in which the specific effective power P_e/m becomes distinguishable.

It has been assumed that the solution to this differential equations can be written as: $\frac{V}{V_o} = k \cdot e^{-\frac{t}{\tau}}$. The time constant τ determines the curve of the forward speed over time, while the combination of constant k and the time constant determine the gradient. This can be illustrated by substituting the time constant τ in the assumed solution and taking its derivative: $\frac{dV/V_o}{dt} = -\frac{k}{\tau} \cdot e^{-\frac{t}{\tau}}$.

By substituting in Equation 2.8 the homogeneous solution can be found as follows:

$$\frac{mV_o}{T_o} \cdot -\frac{k}{\tau} \cdot e^{-\frac{t}{\tau}} + a \cdot k \cdot e^{-\frac{t}{\tau}} = 0 \Rightarrow \tau = \frac{mV_o}{a \cdot T_o} \quad (2.9)$$

The time constant $1/\tau = \frac{a \cdot T_o}{mV_o} = \frac{a \cdot P_e}{mV_o^2}$ clearly shows that the specific power of the ship, the gradient of the resistance curve and the initial forward speed are relevant parameters regarding the time it takes to reach a new equilibrium of Equation 2.4 once the thrust has been altered.

When the thrust has been changed from T_1 to T_2 the ship de- or accelerates to a new forward speed in time: $V_1 \rightarrow V_2$ at $t \rightarrow \infty$. The particular solution for this step change can be found as follows (use Equations 2.5 and 2.8):

$$\frac{mV_o}{T_o} \cdot 0 = \frac{T_2}{T_o} - \left(a \frac{V_2}{V_o} + b \right) \Rightarrow \frac{V_2}{V_o} = \frac{T_2/T_o - b}{a} \quad (2.10)$$

The solution to Equation 2.4 can now be written as:

$$\frac{V}{V_o} = k \cdot e^{-\frac{a \cdot T_o}{mV_o} t} + \frac{T_2/T_o - b}{a} \quad (2.11)$$

By substituting the initial speed V_1 at $t = 0$ in Equation 2.11 factor k can be found.

$$\frac{V_1}{V_o} = k \cdot e^0 + \frac{T_2/T_o - b}{a} \Rightarrow k = \frac{V_1}{V_o} - \frac{T_2/T_o - b}{a} \quad (2.12)$$

This factor takes into account the initial speed and the amount of thrust in- or decrease. A larger thrust in- or decrease implies a steeper slope of the function $\frac{V}{V_o} = k \cdot e^{-\frac{t}{\tau}}$.

Substitution of Equation 2.12 in Equation 2.11 yields the final expression for the ac- and deceleration of a ship:

$$\frac{V}{V_o} = \left(\frac{V_1}{V_o} - \frac{T_2/T_o - b}{a} \right) \cdot e^{\frac{-a \cdot T_o}{m V_o} t} + \frac{T_2/T_o - b}{a} \quad (2.13)$$

Table 2.4 shows time constant and the initial ac- and deceleration for the three example ships given in Figure 2.10 when they:

- accelerate from 0 *kts*, full thrust;
- decelerate from 35 *kts*, no thrust;

The derivative of Equation 2.12 at $t = 0$ s yields the initial ac- and deceleration: $\frac{dV/V_o}{dt} = -k/\tau = -\left(\frac{V_1}{V_o} - \frac{T_2/T_o - b}{a}\right) \cdot \frac{a \cdot T_o}{m V_o}$.

Table 2.3 shows the relevant values used to determine the deceleration over time (Equation 2.11). The difference between the SAR and pilot boat is to show the effect of the gradient of the resistance curve on the speed reduction over time, while all other variables are equal. The difference between the ESC and the other two vessels is to show that a significantly higher mass and half the specific power reduces the ability to reduce speed over a short time interval compared to the two smaller vessels.

Table 2.3: Chosen values to illustrate speed reduction over time for three example ships

Ship	m [t]	L [m]	Rt_o [kN]	V_o [kts]	Pe/W [kW/t]	a [-]	b [-]
SAR boat	30	19	50	35	30	0.25	0.75
Pilot boat	30	20	50	35	30	1	0
ESC	525	50	425	35	15	1	0

Table 2.4 shows that the gradient of the resistance curve introduces an asymmetry between the capacity to ac- and decelerate and that the specific power determines the initial ac- and deceleration. The SAR boat and the pilot boat have an equal initial deceleration. The k constant, however, is 4 times higher for the SAR boat. This means

that it reduces speed much quicker than the pilot boat, even though it has a larger time constant. The initial acceleration of the SAR boat is 4 times smaller than the initial acceleration of the pilot boat. Combined with a much larger time constant (4 times larger) it can already be concluded that it will take much more time to accelerate the SAR boat. The factor 4 is the ratio between the gradient of both resistance curves (0.25 versus 1). For a gradient of the resistance curve equal to 1 (pilot boat and ESC) the initial ac- and deceleration is equal. The ESC has a larger time constant, so it can be concluded that the time to ac- and decelerates is also greater.

Table 2.4: Time constant and initial ac- and deceleration for three example ships

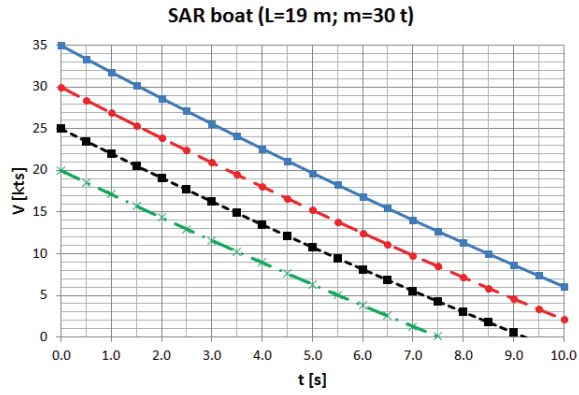
Ship	$\frac{mV_o}{T_o}$ [s]	τ [s]	V_1/V_o [-]	k [-]	$-k/\tau$ [1/s]	V_1/V_o [-]	k [-]	$-k/\tau$ [1/s]
SAR boat	10.8	43.2	0	-1	0.02	1	4	-0.09
Pilot boat	10.8	10.8	0	-1	0.09	1	1	-0.09
ESC	22.2	22.2	0	-1	0.04	1	1	-0.04

Figure 2.11 shows that the capacity to reduce speed in a short time interval is largest for the SAR boat. This ship has a high a high specific power. More importantly is the low gradient of the resistance curve that cause the quick reduction of the forward speed (see Table 2.4). For the pilot boat the speed reduction is less, because of the higher gradient of the resistance curve. For the Enlarged Ship Concept, the time to reduce speed becomes even more due to the much lower specific power of the ship. These results are clearly visible when comparing the speed reductions depicted in Figure 2.11.

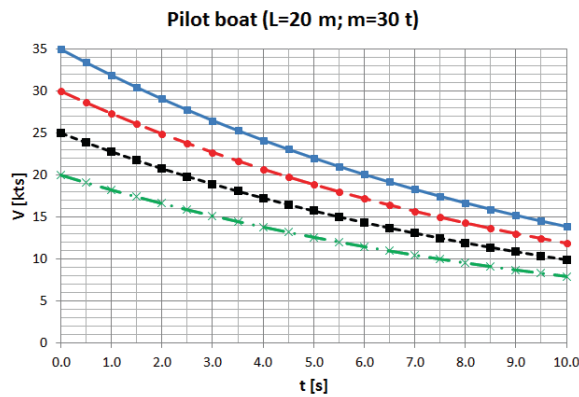
The speed reduction for the SAR boat of the Arie Visser class found analytically compares well with the speed reduction observed during the full scale trials. There, it was observed that the speed reduction before impact were in the order of magnitude of 5 *kts* within a few seconds for maximum 50% throttle reductions. Figure 2.12 shows the deceleration found analytically for 50 and 100% thrust reduction, starting from 30 and 25 *kts*. Within approximately 4 *s* the speed could be reduced 5 *kts* for 50% thrust reduction.

Figure 2.13 shows that the capacity to increase speed is best for the pilot boat. The time constant shown in Table 2.4 showed that the pilot boat should accelerate the quickest, next the ESC and last the SAR boat (the k factor was equal for all three ships). This can be confirmed by Figure 2.13. The low gradient of the resistance curve of the SAR boat causes that this ship takes more even time to restore its speed to 35 *kts* than the ESC, which has a smaller specific power.

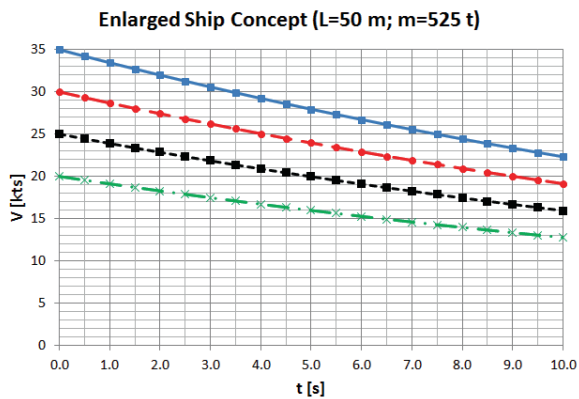
To relate the speed reduction over time to more generic values the speed reduction for specific powers has been analysed. The maximum speed V_o is 35 *kts*. Table 2.5 shows



(a) SAR boat



(b) Pilot boat



(c) Enlarged Ship Concept

Figure 2.11: Speed reduction over time for 100% thrust reduction for three example ships

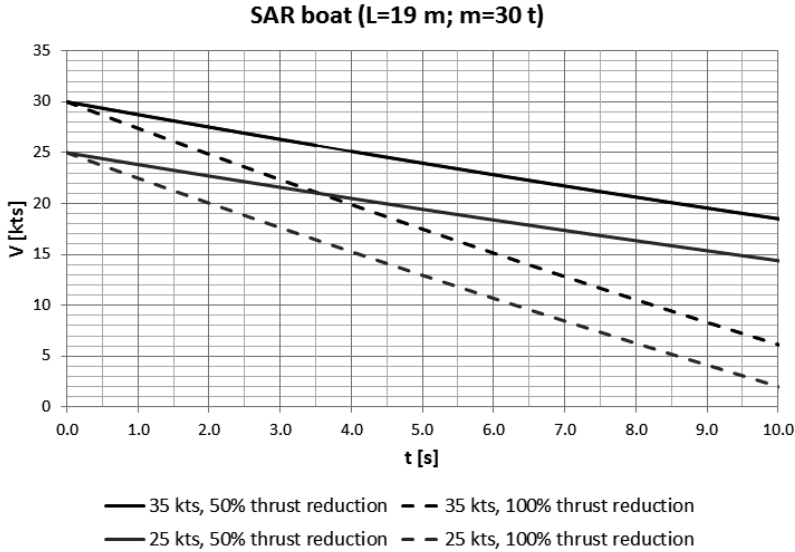
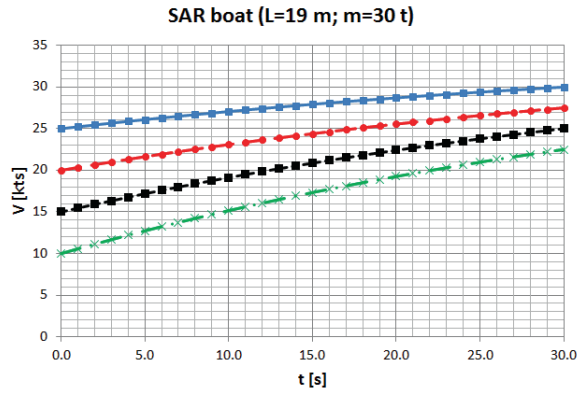


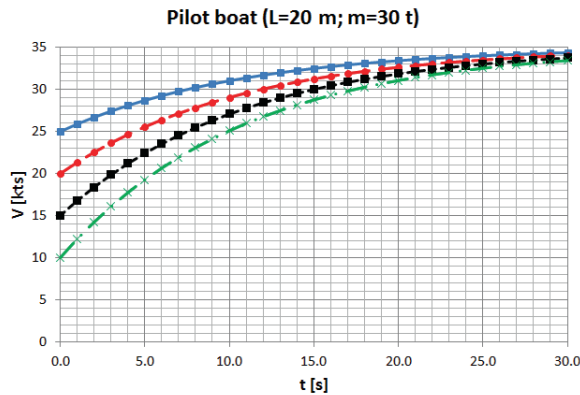
Figure 2.12: Speed reduction over time for 50 and 100% thrust reduction for the SAR boat of the Arie Visser class

the time it takes to reduce the speed from 35 to 30 *kts*, from 35 to 25 *kts*, from 25 to 20 *kts* and from 25 to 15 *kts* for a low gradient of the resistance curve ($a = 0.25$); Table 2.6 for a high gradient ($a = 1$) These tables show the time it takes to reduce the speed related to the specific power, the initial forward speed and the gradient of the resistance curve. The time it takes to restore the speed is relevant with respect to the average forward speed that can be maintained throughout a trip using thrust control. The time it takes dependent on specific power, however, does not provide an indication of the (maximum) average forward speed. For this, the actual thrust reductions, dependent on the incoming waves and the response of the ship should be simulated.

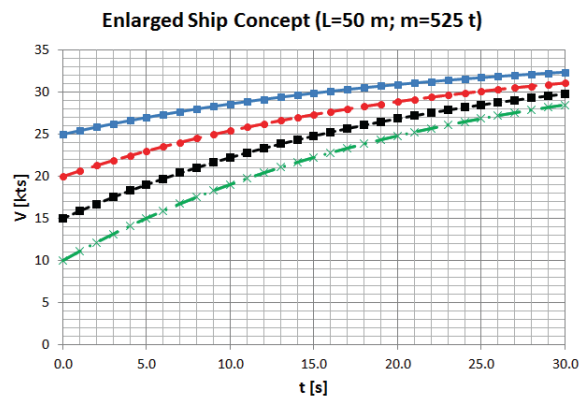
The required speed reduction over time to sufficiently reduce the vertical peak acceleration depends on the nonlinear seakeeping behaviour of the ship. If a ship is able to decelerate quickly, there is a higher probability that the next vertical peak acceleration can be reduced sufficiently. Large horizontal decelerations, however, may not be desired either. The horizontal deceleration (initially) exceeds -2 m/s^2 for a specific power equal or greater than 40 kW/t (for both linearised resistance curves).



(a) SAR boat



(b) Pilot boat



(c) Enlarged Ship Concept

Figure 2.13: Speed increase over time for 100% thrust for three example ships

Table 2.5: Time (in seconds) to reduce speed for a range of specific powers ($a = 0$)

Pe/W [kW/t]	35 to 30 [kts]	35 to 25 [kts]	25 to 20 [kts]	25 to 15 [kts]
10	4.6	9.4	5.0	10.2
15	3.1	6.4	3.4	6.9
20	2.4	4.9	2.6	5.2
25	1.9	3.8	2.0	4.1
30	1.6	3.2	1.7	3.5
35	1.4	2.8	1.5	3.0
40	1.2	2.4	1.3	2.6

Table 2.6: Time (in seconds) to reduce speed for a range of specific powers ($a = 1$)

Pe/W [kW/t]	35 to 30 [kts]	35 to 25 [kts]	25 to 20 [kts]	25 to 15 [kts]
10	4.9	10.7	7.1	16.2
15	3.3	7.3	4.8	11.0
20	2.5	5.5	3.6	8.4
25	2.0	4.3	2.9	6.6
30	1.7	3.6	2.4	5.5
35	1.4	3.1	2.1	4.8
40	1.2	2.7	1.8	4.1

2.2.3 Nonlinear seakeeping behaviour

The nonlinear seakeeping behaviour of planing boats sailing in head seas has been a widely studied subject for nearly 50 years now. Savitsky's paper published in 1968 can probably be considered one of the first publications on this topic. He presented an analysis of the available data on the seakeeping behaviour of planing hulls in order to define and categorize those hydrodynamic problems associated with various speeds of operation in a seaway. He distinguished different behaviour in the low speed range ($F_{N\triangledown} < 2$) (semi-displacement), where the seakeeping characteristics are very similar to the displacement hull and the high speed range ($F_{N\triangledown} > 2$), where the hydrodynamic lift forces are predominant and where high impact forces can occur. At that time, he already noticed that the impact accelerations at high forward speed become quite intolerable and can be considered as the limiting factor when designing a rough-water planing hull for high-speed operation. Fridsma (1969; 1971) was the first to systematically execute model tests with a series of constant-deadrise models, varying in length. His results, presented in the form of response characteristics, cover a wide range of operating conditions and show, quantitatively, the importance of design

parameters on the rough water performance of planing hulls. At this time it already became apparent that planing monohulls show a significant nonlinear behaviour in head waves.

Since then many studies have been published. Their topics varied from the calm water sinkage and trim (Savitsky 1964, Clement and Blount 1963, Keuning and Geritsma 1982, Keuning et al. 1993), the effect of deadrise angle on both the seakeeping behaviour and resistance (see for example Van den Bosch 1970, Blok and Roeloffs 1989, Keuning 1994), to the development and use of computational models (see for example Martin 1978, Zarnick 1978; 1979, Keuning 1994, Troesch 1992; 1996, Garne 2004, De Jong 2011) and to the development of new hull shapes that improve the operability of a planing monohull sailing in head seas: the Enlarged Ship Concept (ESC) and AxeBow Concept (ABC) (Keuning and Pinkster 1995; 1997, Keuning et al. 2001; 2002, Keuning 2006).

Although each previously mentioned study addressed a different issue the underlying physics of the nonlinear seakeeping behaviour of a planing monohull sailing in head seas can be described as follows.

At a high forward speed a large part of the weight of the vessel is carried by a hydrodynamic lift force. There is a significant relative velocity between the hull and water due to the high forward speed and trim of the ship. A hydrodynamic pressure proportional to the square of this relative velocity is generated.

In calm water, the hydrodynamic lift may cause a significant change in calm water reference position, which is expressed in terms of sinkage and trim. The absolute magnitude of the sinkage and trim varies considerably with increasing forward speed and is also strongly dependent on the geometry and layout of the particular ship under consideration.

While sailing in head seas large relative motions cause large variations in the underwater hull geometry, causing large variations in both the hydrodynamic lift and the vertical wave exciting forces, in particular in the forward half of the hull. Moreover, the relative velocity and thus the hydrodynamic lift gets additional contributions from the vessel's motions and from the motion of the waves.

The high forward speed and the large geometry changes are the source for the development of the nonlinear hydrodynamic lift and the nonlinear wave exciting forces. The rate of change of the hydrodynamic lift while performing large relative motions with respect to the incoming waves is largely dependent on the change of the sectional wetted beam. The sectional beam is a function of sectional submergence and sectional deadrise angle (V-shaped sections). The large water entry velocity in the foreship (due to an additional contribution of the pitch velocity) causes large changes of the wetted beam, yielding a large change of the hydrodynamic lift in a short time interval. The change of wetted beam is largely dependent on the deadrise angle in the foreship as well as on the shape of the bow (convex, concave or straight lines). The large change of the hydrodynamic lift can be considered a strongly nonlinear hydrodynamic reaction force in heave and pitch direction. The wave exciting forces of a planing mono-

hull are dominated by the undisturbed wave component (Froude-Krylov); diffraction is considered to be small (Zarnick 1978, Keuning 1994). The Froude-Krylov force is calculated by integration of the dynamic pressure in the undisturbed incoming wave over the actual instantaneous submerged area of the hull. The large relative motions of the ship cause that the instantaneous submerged area changes significantly over time, most profoundly in the fore ship. The rate of change of the wave excitation force may become significant, causing its strongly nonlinear character.

The nonlinear hydrodynamic lift and the nonlinear wave exciting forces are the distinct features of the seakeeping behaviour of a planing monohull sailing in head seas. The response is considered nonlinear to the amplitude of the incoming wave. The extent of nonlinearity of the response is determined by the hull geometry (deadrise angle fore ship, length over beam ratio), sea state (relative motions) and the forward speed (magnitude hydrodynamic lift). The nonlinear impact loads have a significant influence on the motions and accelerations and are crucial for the extreme responses. They result in violent motions and large vertical accelerations (see for example Keuning 1994; 2006).

The effect of hull geometry, sea state and forward speed will be illustrated by means of results of model tests. Model tests in the towing tank of the Delft University of Technology were carried out to investigate the seakeeping behaviour of the pilot boat mentioned in the previous section. Its behaviour in head seas was compared with an AxeBow Concept (ABC) of the same size (Visch 2007). The main dimensions are given in table 2.7. Figures 2.14 and 2.15 depict sketches of the hull geometries. Table 2.8 shows the wave conditions and speed during the model tests.

Table 2.7: Main dimensions pilot boat

Designation	Symbol	DCH	ABC	Unit
Length over all	L_{oa}	19.3	20.0	m
Beam over all	B_{oa}	6.30	5.65	m
Draft amidships	T	0.96	0.90	m
Displacement	∇	33.66	35.22	m^3
Longitudinal Centre of Gravity	LCG	6.8	8.2	m
Vertical Centre of Gravity	VCG	1.67	1.67	m
Radius of gyration y-axis	k	5.45	5.5	m

Figures 2.16 and 2.17 show the distributions of the vertical accelerations. The vertical accelerations were measured at 90% of the length, measured from the transom stern. The troughs represent the vertical accelerations upwards (z -axis pointing downwards). The vertical accelerations downwards are naturally much smaller than the accelerations upwards. A ship cannot fall faster than the gravitational acceleration. A additional pitch component causes that the downward vertical acceleration at

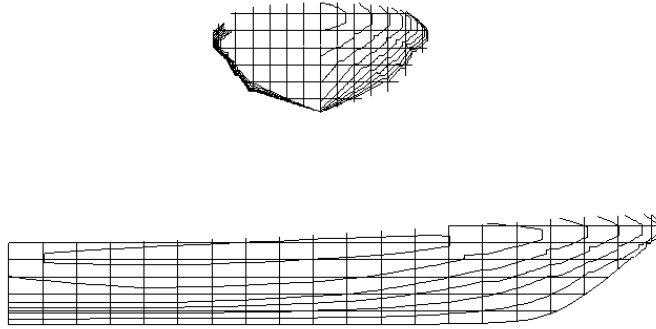


Figure 2.14: Sketch hull geometry pilot boat

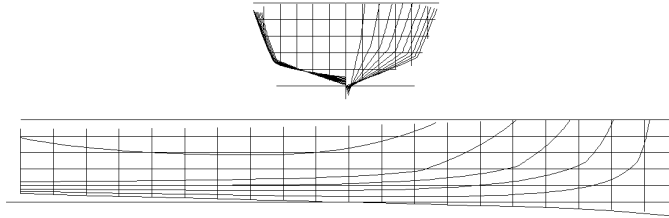


Figure 2.15: Sketch hull geometry ABC

Table 2.8: Tested conditions

Name	H_s	T_p	V_s
—	[m]	[s]	[kts]
Condition 1	1.5	5.3	15
Condition 2	1.5	5.3	30
Condition 3	2.5	7.15	15
Condition 4	2.5	7.15	30

the bow is more than $g \text{ m/s}^2$. The generated wave crests and troughs in the towing tank were Rayleigh distributed. If the response was linear to the amplitude incoming wave, the probability of exceedance of the maxima and minima would appear as the straight blue line in the Rayleigh plot. The vertical peak accelerations clearly show a nonlinear relation with the amplitude of the incoming wave.

Comparison between the Rayleigh plots left and right shows the influence of forward speed; between top and bottom the influence of sea state. For both ships the effect of forward speed is clearly visible. A higher forward speed implies a higher

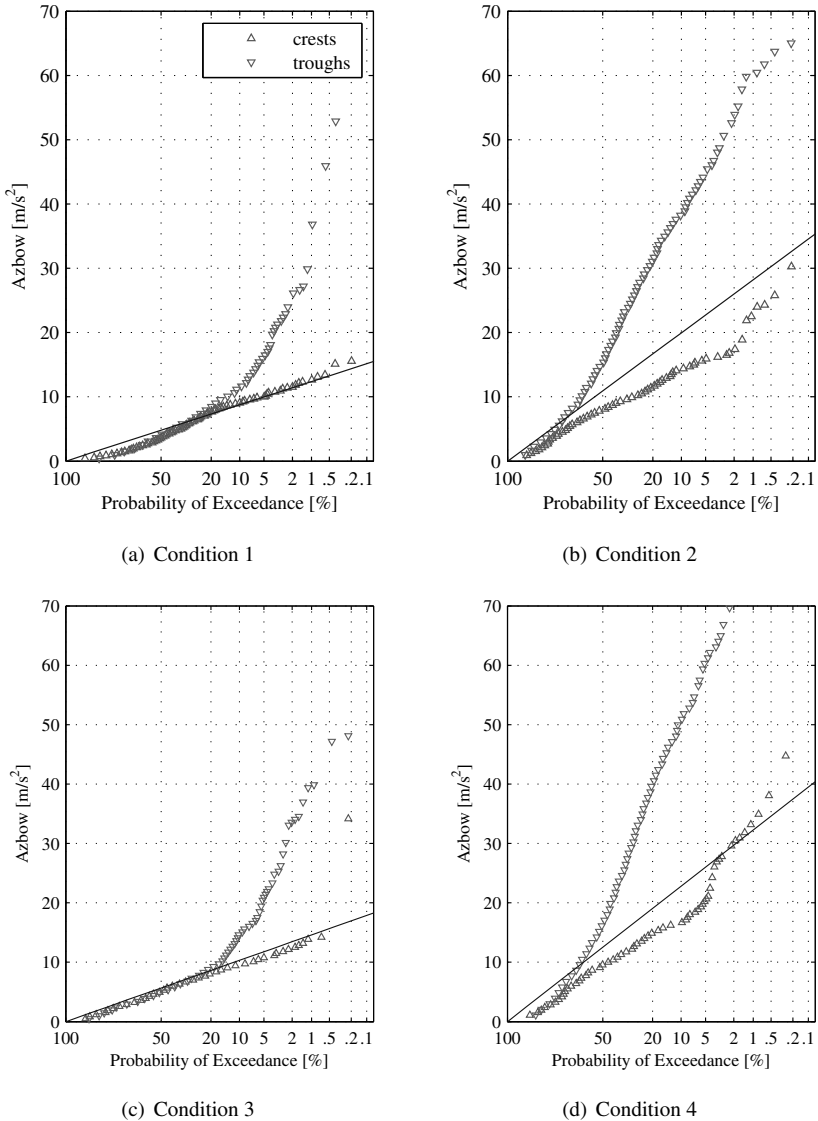
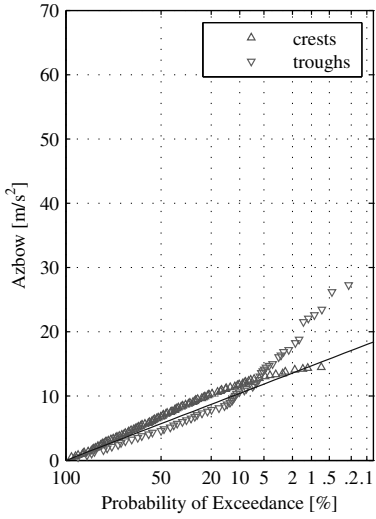
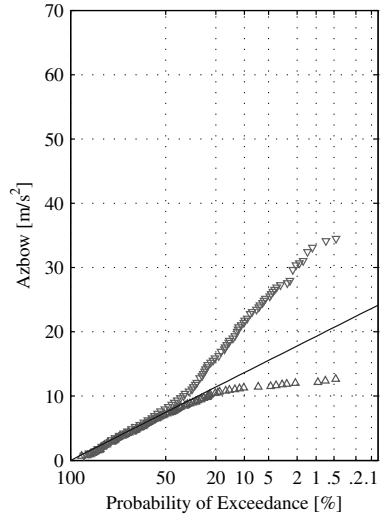


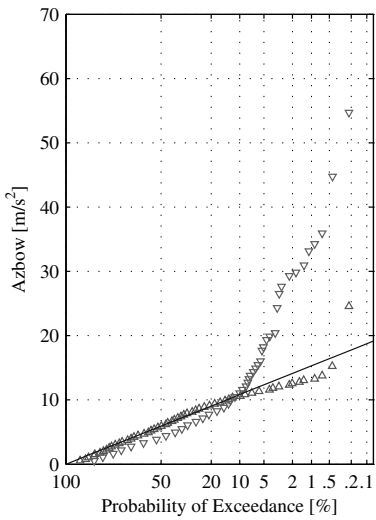
Figure 2.16: Rayleigh plots of the vertical accelerations pilot boat for two sea states and two forward speeds



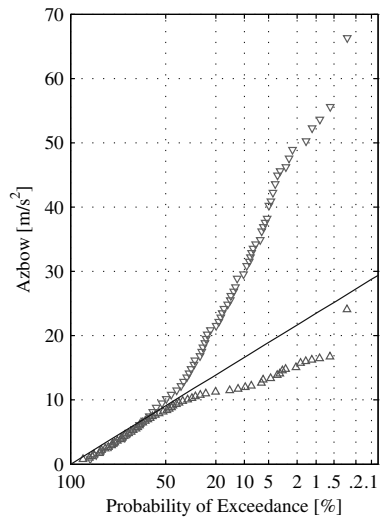
(a) Condition 1



(b) Condition 2



(c) Condition 3



(d) Condition 4

Figure 2.17: Rayleigh plots of the vertical accelerations ABC for two sea states and two forward speeds

level of accelerations. The effect of sea state is less clear for the pilot boat. Comparing both sea states at a forward speed of 15 *kts* shows that the level of vertical accelerations is slightly higher in a higher sea state. Sailing at 30 *kts* in the higher sea state yields the highest level of accelerations. The difference between sea states is clearer for the ABC.

The level of accelerations is less for all conditions for the ABC. The rate of change of both the hydrodynamic lift and wave excitation is less than for the pilot boat. This yields significantly lower level of vertical accelerations.

Similar results were found during other model tests, where the seakeeping behaviour of a much larger ESC (see also previous section) and ABC was analysed for a range of speeds and significant wave heights (Vermeulen 2005, Keuning and van Walree 2006). The peak period of the spectrum was not varied ($T_p = 7.8$ s). Table 2.9 shows the main dimensions of the ships. Tables 2.10 and 2.11 present the measured maximum vertical peak accelerations in each condition (upward vertical accelerations). The maximum vertical acceleration depends on the encountered wave train during the experiments due to the nonlinearity of the response. The encountered wave train is different for different speeds. It may have been different for both ships in the same condition since the start of each run may have been different (dispersion of the wave). The maximum vertical peak accelerations depicted in Tables 2.10 and 2.11 may therefore only be used as a indicative, comparative value.

Table 2.9: Main dimensions ESC & ABC

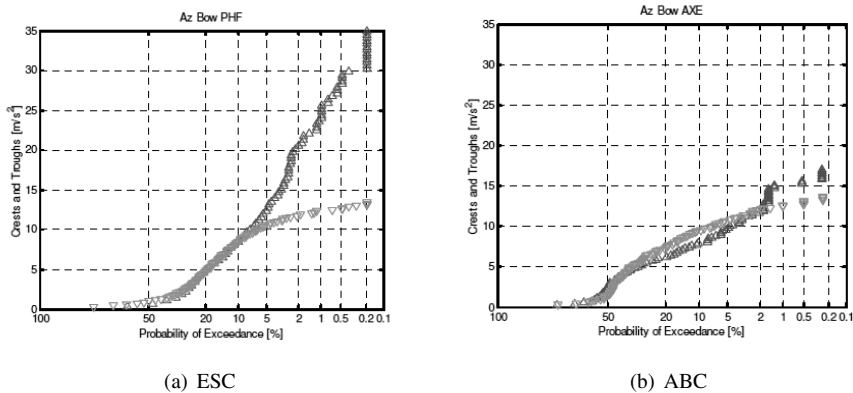
Designation	Symbol	ESC	ABC	Unit
Length waterline	L_{wl}	55	55	<i>m</i>
Beam over all	B_{wl}	8.46	8.46	<i>m</i>
Draft (maximum)	T	2.66	4.38	<i>m</i>
Displacement	∇	516.0	517.4	m^3
Longitudinal Centre of Gravity	LCG	32.5	30.6	<i>m</i>
Vertical Centre of Gravity	VCG	3.85	3.53	<i>m</i>
Radius of gyration y-axis	k	13.75	13.75	<i>m</i>

Table 2.10: Measured maximum vertical peak acceleration ESC [m/s^2]

V_s	H_s [<i>m</i>]			
[<i>kts</i>]	2	2.5	3	3.5
25	12	N.A.	30	43
35	18	N.A.	39	56
50	21	N.A.	42	50

Table 2.11: Measured maximum vertical peak acceleration ABC [m/s^2]

V_s	H_s	[m]		
[kts]	2	2.5	3	3.5
25	4	N.A.	21	21
35	N.A.	13	17	28
50	10	10	14	21

**Figure 2.18:** Rayleigh plots of the vertical accelerations ESC & ABC ($H_s = 3$ m, $T_p = 7.8$ m, $V_s = 35$ kts ; Keuning and van Walree 2006)

By comparing Tables 2.10 and 2.11 the effect significant wave height, forward speed and hull geometry can be seen. The maximum vertical peak accelerations increases with increasing significant wave height. From 25 to 35 kts the magnitude of the maximum vertical peak acceleration increases; from 35 to 50 kts it generally does not increase much for the ESC and it even decreases for the ABC. This may be because an increased damping at such a high speed of 50 kts . Furthermore, the encountered wave train was not exactly equal. The maximum acceleration is smaller for the ABC than for the ESC for all conditions. Figure 2.18 shows the distribution of the vertical accelerations for both ships sailing at 35 kts in 3 m significant wave height and 7.8 s peak period of the wave spectrum. This figure shows the lower level of accelerations for the ABC than the ESC in the same sea state at an equal forward speed.

The presented results of model tests show that hull geometry, sea state and forward speed determine the level of accelerations of a planing monohull sailing at a high constant forward speed in head seas. For thrust control is important to know that generally the vertical accelerations reduce with decreasing forward speed. This may, however, not always be valid for a temporary speed reduction.

A change of trim and sinkage, when the thrust has been reduced, influences the magnitude of the vertical peak acceleration. It may cause that the next vertical peak acceleration is larger than when the speed would not have been reduced. The rate of change of the hydrodynamic lift and wave excitation may have been increased due to an unfavourable trim and sinkage.

It has been assumed that the major contribution to changes in trim and sinkage when the speed reduces comes from a change of the hydrodynamic lift and buoyancy force (both in magnitude and centre of effort). The thrust force itself also has a contribution. Its line of action is not always parallel to the keel line and it may have a (small) contribution to the pitch moment. This is, however, different for each ship. For the purpose of this study it is not (yet) relevant to take into account these additional effects. The line of action of the thrust force is assumed to be horizontal through the centre of gravity of the ship, regardless of the current pitch angle. The line of action of the resistance of the ship is also assumed to be horizontal through the centre of gravity of the ship, regardless of the current pitch angle.

Figure 2.19 depicts the total forces acting on a planing boat and their line of action assumed throughout the rest of this study. This figure shows the forces during calm water planing. In waves an additional wave excitation is present. The thrust force is controlled by the bridge handle. The resistance is based on the calm water resistance curve as discussed in Section 2.2.2. The weight of the ship is carried by the hydrostatic and hydrodynamic force. The hydrodynamic lift acts perpendicular to the keel.

It can be concluded that the hull geometry of the ship, the heave and pitch motion, the forward speed at impact and the incoming wave are the relevant variables that determine the magnitude of the vertical peak acceleration. These variables should be incorporated in the computational model used to predict the response.

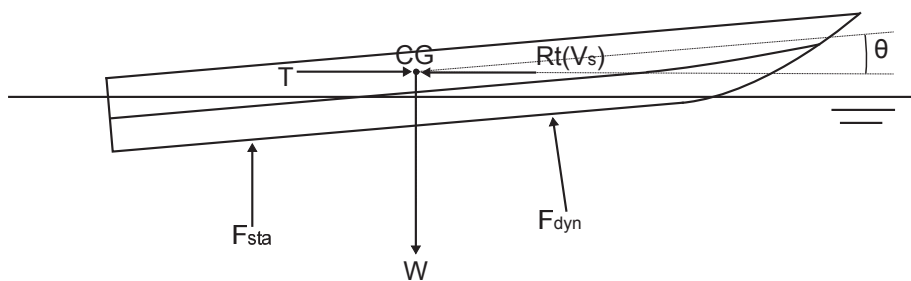


Figure 2.19: Overview total forces acting on the ship

2.2.4 Acceptance level vertical accelerations

The limited number of full scale trials on board of the Dutch SAR boat of the Arie Visser class showed a large spreading of the measured level of vertical accelerations

(see Figure 2.5). There are many factors that influence the level of accelerations that a crew on high speed craft generally considers acceptable. Examples of these factors are the mission purpose and the anticipated duration of the trip, the motivation of the crew, fatigue and there are probably more.

Townsend et al. (2012) carried out a study into the high speed craft motion effects and the hazards of whole human body vibration and repeated shock. He stated that:

Human tolerance to vibration primarily depends on the complex interactions of motion duration, direction, frequency, magnitude and biodynamical, psychological, physiological, pathological and intra- and inter-subject variabilities. The complex interactions and their effects on humans are not fully understood. However, whole body vibration, especially those associated with rough vehicle rides, can damage the human body.

Various injuries and injury mechanisms are associated with whole body vibrations and repeated shock. With very few studies into the effects of repeated impacts associated with high speed marine craft motions, in spite of the reported significant risk of injury, limited data is available to identify the injury mechanisms. This is further compounded by the ethical difficulties in reproducing the dangerous motions in a laboratory.

It is recognised that whole body vibrations and repeated shock associated with high speed marine craft motions may cause significant injuries. The injury mechanisms, however, are not fully understood and the data to identify them is limited.

Keuning and van Walree (2006) describe full scale trials that were carried to determine the most important limiting criterion or criteria for the operation of a fast ship in irregular waves. The paper states that:

Generally spoken all crews imposed a voluntary speed reduction at roughly the same conditions on board the ship. It also showed clearly that the real measure for imposing a voluntary speed reduction was not the prevailing magnitude of the significant amplitude of the motions or vertical accelerations at that time, but the occurrence of the high peaks in particular in the vertical acceleration. The occurrence of such a 'one big peak' generally provoked a speed reduction by all the crews just to 'prevent it from happening again'. In fact such a reaction is more or less in line with a well known more general aspect of human behaviour, namely that most people are inclined to react to 'extremes' rather than to 'averages'.

This illustrates that for each crew a value exists for which they consider the vertical peak acceleration ('one big peak') unacceptable. If this 'unacceptably' large vertical peak acceleration does not occur throughout the trip they do not feel obliged to reduce the speed.

To prove that automated proactive thrust control reduces the level of accelerations compared to a trip at an equal, but constant forward speed it is therefore sufficient to assume a value for the vertical accelerations that the crew considers unacceptable. If a vertical peak acceleration is anticipated that exceeds this value the proactive control system should reduce the thrust. The exact value of the assumed maximum allowable vertical peak acceleration may differ per crew, mission purpose, trip, etc. It may even change during a trip. The development of a criterion for the vertical accelerations on board of a planing monohull in head seas is not within the scope of this study.

The vertical acceleration at the bow has been chosen as criterion for automated proactive thrust control. It is more profound and has a stronger nonlinear relation with the amplitude of the incoming wave than a vertical acceleration defined in the vicinity of the centre of gravity. This is because of the additional pitch acceleration component. The vertical acceleration at the bow is defined as:

$$A_{z_{bow}} = \ddot{z} - L_{bow} \cdot \ddot{\theta} \quad (2.14)$$

In each chapter in this dissertation the value used will be explicitly stated. It varies between Chapter 3 and 4 due to the different computational models used to calculate the response of a planing monohull sailing in head seas. During the model tests (Chapter 5) a value was chosen that best suited the speed range of the carriage in relation to the generated waves.

Note to horizontal and lateral accelerations

Horizontal and lateral accelerations are not evaluated in this dissertation. Horizontal and lateral accelerations may also contribute to undesirable motion effects. In this study, the response on 3 DoF is considered. So, lateral accelerations (due to roll) are not considered. Large horizontal accelerations may occur, when the ship has a large (axial) deceleration. The effect of large decelerations on the crew has not been considered. It is not the purpose of this dissertation to address the horizontal acceleration level. For this, wave action should also be taken into account. Wave forces may contribute significantly to large horizontal acceleration peaks. To prove that automated proactive thrust control reduces the level of accelerations it is sufficient to use a realistic value for the deceleration.

2.3 Proposed control system

The full scale trials carried out on board of the SAR boat of the Arie Visser class show that thrust control is actuated before impact (proactive control of the thrust). Control is based on the anticipated vertical peak accelerations. If they anticipate that the next impact will result in an unacceptably large acceleration, they temporarily reduce the speed. They have little time to react; there is little time to effectuate control. If a sequence of large vertical peak accelerations is anticipated, the thrust remains reduced.

In relation to the setup of automated proactive thrust control it can be concluded that an operator:

- chooses a desired forward speed that he would like to maintain during the trip on forehand,
- continuously observes and judges the incoming wave,
- predicts the response using his experience and intuition and
- determines and applies an amount of the thrust reduction that he thinks will result in a sufficient reduction of the next occurring vertical peak acceleration.

If based on this knowledge automated proactive thrust control is set up, the following three components are essential:

1. A shipboard wave measurement system that provides a sufficiently accurate description of the incoming wave(s) over the next few seconds;
2. A computational model that predicts the response (the vertical peak accelerations) of the ship based on the measured incoming wave faster than real-time;
3. A stable control system that determines the thrust force continuously;

In this part of the project, it is assumed that the waves used for predicting the response can be measured by a laser, radar or lidar in the near future. At present, a thorough research into possibilities to measure the incoming wave on board of violently moving ship having a high forward speed is not of interest at this stage. Real-time wave measurements from an object moving in waves and its transformation in time to the ship's location are not available on the market yet. Recently, a few papers have been published on this subject (see for example Fu et al. (2011), Grilli et al. (2011), Story et al. (2011)).

Throughout the rest of this study the waves, including their propagation and dispersion, are assumed to be known (at each time instant). The aim of this study is to show that using automated proactive thrust control a reduction of the vertical accelerations can be realised and to prove that proactive control for a planing boat based on predicted vertical peak accelerations is possible. If automated proactive thrust control yields the desired outcome the development of a shipboard wave measurement system for this specific purpose becomes more relevant.

The computational model should be able predict both the speed reduction over time and the next vertical peak acceleration accurately. The calculations need to be carried out faster than real-time since the time interval to effectuate control is quite short (high relative velocity between ship and incoming wave). The axial deceleration is based on the calm water resistance of the ship (wave action in horizontal direction has been neglected). The mass of the ship, the initial forward speed and the amount of thrust reduction should be taken into account to determine the actual speed reduction over time (see Section 2.2.2). The vertical peak acceleration depends on the speed at

impact. The hull geometry of the ship, the heave and pitch motion and the incoming wave should also be taken into account to determine the actual acceleration peak (see Section 2.2.3).

The control system incorporates an assumed relation between bridge handle and thrust force (as explained in Section 2.2.1). The controlled variable is the speed; the speed is controlled by the thrust. The controlling variable is the bridge handle.

Figure 2.20 depicts the principle of the proactive control system. The dashed frame represents the control system. The elements outside the frame are elements in the real world. The control strategy is that the response should be predicted for a certain time interval, called the prediction window, dependent on the control setting. The control setting in this case is the magnitude of the thrust force. The real-time simulations are performed at a certain frequency, preferably at 1, 2 or 4 Hz . The response should be predicted a number of times each wave encounter. If it has been predicted a number of times each wave encounter, the probability that the next occurring vertical peak acceleration has been predicted in time increases.

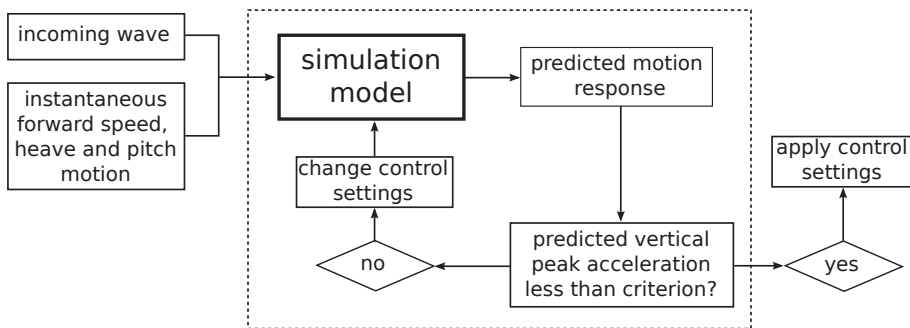


Figure 2.20: Overview proactive control system

At first, on time t_i , the response for the duration of the prediction window will be predicted using an unchanged thrust. If the predicted vertical peak acceleration does not exceed the preset criterion, nothing has to be done; the thrust remains unchanged. If it does speed reduction will be necessary. Dependent on the time available the response will be predicted using a reduced thrust. For a number of control settings the response must be predicted before the actual impact. In this way, a relation between the control setting, here the thrust force, and the predicted magnitude of the vertical acceleration can be found. Figure 2.21 depicts an example of the determined relation between reduced thrusts and predicted vertical peak accelerations. It should be stressed that each t_i the number of response predictions should be carried out much faster than real-time, leaving sufficient time to decelerate. The maximum possible thrust force, for which the predicted vertical acceleration is smaller than the preset criterion, is chosen (min-

imum speed loss). After impact the thrust may be restored to its original value, if no new unacceptable vertical peak acceleration has been predicted.

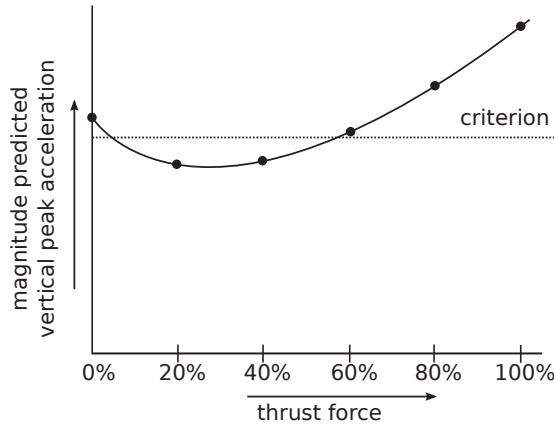


Figure 2.21: Example of determined relation between thrust reduction and predicted vertical peak acceleration

2.4 Important issues concerning automated proactive thrust control

Carrying out real-time simulations on board of a planing ship sailing in waves and moreover using the outcome for control of the vertical motions is a new concept. If the predicted vertical accelerations (output computational model) prove to be inaccurate, the chosen amount of thrust reduction might be inaccurate. The cause of inaccurate predicted vertical peak accelerations may be found in two factors:

1. The computational model might not provide satisfactory results (it does not describe the reality sufficiently accurate);
2. The input to the model is incorrect: measurement incoming wave and instantaneous forward speed, heave and pitch motion at the beginning of each response prediction;

If the magnitude of the vertical peak accelerations is not predicted accurately, incorrect thrust reductions may be applied. This affects the level of reduction of the vertical accelerations possible with automated proactive thrust control.

The time step used for the response predictions may also have a large influence on the predicted magnitude of the vertical peak accelerations. For an accurate description of the peaks a small time step is desired. On the other hand, the response predictions

should be carried out faster than real-time, which imposes limits to the minimum time step that may be used. A trade-off exists between little calculation time (large time step) and the accuracy of the predicted vertical peak accelerations (small time step).

The calculation time required to predict the response for a number of control settings takes time, introducing a time delay before the actual realisation of the required thrust reduction. As was stated in Section 2.2.1 significant time delay may jeopardise the feasibility of automated proactive thrust control, since the available time left to decelerate may become too short.

The influence of the minimum speed that can be realised before impact (see Section 2.2.2) and the accuracy of the predicted vertical peak accelerations (also dependent on the calculation time step) are important aspects regarding the performance of automated proactive thrust control and are further elaborated throughout this dissertation. For the conceptual model of automated proactive thrust control, discussed in Chapter 3, the reduction of the vertical acceleration level is determined for a range of specific powers and prediction windows. For the idealised model of automated proactive thrust control, discussed in Chapter 4, the reduction of the vertical acceleration level is determined for a benchmark ship and a range of prediction windows. The effect of the accuracy of the predicted vertical peak accelerations, including time step, on the level of reduction of the level of accelerations is also addressed in this chapter.

The influence of incorrect input to the computational model is not further elaborated. In this study the waves are assumed to be known. It may be expected that in reality the incoming wave cannot be measured 100% accurately. Inaccurate wave predictions cause inaccurate response predictions. The instantaneous forward speed, heave and pitch motion on time-instant t_i are important for an accurate response prediction. Starting off with incorrect values for the instantaneous forward speed, heave and pitch motion may also yield inaccurate response predictions. The exact effect inaccurate wave or motion measurements on the response predictions and consequently on the performance of automated proactive thrust control is not analysed. The effect of inaccurate response predictions, irrespective of their origin, is further analysed.

The effect of a time delay introduced by the required calculation time to predict the response has not been taken into account in Chapter 4 and 5. A time delay shortens the available time to decelerate. Results of simulations for short prediction windows show the effect on the reduction of the level accelerations using automated proactive thrust control when a significant time delay would exist. When the control scheme is implemented in model experiments (proof of concept, Chapter 5) calculation time does exist.

Chapter 3

Conceptual model of automated proactive thrust control

In the previous chapter the setup of automated proactive thrust control was explained, derived from what was observed during full scale trials. Results of full scale trials suggested that using thrust control it is possible to sail at a higher forward speed without increasing the discomfort on board, but a conclusive statement could not be given. To investigate if automated proactive thrust control reduces the level of accelerations in an early stage of this study a conceptual model of automated proactive thrust control has been developed.

Section 3.1 explains the setup of the conceptual model. The elementary response model, used to mimic the response of the ship, is discussed in Section 3.2. Section 3.3 provides the input to the conceptual model. Section 3.4 illustrates the applicability of the conceptual model. Section 3.5 shows the relation between minimum attainable speed before impact and the reduction of the level of accelerations. Section 3.6 discusses the results generated with this conceptual model of automated proactive thrust control.

3.1 Setup conceptual model

This conceptual simulation model of automated proactive thrust control has been setup to show that a reduction of the vertical acceleration level may be expected if automated proactive thrust control would be applied on board of a planing monohull sailing in head seas. This is done by showing the reduction of the vertical acceleration level for a range of specific powers and prediction windows. Using a conceptual model a fair comparison can be made between a simulation with and without thrust control. The level of accelerations will be compared at an equal average forward speed.

Figure 3.1 depicts the relation between independent, controlled and dependent variables associated with automated proactive thrust control. The ship under consideration and the sea state are the independent variables. During the full scale trials it was observed that the operators tried to maintain a desired forward speed (see Section 2.1.2). The desired forward speed can also be regarded as an independent variable. The variables ship (hull geometry and inertia), sea state and forward speed determine the extent of nonlinearity of the heave and pitch response (see Section 2.2.3). The dependent variable is the response of the ship, where the vertical peak accelerations is the variable of interest. The variable that affects the magnitude of the next vertical peak acceleration is the actual forward speed at impact. This is the controlled variable. The speed is controlled by the thrust; the actual controlling variable is the bridge handle (see Section 2.2.1). The actual speed reduction, once the thrust has been reduced, is the integral of the deceleration over the time interval between the start of a thrust reduction and the actual impact. This time interval has been defined as the net available time interval for deceleration (T_{dw}). The minimum speed that can be realised before impact depends on the specific power of the ship, the initial forward speed, the shape of the resistance curve and the time available to decelerate (see Section 2.2.2).

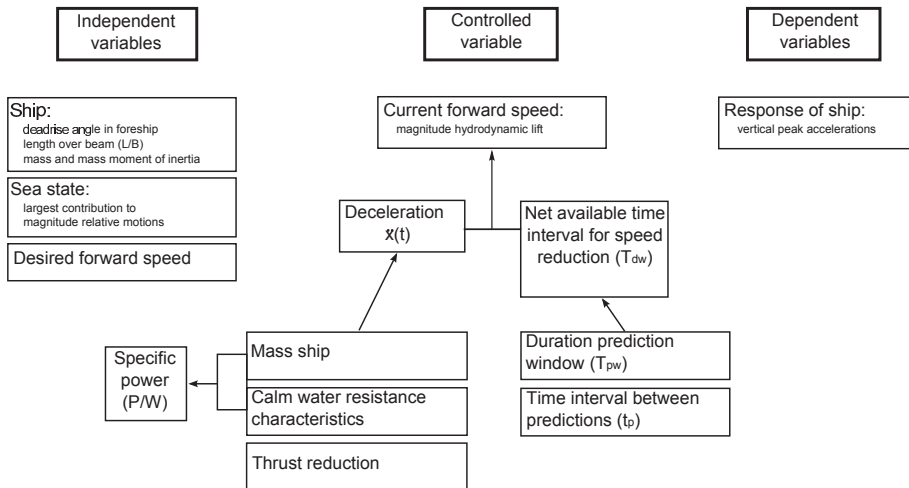


Figure 3.1: Variables associated with automated proactive thrust control

In Figure 3.2 an overview of the conceptual model is depicted. On time t_i the response will be predicted for the duration of the prediction window (T_{pw}) using the elementary response model. If thrust reduction is necessary, more predictions are carried out using reduced thrusts (see Figure 2.21). If an appropriate thrust reduction has been determined, the response will be saved for t_p s. t_p is the frequency at which the real-time simulations are performed (see Section 2.3). This process repeats itself on $t_{i+1} = t_i + t_p$ s. It has been assumed that the response predictions do not consume

time.

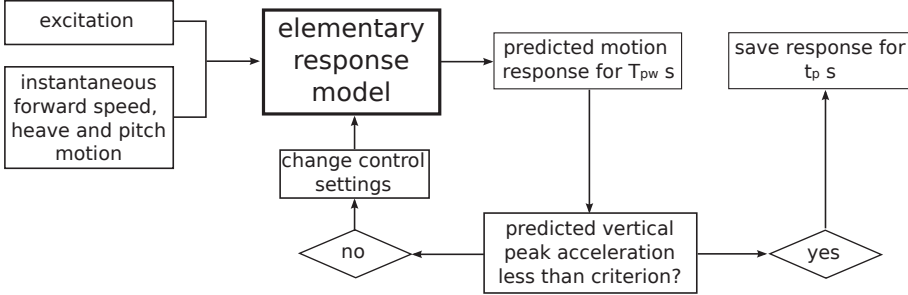


Figure 3.2: Overview conceptual model

The net time interval available to decelerate T_{dw} , is always smaller than the prediction window T_{pw} . The net available time interval for speed reduction is at most t_p s shorter than the prediction window ($T_{pw} - t_p < T_{dw} \leq T_{pw}$, see Figure 3.3).

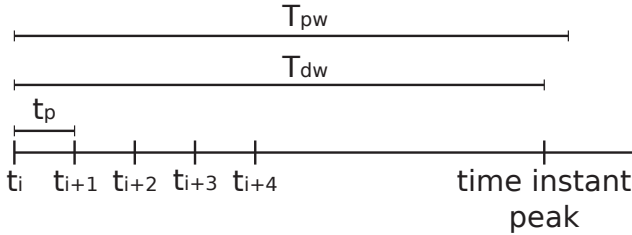


Figure 3.3: Time line with respect to response predictions

The accuracy of the response predictions, also dependent on the chosen calculation time step, has not been analysed using this conceptual model. The response predictions and the presumed actual response were calculated using the elementary model. The calculation time step for both the response predictions and the presumed actual response was also equal. This implies that the response is 100% accurately predicted. The input for the response predictions, the excitation and the instantaneous forward speed, heave and pitch motion, are assumed to be known (see Section 2.3).

3.2 Elementary response model

The equations of motion in the elementary model are derived from an ordinary nonlinear-mass spring system. Three issues must be incorporated in the equations of motion of the nonlinear mass-spring system in order to effectively mimic the behaviour of a planing boat in head waves:

1. The nonlinear relation of the vertical response with the excitation resulting in vertical peak accelerations;
2. A relation between the forward speed and the vertical accelerations;
3. A description of the nonlinear relation between resistance, thrust and forward speed;

The nonlinear relation of the vertical response with the excitation resulting in vertical peak accelerations is found by assuming a nonlinear restoring force in heave and pitch direction and a nonlinear damping force in pitch direction. A relation between the forward speed and the vertical accelerations has been found by assuming nonlinear coupling terms between heave and pitch and the forward speed. The calm water resistance has been used to describe the nonlinear relation between resistance, thrust and forward speed (see Section 2.2.2).

The relation between forward speed and the vertical accelerations describes the reduction of the vertical peak acceleration when the speed has been reduced temporary. A temporary speed reduction decreases the hydrodynamic lift. Consequently, its rate of change while the ship is performing large relative motions decreases. The vertical peak acceleration, which is experienced by the ship and the crew, is therefore much smaller.

The coordinate system of the elementary model is defined earth fixed. It has its origin at a height equal to the height of the centre of gravity above the undisturbed water surface. The x -axis points in the direction of the forward speed. The z -axis is pointing downwards (see Figure 3.4).

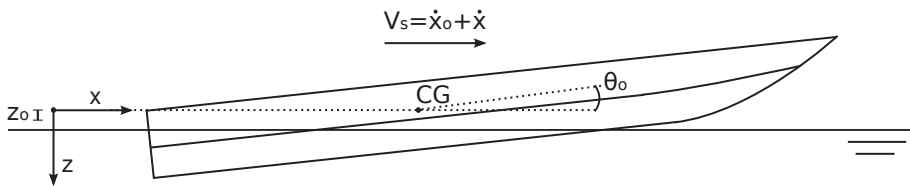


Figure 3.4: *Coordinate system and equilibrium position*

The equations of motion are developed around a certain steady-state equilibrium. The ship sails at a certain steady-state forward speed \dot{x}_o at a certain steady-state rise z_o and steady-state pitch angle θ_o . The total forward speed can be written as: $V_s = \dot{x}_o + \dot{x}$ (consisting of a constant and a variable part, see Figure 3.4). The corresponding steady-state resistance is equal to Rt_o . T_{max} is the maximum thrust force. γ is the position of the bridge handle (100% is full speed ahead). The heave and pitch displacements, z and θ , represent deviations from the steady-state equilibrium position. The total heave and pitch motion are written as $z_o + z$ and $\theta_o + \theta$ respectively.

We assume that each nonlinear hydromechanic reaction force in a certain direction consists of independent reaction forces dependent either on an acceleration, a velocity or a displacement in its motion direction (no relations such as $\dot{x}z$, or $z\dot{z}$, etcetera). For example:

$$F_{r_z}(\bar{x}) = f_z(\ddot{x}) + f_z(\dot{x}) + f_z(x) + f_z(\ddot{z}) + f_z(\dot{z}) + f_z(z) + f_z(\ddot{\theta}) + f_z(\dot{\theta}) + f_z(\theta)$$

Nonlinearity in heave direction is found using a strongly nonlinear restoring force; acceleration, damping and coupling terms are assumed to be linear. An assumed continuous increasing quadratic function represents the relation between the vertical restoring force and the heave displacement (see Figure 3.5):

$$\begin{aligned} z \geq 0 : f_z(z) &= c_{zz} \cdot z + c_{zz} \cdot z^2 \\ -1.5 < z < 0 : f_z(z) &= c_{zz} \cdot z + c_{zz}/3 \cdot z^2 \\ z \leq -1.5 : f_z(z) &= -0.75 \cdot c_{zz} \end{aligned} \quad (3.1)$$

For $z \leq -1.5 \text{ m}$ the ship is assumed to be airborne; a constant reaction force pulls the ship down.

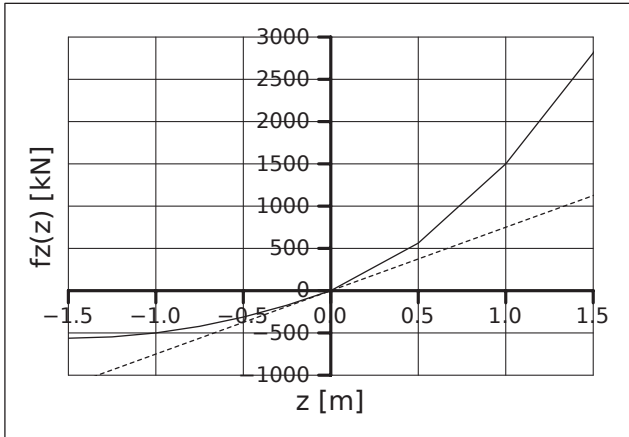


Figure 3.5: Assumed nonlinear restoring force in heave direction

In pitch direction both the damping and restoring force are nonlinear; acceleration and coupling terms (except in phase with forward speed) are assumed to be linear (see Figures 3.6 and 3.7):

$$\begin{aligned} \theta \geq 0 : f_\theta(\theta) &= c_{\theta\theta} \cdot \theta + c_{\theta\theta} \cdot \theta^2 \\ \theta < 0 : f_\theta(\theta) &= c_{\theta\theta} \cdot \theta - c_{\theta\theta} \cdot \theta^2 \end{aligned} \quad (3.2)$$

$$\begin{aligned} \dot{\theta} \geq 0 : f_{\theta}(\dot{\theta}) &= b_{\theta\theta} \cdot \dot{\theta} \\ \dot{\theta} < 0 : f_{\theta}(\dot{\theta}) &= b_{\theta\theta} \cdot \dot{\theta} - b_{\theta\theta} \cdot \dot{\theta}^2 \end{aligned} \quad (3.3)$$

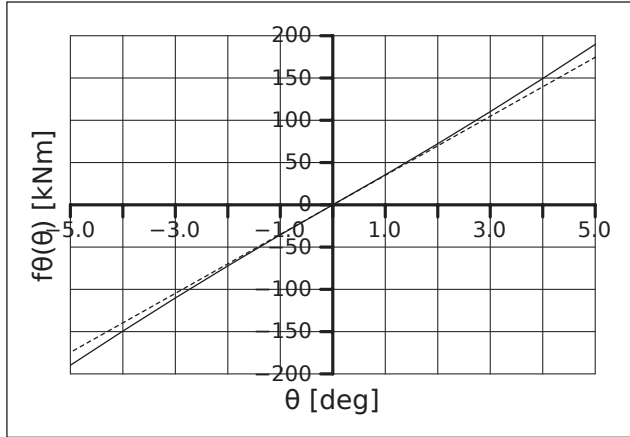


Figure 3.6: Assumed nonlinear restoring force in pitch direction

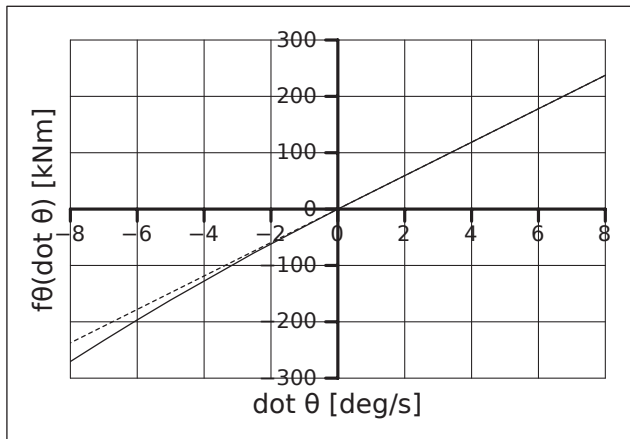


Figure 3.7: Assumed nonlinear damping force in pitch direction

The nonlinear relation between forward speed and the hydrodynamic lift has been represented by nonlinear coupling terms in the heave and pitch equation of motion which are dependent on the forward speed. These reaction forces are assumed to be

equal to (see Figures 3.8 and 3.9):

$$\begin{aligned} f_z(\dot{x}) &= b_{zx} \cdot \dot{x} - b_{zx}/8 \cdot \dot{x}^2 \\ f_\theta(\dot{x}) &= b_{\theta x} \cdot \dot{x} - b_{\theta x}/6 \cdot \dot{x}^2 \end{aligned} \quad (3.4)$$

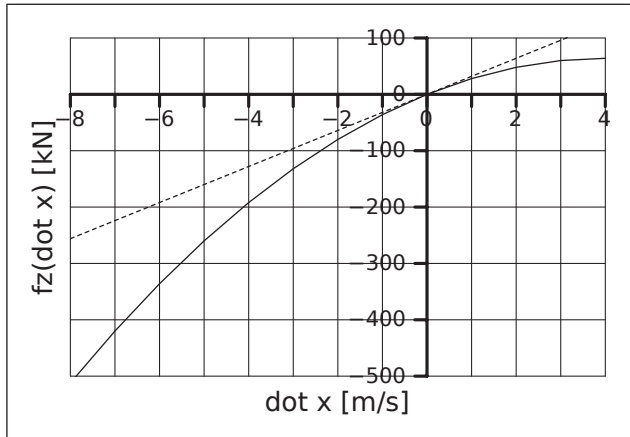


Figure 3.8: Assumed nonlinear coupling term between forward speed and heave motion

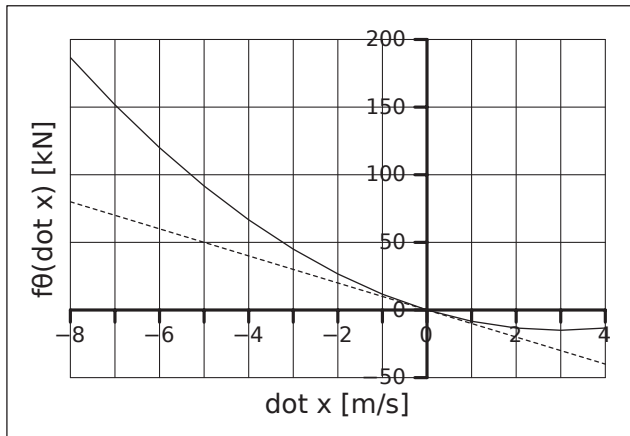


Figure 3.9: Assumed nonlinear coupling term between forward speed and pitch motions

The horizontal reaction force F_{T_x} is assumed to be equal to the calm water resistance curve (see Section 2.2.2). It is assumed to be speed dependent only. Coupling between the surge motion and the vertical motions has been neglected.

The calm water resistance is described by a 3rd polynomial function. For the present setup a continuous and increasing polynomial function is desired in order to avoid horizontal instabilities. The polynomial expression has been defined around $\dot{x} = 0$ (see Figure 3.10):

$$f_x(\dot{x}) = 0.05 \cdot \dot{x}^3 - 0.05 \cdot \dot{x}^2 + 0.15 \cdot \dot{x} \quad (3.5)$$

The total resistance can be expressed as $Rt = Rt_o + f_x(\dot{x})$.

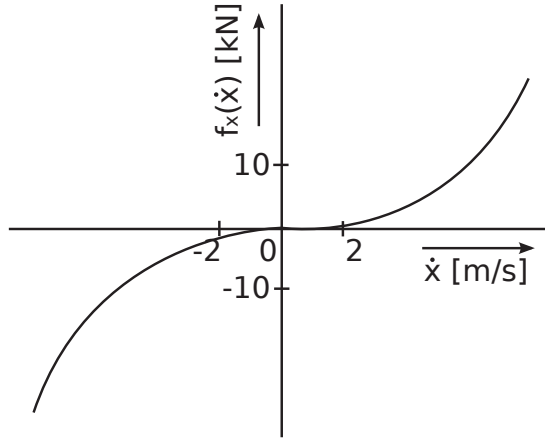


Figure 3.10: Calm water resistance

The wave excitation has been introduced into the elementary model as external forces in heave and pitch direction (force and moment). Actual waves are not modelled. Hence, relative motions between the waves and the ship do not exist in this model. Besides that, the vertical wave excitation is chosen to be independent on the instantaneous displacements in heave and pitch direction of the ship. The horizontal wave excitation has been neglected. Since coupling between surge and the heave and pitch motion was neglected as well, there are no surge oscillations.

The equations of motion of the elementary model are written as (there are no horizontal restoring forces):

$$\begin{aligned} m \cdot \ddot{x} + f_x(\dot{x}) &= \gamma \cdot T_{max} - Rt_o \\ (m + a_{zz}) \cdot \ddot{z} + b_{zz}\dot{z} + f_z(z) + a_{z\theta}\ddot{\theta} + b_{z\theta}\dot{\theta} + c_{z\theta}\theta + a_{zx}\ddot{x} &= F_{w_z} - f_z(\dot{x}) \\ (I + a_{\theta\theta}) \cdot \ddot{\theta} + f_{\theta}(\dot{\theta}) + f_{\theta}(\theta) + a_{\theta z}\ddot{z} + b_{\theta z}\dot{z} + c_{\theta z}z + a_{\theta x}\ddot{x} &= M_{w_{\theta}} - f_{\theta}(\dot{x}) \end{aligned} \quad (3.6)$$

The forces, that represent the relation between forward speed and the hydrodynamic lift, $f_z(\dot{x})$ and $f_{\theta}(\dot{x})$, can be considered as external forces, which can be manipulated

by changing the forward speed. Except the nonlinear restoring force in heave and pitch direction, the nonlinear damping force in pitch direction, the nonlinear resistance and the nonlinear coupling terms between heave and pitch and the forward speed all other terms in Equation 3.6 are assumed to be linear (constants; see Appendix A).

The nonlinearity of this system approximates the nonlinear seakeeping behaviour a planing monohull sailing in head seas. It is set up in such a way that the reaction forces represent the nonlinear hydromechanic reaction forces (with the largest contribution from the nonlinear hydrodynamic lift) of a certain monohull planing around a chosen steady-state equilibrium (steady-state forward speed, sinkage and trim). The nonlinear character of the vertical wave exciting forces (Froude-Krylov force) due to the large relative motions is not incorporated. The dependency of the vertical wave exciting forces on the instantaneous submergence has not been modelled.

In reality, the instantaneous wave pressure of the undisturbed wave over the actual wetted surface of the craft, yielding the instantaneous Froude-Krylov force, introduces a significant nonlinear effect into the wave exciting forces on a fast ship. Together with large changes in hydrodynamic lift force, this will result in large peaks in the vertical accelerations having a very short duration. In the present model these nonlinear effects are not present. The rise time of the vertical peak accelerations at the bow is therefore somewhat larger than of the accelerations of a planing monohull sailing in head seas and the peaks are less profound.

By choosing one set of coefficients the nonlinearity of the response is fixed. The possibility to vary the ship's geometry and the sea state has been excluded using this elementary model to mimic the response of a planing monohull sailing in head seas. Choosing another steady-state forward speed has no effect on the generated outcome. The influence of these factors can be analysed when the elementary model is replaced by a computational model that describes the nonlinear seakeeping behaviour more accurately than the present model (this model should incorporate the influence of the ship, sea state and desired forward speed on the response; see Chapter 4).

The deceleration, once the thrust has been reduced, is determined by equilibrium between the thrust force and the the speed dependent reaction force. The relation between bridge handle and thrust force is assumed to be one to one, implying that the path for $T(t)$ is dictated by $\gamma(t)$: $\gamma(t) \cdot T_{max} = T(t)$. It has been assumed that a 100% change (in-/decrease) can be realised in 1 second ($d\gamma/dt = dT/dt = 1 \text{ 1/s}$). This assumption has been explained in Section 2.2.1.

When a temporary speed reduction is required, the bridge handle position will be changed using a continuous function, yielding a continuous function for the thrust force and hence for the speed (see Figure 3.11). The maximum speed reduction before impact is dependent on:

- The maximum deceleration;
- The net available time interval for speed reduction (T_{dw} ; time interval between detection and impact, t_1 to t_2);

- The path of the deceleration $\ddot{x}(t)$;

The maximum deceleration depends on the mass of the ship, the resistance characteristics and the initial forward speed. This has been explained in Section 2.2.2. The maximum deceleration in this model is equal to:

$$\ddot{x} = -\frac{Rt_o + f_x(\dot{x})}{m} \text{ using equation 3.6}$$

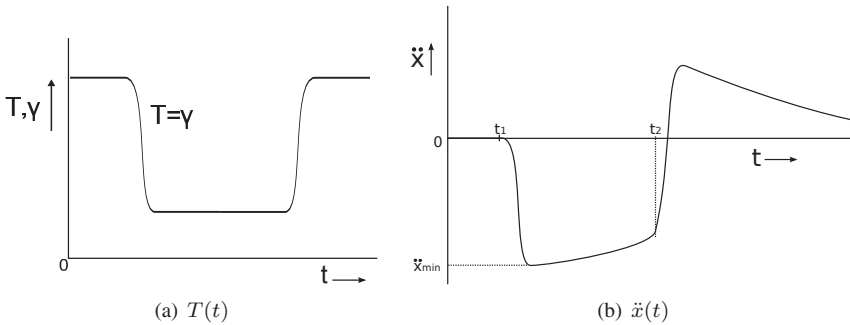


Figure 3.11: Relation between thrust and deceleration

The actual speed reduction is equal to the area under $\ddot{x}(t)$:

$$\dot{x}(t_2) - \dot{x}(t_1) = \int_{t_1}^{t_2} \ddot{x}(t) dt \quad (3.7)$$

The minimum attainable speed within the time-interval $t_2 - t_1$ can be considered the maximum control force possible. A large speed reduction can be obtained if the maximum deceleration is large (large ratio Rt/m , related to a large specific power P_e/m), if the deceleration remains large between t_1 and t_2 (low gradient of the resistance curve around $\dot{x} = 0$ m/s) and if the vertical peak acceleration is detected early (a large prediction window T_{pw}).

3.3 Calculation input

A typical mass and mass moment of inertia were chosen based on the values used for the DSDS (Keuning et al. 1993). The steady-state equilibrium position was chosen using the calm water trim and sinkage of the 19° deadrise parent hull of the DSDS with a length of 15 m and with a typical loading $A_p/\nabla^{2/3}$ and position of *LCG*.

The chosen steady-state equilibrium was: $u_o = 1$, $\dot{x}_o = 12 \text{ m/s}$ ($F_{N\varphi} \approx 2.25$), $z_o = -0.20 \text{ m}$, $\theta_o = 5^\circ$. T_{max} is always equal to the steady-state resistance Rt_o . The centre of gravity in this model was situated at midships ($\xi_{bow} = 7.5 \text{ m}$). A mass of 23.4 t has been chosen. The radius of gyration was estimated on $L_p/4 = 3.75 \text{ m}$, yielding a mass moment of inertia of $I = m \cdot k_{yy}^2 = 329062.5 \text{ kgm}^2$. The calm water resistance of this ship with a typical loading $A_p/\nabla^{2/3}$ and position of *LCG* (calculated using Savitsky's method and PHF) and the resistance curve used in the elementary model are given in Appendix A. The values of the coefficients used in the equations of motion are also given in Appendix A.

The time interval between two predictions (t_p) was chosen to be 0.5 s . The discretization of bridge handle positions used for the predictions was chosen to be 5% . If an unacceptably large vertical peak acceleration had been predicted, 21 simulations using reduced thrusts (0 to 100%) were carried out.

The criterion was set on -10 m/s^2 for the vertical acceleration at the bow (only troughs are considered). The elementary model mimics the nonlinear seakeeping behaviour of a planing monohull sailing in head seas, but the vertical peak accelerations are less profound. The chosen criterion for the conceptual simulation model of automated proactive thrust control is therefore less than what would be expected in reality (see for example Figure 2.5).

Table 3.1 shows the chosen range of maximum speed reductions before impact (starting from $\dot{x}_o = 12 \text{ m/s}$, assuming a 100% thrust reduction and $T_{dw} = T_{pw}$). This range was realised using a range of steady-state resistances and prediction windows. The chosen predictions window were 2, 3, 4, and 5 s. A higher steady-state resistance implies a higher specific power. Increasing the specific power means increasing the speed reduction before impact. Increasing the prediction window means increasing the time interval to decelerate (see Equation 3.7). \ddot{x}_{max} is the initial deceleration. The chosen combinations of steady-state resistances (and specific powers) and prediction windows cover a realistic range of maximum speed reductions before impact (see Section 2.2.2).

Table 3.1: Maximum possible speed reduction within prediction window

P_e/m [kW/t]	Rt_o [kN]	\ddot{x}_{max} [m/s ²]	T_{pw} [s]:				
			2	3	4	5	
15.4	30	-1.3	1.9	3.1	4.3	5.2	[m/s]
20.5	40	-1.7	2.5	4.1	5.5	6.6	[m/s]
25.6	50	-2.1	3.2	5.1	6.7	7.8	[m/s]

The wave excitation was irregular, built up out of 40 components with random phases ($d\omega = 0.05 \text{ rad/s}$). The peak period was 6.28 s . The assumed force spectrum for

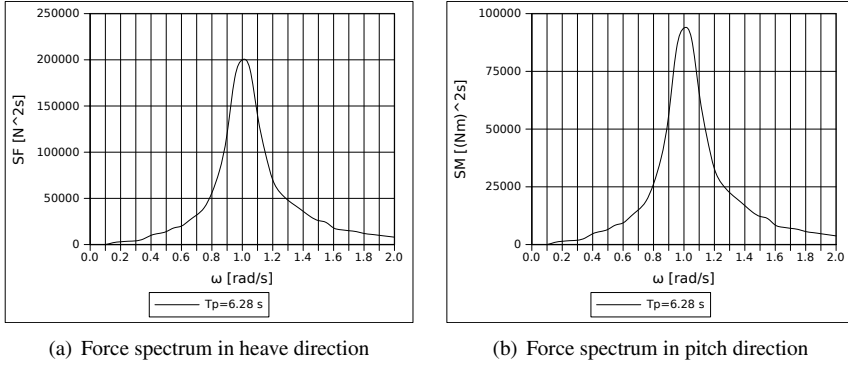


Figure 3.12: Wave excitation

both heave and pitch direction used is given in Figure 3.12. Neither variations of force and moment spectra, nor variations of their realisations are relevant at this stage. We are solely interested whether by means of temporary speed reductions a significant reduction of the level of accelerations can be expected.

The run length was 2400 s, corresponding with a total number of approximately 1000 counted peaks for the vertical acceleration at the bow. The repetition time of the wave train for a ship sailing in head seas is dependent on the forward speed (see Appendix B). For a forward speed of 9.5 m/s (see next section) and a frequency step of 0.05 rad/s the wave train the ship encounters is unique for 2500 s. The corresponding repetition distance is 24 km.

The equations of motion (Equation 3.6) are solved using the Euler method. The time step was 0.05 s. Each time step the forces were calculated. The acceleration in 3 DoF could be determined. Integration yielded the velocities and displacements.

The calculated responses were compared with respect to the maximum vertical acceleration found during the simulation, the number of vertical peak accelerations above the preset criterion and the level of the accelerations. The level of accelerations was visualised by plotting the distributions of the vertical peak accelerations using Rayleigh plots.

The maximum vertical acceleration found during the calculations cannot be considered as an absolute value, but should rather be considered a measure of performance. The largest vertical acceleration found is dependent on the encountered wave train and the duration of the simulation. This maximum vertical acceleration gives us an indication of the largest vertical acceleration that can be expected and is used as a comparative value.

3.4 Applicability conceptual model

The equations of motion in the elementary model should mimic the nonlinear sea-keeping behaviour of a planing monohull sailing in head seas. The relation of the vertical accelerations with the amplitude of the excitation should be nonlinear, yielding large vertical peak accelerations. Their magnitude should be speed dependent. Thrust reductions should yield realistic speed reductions and reduced vertical peak accelerations.

Typical time-traces of the calculated motions and accelerations at the bow using thrust control are given in Figure 3.13 ($P_e/m = 20.5 \text{ kW/t}$ and $T_{pw} = 4 \text{ s}$). Peaks do occur. They are, however, not as profound and their rise time is not as short as what would happen in reality ($0.3 \sim 0.5 \text{ s}$ compared to $0.1 \sim 0.2 \text{ s}$, see Figures 2.3 and 2.4). This time-series shows that three thrust reductions were required. The speed reductions were realistic (approximately 2 and 4 m/s). Figure 3.14 shows what would have happened if thrust control was not applied. The first peak clearly would have exceeded the criterion when the speed would have been 12 m/s . A forward speed of 10 m/s more or less corresponds with the average forward speed using thrust control. The second and third speed reduction clearly yield lower peak accelerations compared to a constant forward speed of 10 m/s . The exact time instant that these peaks occurred did not correspond because the encounter wave train was not exactly equal for a simulation with constant forward speed compared to the simulation with thrust control. When thrust control had been applied the three peaks exceeding the criterion had been reduced to -10 m/s^2 , exactly equal to the criterion. Figure 3.13 also shows that it takes significantly more time to accelerate than to decelerate. This is because of the low gradient of the resistance curve (see Section 2.2.2, Figures 2.11 and 2.13).

Figure 3.15 shows the distributions of the vertical peak accelerations of simulations carried out at a constant forward speed of 8, 10 and 12 m/s . The positive peaks of the calculated signal were omitted in this figure since only the troughs (upward vertical accelerations, z -axis pointing downwards) were considered. The peaks and troughs of the excitation, both the heave force F_{wz} and pitch moment $M_{w\theta}$, were Rayleigh distributed. If the vertical accelerations were linear to the excitation, the response would also be Rayleigh distributed. The probability would be plotted on top of the given straight line, which in this case corresponds with the steady-state forward speed of 10 m/s . The deviation from this line displays the nonlinearity of the elementary model. The vertical accelerations at the bow show a nonlinear relation with the amplitude of the excitation. The speed dependency of the level of accelerations is also visible.

The time-traces given in Figures 3.13 and 3.14 show that vertical peak accelerations occur. Temporary speed reductions yield diminished vertical accelerations. The Rayleigh plot depicted in Figure 3.15 shows that the elementary model (Equation 3.6)

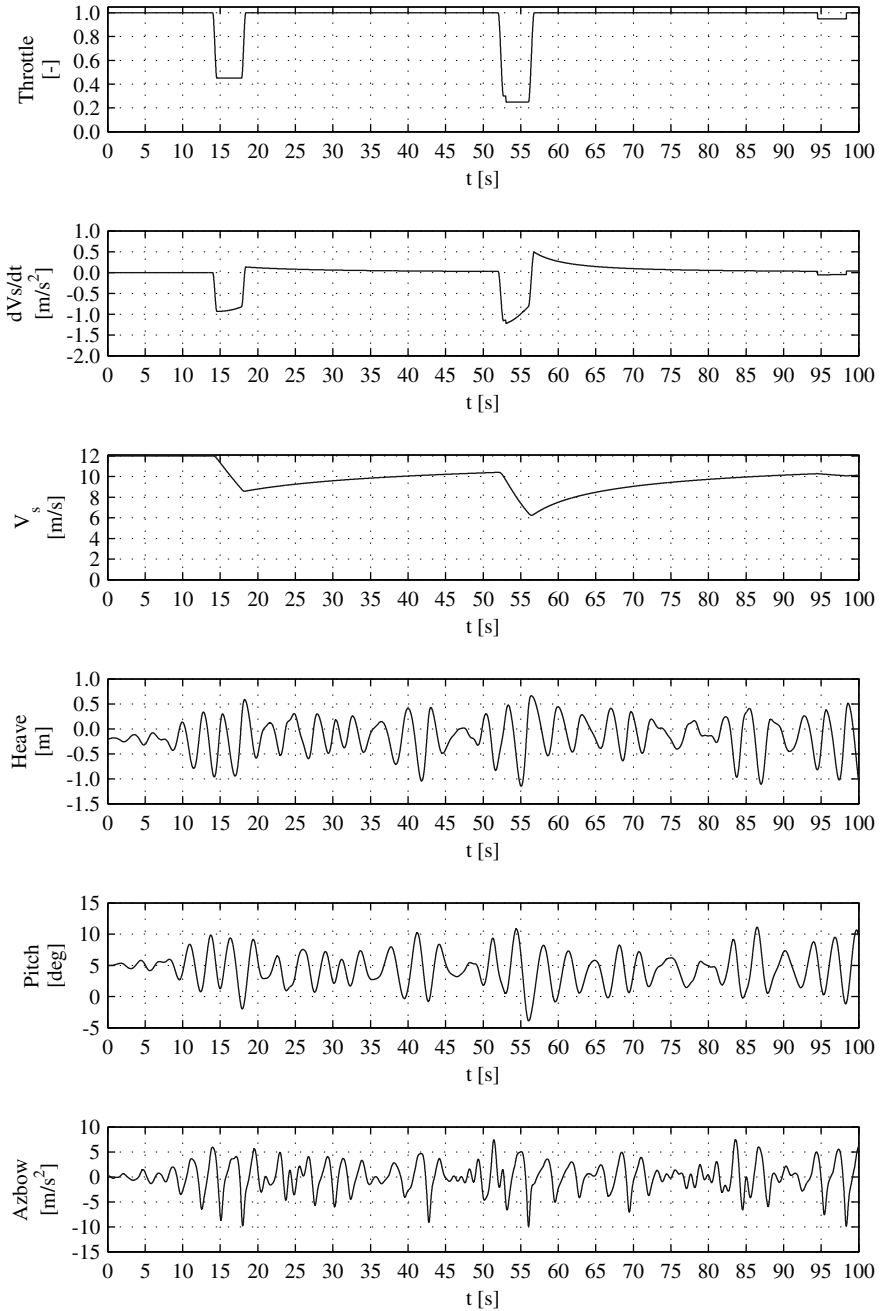
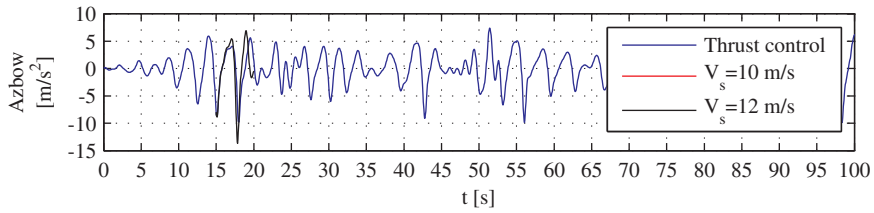
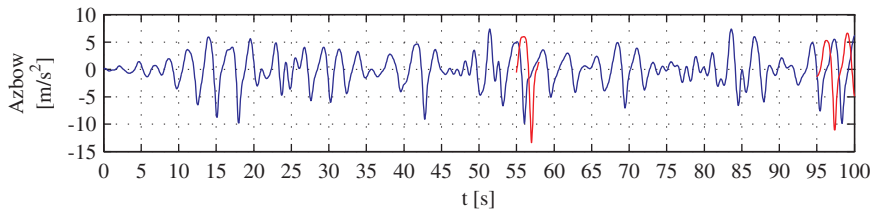


Figure 3.13: Typical time-traces of the calculated response using thrust control ($P_e/m = 20.5$ kW/t and $T_{pw} = 4$ s)



(a) constant $V_s = 12 \text{ m/s}$



(b) constant $V_s = 10 \text{ m/s}$

Figure 3.14: Comparison vertical accelerations at the bow

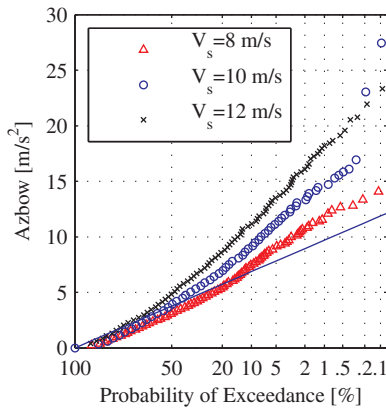


Figure 3.15: Rayleigh plots of the vertical accelerations at the bow, showing the influence of different constant forward speeds

yields a nonlinear, speed dependent response. The conceptual model of automated pro-active thrust control, using the equations of motion of a nonlinear mass-spring system as a representation for the response of a planing monohull sailing in head seas, is therefore an applicable approach to show that a reduction of the vertical acceleration level may be expected if automated proactive thrust control would be applied on

board of a planing monohull sailing in head seas.

3.5 Expected influence automated proactive thrust control

In Tables 3.2 and 3.3 the percentage of the vertical accelerations exceeding the preset criterion of -10 m/s^2 and the maximum vertical acceleration at the bow of each simulation are given. The average forward speed was about $9.2 \sim 9.7 \text{ m/s}$ for all simulations with control (see Table 3.4). For comparison, the results of the simulation carried out at a constant speed of 9.5 m/s are also given (see Tables 3.2 and 3.3).

Table 3.2: Number of vertical peak accelerations at the bow exceeding preset criterion as percentage of total number of peaks

P_e/m [kW/t]	Rt_o [kN]	\ddot{x}_{max} [m/s ²]	no control	T_{pw} [s]:			
			9.5 [m/s]	2	3	4	5
15.4	30	-1.3	6.9	6.7	3.5	1.8	0.9 [%]
20.5	40	-1.7	6.9	5.5	3.3	1.2	0.2 [%]
25.6	50	-2.1	6.9	5.1	2.1	0.3	0.0 [%]

Table 3.3: Maximum vertical acceleration at the bow during each simulation

P_e/m [kW/t]	Rt_o [kN]	\ddot{x}_{max} [m/s ²]	no control	T_{pw} [s]:			
			9.5 [m/s]	2	3	4	5
15.4	30	-1.3	-22.1	-21.6	-26.1	-20.7	-19.8 [m/s ²]
20.5	40	-1.7	-22.1	-24.8	-18.0	-18.6	-13.6 [m/s ²]
25.6	50	-2.1	-22.1	-25.5	-14.0	-11.3	-10.0 [m/s ²]

Table 3.4: Average forward speed

P_e/m [kW/t]	Rt_o [kN]	\ddot{x}_{max} [m/s ²]	T_{pw} [s]:			
			2	3	4	5
15.4	30	-1.3	9.7	9.6	9.5	9.4 [m/s]
20.5	40	-1.7	9.5	9.3	9.3	9.3 [m/s]
25.6	50	-2.1	9.5	9.2	9.2	9.3 [m/s]

The number of large vertical peak accelerations above the preset criterion were less than half for $T_{pw} \geq 3 \text{ s}$, compared to the simulation carried out at a constant speed. A

significant decrease was found for $T_{pw} \geq 4$ s (corresponding with a maximum speed reduction greater than 4 m/s, see Table 3.1). The number of vertical peak accelerations at the bow exceeding preset criterion was percentage less than 1/3rd than what was found at a constant forward speed. The maximum acceleration only decreased to a value close or equal to the criterion for larger maximum speed reductions, ≥ 6.5 m/s ($P_e/m = 20.5$ kW/t & $T_{pw} = 5$ s and $P_e/m = 25.6$ kW/t $T_{pw} \geq 4$ s) compared to the simulation carried out at a constant speed.

Tables 3.2 and 3.3 also show that if there is little time left to decelerate (thus for $T_{pw} = 2$ s, for example when a considerable time delay would exist), the reduction of the vertical accelerations was limited. The percentage of the vertical peak accelerations exceeding the preset criterion did not decrease significantly. The maximum vertical acceleration was in the same order of magnitude as what was found using a constant forward speed (more than twice the criterion). The distributions of the vertical peak accelerations were very similar to the distribution of the peaks taken from a simulation carried out with an equal constant forward speed (see Figure 3.16).

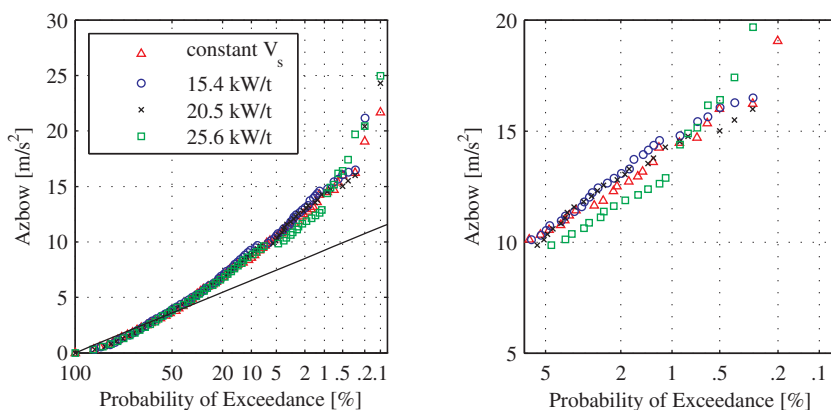


Figure 3.16: Rayleigh plot of the vertical accelerations at the bow for a short prediction window ($T_{pw} = 2$ s)

Figure 3.17 shows the distributions of the vertical peak accelerations at the bow using the following combinations of specific power and prediction window: 15.4 kW/t and 3 s, 20.5 kW/t and 4 s, and 20.6 kW/t and 5 s. These combinations correspond with a range of increasing maximum speed reduction before impact, respectively 3.1, 5.5 and 7.8 m/s (see Table 3.1). For comparison, the distribution of the peaks taken from a simulation carried out at a constant speed of 9.5 m/s is also given. If the maximum speed reduction within the prediction was small, proactive thrust control did not have any effect on the level of accelerations. For the second combination of specific power and prediction window, representing a maximum speed reduction before impact of 5.5 m/s, the reduction was more significant. If the maximum speed reduction within the

prediction window was large, all unacceptable vertical peak accelerations could be counteracted.

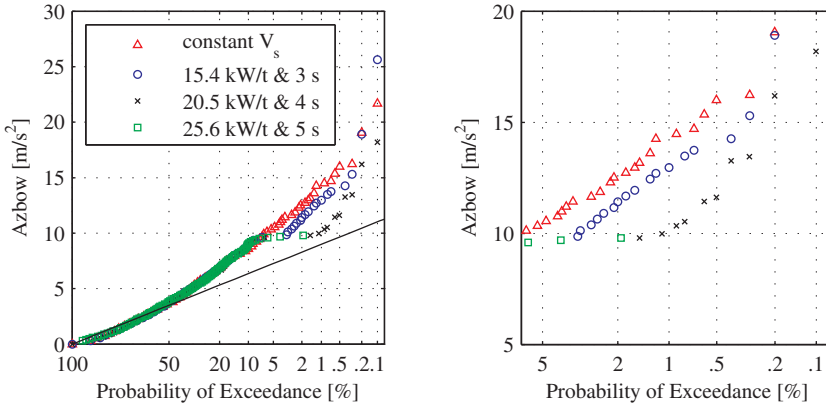


Figure 3.17: Rayleigh plot of the vertical accelerations at the bow, showing the influence of maximum speed reduction before impact

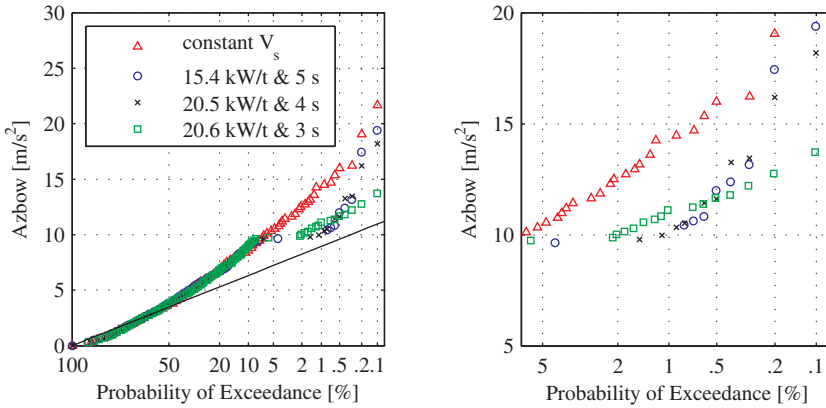


Figure 3.18: Rayleigh plot of the vertical accelerations at the bow for a maximum speed reduction before impact of 5 m/s

Figure 3.18 shows the distributions of the vertical peak accelerations at the bow where the maximum speed reduction was more or less equal. The combinations specific power and prediction window of 15.4 kW/t and 5 s, 20.5 kW/t and 4 s, and 20.6 kW/t and 3 s resulted in a maximum speed reduction of respectively 5.2, 5.5 and 5.1 m/s. The reduction of the acceleration level is clearly visible. For a lower specific

power, however, there is a higher chance that a large peaks still occur. A higher deceleration capacity is probably more beneficial to eliminate the extreme values.

From Tables 3.2 and 3.3 and from Figures 3.16 and 3.18 it can be concluded that for a maximum speed reduction greater than 5 m/s a significant better seakeeping behaviour could be established. The level of accelerations has been decreased, while the average forward speed was more or less equal. In most cases, however, not all unacceptable vertical peak accelerations were counteracted. For very large maximum speed reductions (here $\geq 6.5\text{ m/s}$) automated proactive thrust control is able to counteract all vertical peak accelerations above the preset criterion (optimal functionality).

3.6 Conclusions

Based on the results generated with this conceptual model it can be concluded that a reduction of the vertical accelerations can be expected if automated proactive thrust control has been applied on board of a planing monohull. The level of accelerations above the criterion decreased for increasing specific power and increasing prediction windows. For large maximum possible speed reduction before impact all vertical peak accelerations are counteracted (optimal functionality). The dependency of the average forward speed on variations of the specific power and the prediction window was small. It can be concluded that the reduction of the vertical acceleration level is more when a large speed reduction before impact can be realised. If the time to decelerate was limited, when for example a considerable time delay exists, the reduction was nil.

From the results generated in this chapter follows the hypothesis that:

Using automated proactive thrust control the vertical acceleration level on board of a planing monohull sailing in head seas can be reduced, if sufficient time to decelerate to a sufficiently low speed before impact is available, provided that the vertical peak accelerations are estimated accurately.

The required minimum amount of speed reduction before some effect on the vertical peak accelerations is noticeable is largely dependent on the nonlinearity of the response of the ship. The variables that determine the nonlinearity of the response are the sea state, the ship's geometry, the ship's inertia (mass and mass moment of inertia) and the desired forward speed (see Figure 3.1). They determine whether an unacceptably large vertical peak acceleration is likely to occur (related to rate of change of nonlinear hydromechanic lift force and nonlinear wave excitation). These variables could not be varied in the conceptual model (see Section 3.2). The nonlinearity of the response was therefore fixed.

The specific power of the ship under consideration determines the maximum possible deceleration. The required minimum amount of speed reduction, while sailing at a certain desired forward speed, and the deceleration determine the minimum net time

interval required to decelerate. In other words, they determine the required length of the prediction window.

It may therefore be stated that the order of magnitude of the independent variables ship, sea state and desired forward speed in relation to the maximum speed reduction within the prediction window (minimum possible value of the control variable) are important variables regarding the performance of automated proactive thrust control. They determine to what extent the vertical acceleration level can be reduced.

In the conceptual model it has been assumed that the predicted response was equal to the presumed actual response. The vertical peak accelerations were therefore 100% accurately predicted. The amount of thrust reduction, if an unacceptable vertical peak acceleration has been predicted, is based on its estimated magnitude. If the vertical peak accelerations are not predicted with a certain degree of accuracy, incorrect amount of thrust reductions may be applied. The reduction of the level of accelerations is expected to diminish.

Chapter 4

Idealised model of automated proactive thrust control

In the previous chapter it was shown that a reduction of the vertical acceleration level can be expected when automated proactive thrust control is applied on board of a planing monohull sailing in head seas. Parameters that determine the nonlinearity of the response (ship, sea state and desired forward speed) were not varied. The influence of the accuracy of the response predictions was not addressed either. The purpose of this chapter is to show to what extent the vertical accelerations are expected to be reduced when automated proactive thrust functions in more realistic conditions on board of a planing monohull sailing in head seas.

Section 4.1 explains the idealised model of automated proactive thrust control used in this chapter. More background to the computational model used for calculating the response, which replaces the elementary model, is given in Section 4.2. The input to the calculations is given in Section 4.3 and Section 4.4 illustrates the applicability of this idealised model. Section 4.5 discusses the influence of the minimum attainable speed before impact on the reduction of the level of accelerations. Section 4.6 shows the influence of inaccurate response predictions, including the influence of the calculation time step. In Section 4.7 conclusions are drawn based on the generated results.

4.1 Setup idealised model

This idealised model of automated proactive thrust control has been setup:

- To show the level of reduction possible with automated proactive thrust control;
- To show the influence of inaccurate response predictions on the expected reduction of the level of accelerations;

The response has been calculated using a computational model for calculating the response of a planing monohull sailing in head seas. The surge equation of motion in this model is a function of forward speed only (see Section 2.2.2). The relation between bridge handle and thrust force has been modelled as one to one (see Section 2.2.1). Calculation time (time delay) has not been taken into consideration; The response predictions do not consume time. Furthermore, the incoming wave and instantaneous forward speed, heave and pitch motion at the beginning of a response prediction are assumed to be known (see Section 2.4).

To show the level of reduction possible with automated proactive thrust control simulations have been carried out in an ideal setup: The predicted response is equal to the presumed actual response. The generated results show the relation between the desired forward speed, the maximum speed reduction before impact (dependent on prediction window) and the reduction of the vertical accelerations and the average forward speed during a trip. The time interval required for deceleration for the chosen benchmark ship (having a certain specific power) and the corresponding required maximum speed reduction before impact for which a significant reduction of the vertical acceleration level may be expected are estimated.

In reality it is expected that the response predictions are not 100% accurate. The computational model might not provide satisfactory results and/or the input to the model is incorrect (inaccurate measurement incoming wave and instantaneous forward speed, heave and pitch motion, see Section 2.4). Therefore, simulations are also carried out for the case where the predicted vertical peak accelerations were assumed to be over- and underestimated compared to the presumed actual peaks. The chosen calculation time step influences the accuracy of the predictions. On the other hand, a large time step benefits the calculation time required to predict the response (see Section 2.4). Simulations using a range of calculation time steps are therefore also carried out. These simulations address the effect of the accuracy of the predictions of the vertical accelerations in relation to the reduction of the level of accelerations possible with automated proactive thrust control.

Figure 4.1 depicts the independent, control and dependent variables associated with automated proactive thrust control. The results in this chapter were generated using a benchmark ship. The specific power of the benchmark ship was a constant. The results were generated for a range of prediction windows, resulting in a range of maximum speed reductions before impact. A time interval between two predictions has been chosen. The time interval available for speed reduction is always smaller or equal to the prediction window: $T_{pw} - t_p < T_{dw} \leq T_{pw}$ (see Figure 4.2). t_p is the frequency at which the real-time simulations are performed (see Section 2.3).

In Figure 4.3 an overview of the idealised model of automated proactive thrust control is depicted. The computational model used for the simulations includes the influence of the ship, sea state and forward speed on the response. The specifications of the ship under consideration are incorporated in the input for the computational model.

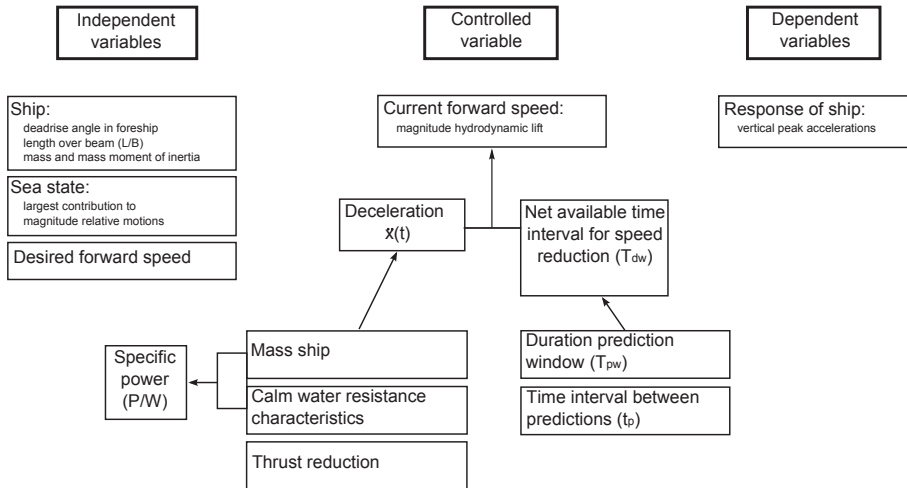


Figure 4.1: Variables associated with automated proactive thrust control

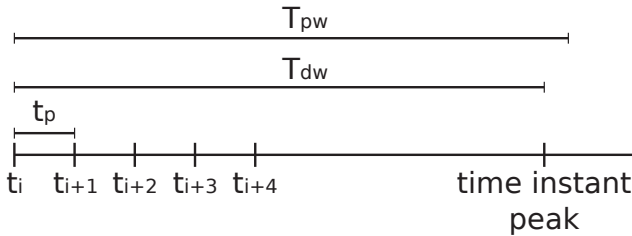


Figure 4.2: Time line with respect to response predictions

The response is calculated in two parts. First, on time t_i the response will be predicted for the duration of the prediction window using the computational model. This is done in a separate calculation loop (top figure in Figure 4.3). If thrust control is required, the response will be predicted for a number of thrust reductions (see also Section 2.3). The relation between the thrust force and the corresponding predicted vertical peak acceleration will be determined (see Figure 4.4). The largest possible thrust for which the predicted vertical peak acceleration meets the criterion is chosen. Last, the presumed actual motions are calculated for t_p s using the chosen control setting (bottom figure in Figure 4.3). This process repeats itself on $t_{i+1} = t_i + t_p$. Each time the response has been predicted and the presumed actual motions are calculated the moment in time is frozen. The response predictions and the calculation of the presumed actual response are carried out separately, because when the influence of the accuracy of the predicted vertical peak accelerations is analysed the predicted vertical peak accelerations differ from the presumed actual ones.

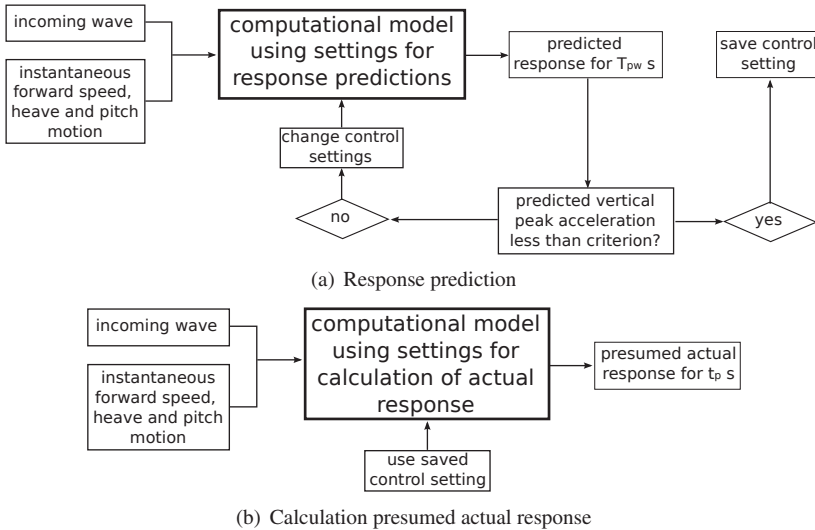


Figure 4.3: Overview idealised model

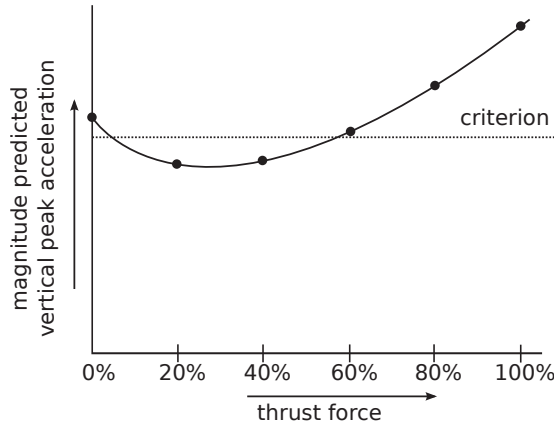


Figure 4.4: Example of determined relation between thrust reduction and predicted vertical peak acceleration

4.2 Used computational model

4.2.1 Applicability

The computational model should describe the nonlinear response of a planing mono-hull sailing in head seas (see Section 2.2.3). In the current setup it is not necessary

to predict the response faster than real-time; the calculation time is assumed to be zero. For model tests (Chapter 5) and for the future real case scenario, however, a short CPU time is required. The actual parameters determining the nonlinear seakeeping behaviour (the mass and geometry of the ship, the forward speed, the hydrodynamic lift, the nonlinear wave excitation and the dependency of the wave exciting forces and hydrodynamic reaction forces on the large relative motion amplitudes and the time dependent hull shape) need to be incorporated in this model. It must be able to calculate large vertical peak accelerations, with their typical short duration of 0.1 to 0.2 s.

Computational models used for simulating the behaviour of a planing monohull in head seas are either based on 2-dimensional strip theory or 3-dimensional panel methods. To account for the large changes in wetted length, pitch angle and consequently the under water hull shape the force integration to be carried out in the time domain.

3-dimensional simulation models for calculating the motions of a fast ship in waves exists, but they mostly require too much calculation time for the purpose of this study. For example, even for a simplified version of the 3-dimensional time domain panel method simulation model explained by Van Walree (1999) and De Jong (2011), where memory effects are neglected, the calculation time is too large for the purpose of pro-active control (slower than real-time). Moreover, at this point it is unable to predict the peaks in the vertical acceleration, which is essential for automated proactive thrust control (Recommendations with respect to an impact model are given by De Jong (2011, pages 205-207)).

2-dimensional simulation models require much less calculation time than 3-dimensional models. The nonlinear mathematical model of motions of a planing monohull in head seas developed by Zarnick (1978) and Keuning (1994) is based on strip theory and requires little calculation time. The CPU time depends on the number of stations in which the hull is divided and the time step used for the calculations, but generally speaking it is much faster than real-time. Moreover, this model is able to predict the short vertical peak accelerations. Figure 4.5 shows typical time-traces of the vertical accelerations at the bow for the SAR boat of the Arie Visser class, both measured and calculated. The measured time-traces were obtained during model tests. The encountered wave train was different for both situations. The figure clearly shows that the computational model is able to reproduce the typical shape of a vertical peak acceleration.

The computational model developed by Zarnick (1978) and Keuning (1994) calculates the response of a hard-chined monohull at a constant forward speed in 2 degrees of freedom (heave and pitch motion). The model is valid for a speed range of $F_{N\triangledown} \approx 1.5 - 4.0$. The equations of motion are solved in the time domain using Kutta-Merson integration scheme. For this study an extension to 3 degrees of freedom (surge motion) was required.

The effects of the forward speed, the hydrodynamic lift, the change in reference position, the irregularity of the waves and the dependency of the wave exciting forces and hydrodynamic reaction forces on the large relative motion amplitudes and the

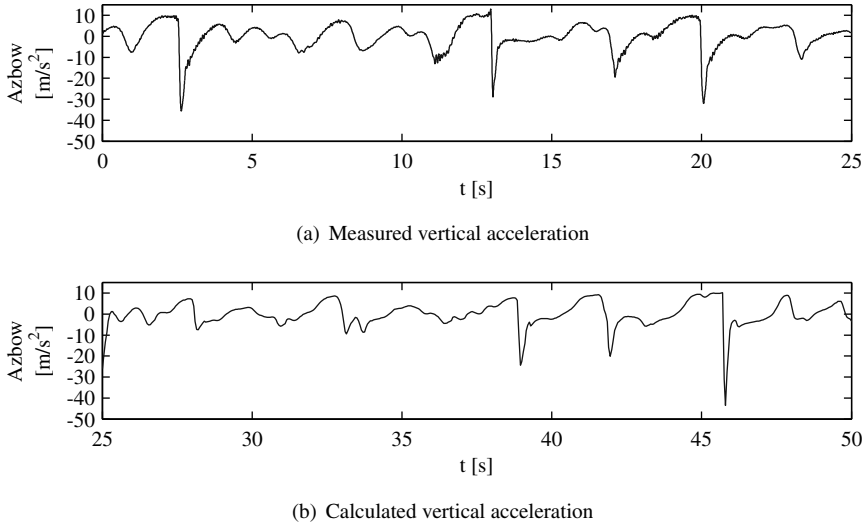


Figure 4.5: Typical time-traces of the vertical accelerations at the bow for the SAR boat of the Arie Visser class

time dependent hull shape are properly implemented Keuning (1994). The vertical accelerations are dependent of the ship's geometry, sea state and forward speed. The hull must be divided in an arbitrary number of transverse sections along the hull. If strip theory is used the assumptions are made that interaction effects within the 2-dimensional flows of the cross sections are negligible and thus that the hydromechanic forces, acting on the hull, can be approximated by integrating forces on the cross sections over the ship's length.

Zarnick used the theory of a calm water penetrating wedge for determining the forces acting on a cross section. When looking at a slice of water (no waves), a planing monohull passing through it is like a wedge penetrating the water surface with a constant velocity. The force acting on a calm water penetrating wedge consists of a hydrostatic component related to the displaced water (f_b) and a hydrodynamic part consisting of a component related to the change of fluid momentum and a viscous component (f_i). The water entry velocity of a cross section in calm water is equal to the velocity vector perpendicular to the keel. In waves, it gets additional contributions due to the heave and pitch motion.

The wave lengths are assumed to be large in comparison with the ship's dimensions ($\lambda/L \geq 1$) and the wave slope is assumed to be small (less than 6°). Because of the large wavelengths, diffraction forces can be neglected; only the Froude-Krylov forces are of importance. The nonlinear wave excitation is directly integrated in the expressions for hydromechanic forces and is caused by:

1. The geometrical properties of the wave, altering the total wetted length, the sectional wetted breadth and immersion;
2. The vertical orbital velocity;

Because the ships under consideration are generally shallow with respect to the height of the waves, the orbital velocity is taken at the undisturbed water surface in the plane $z = 0$.

For further details about this simulation model the reader is referred to Zarnick (1978), Keuning (1994) or Van Deyzen (2008).

4.2.2 Equations of motion

The coordinate system is defined as an earth fixed coordinate system with the x -axis lying in the undisturbed water surface pointing in the direction of the forward speed and a body fixed coordinate system with the origin in the centre of gravity of the ship and of which the ξ -axis is the longitudinal axis pointing forward. The z - and ζ -axes are pointing down. The total forces acting on a fast monohull using nonlinear strip theory are visualised in Figure 4.6.

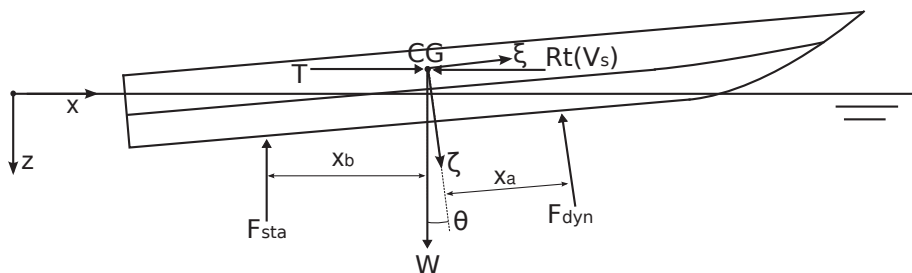


Figure 4.6: Definition of the total forces acting on the ship

The equations of motion are written as:

$$\begin{aligned}
 \text{Surge: } & M \cdot \ddot{x}_{CG} = \gamma \cdot T_{max} - Rt(V_s) \\
 \text{Heave: } & M \cdot \ddot{z}_{CG} = W - F_{dyn} \cos \theta - F_{sta} \\
 \text{Pitch: } & I \cdot \ddot{\theta} = F_{dyn} x_a + F_{sta} x_b
 \end{aligned} \tag{4.1}$$

in which F_{dyn} represent the total hydrodynamic force and F_{sta} the total hydrostatic force. These forces are found by integrating the sectional forces:

$$\begin{aligned}
 F_{dyn} &= \int_L f_l d\xi \\
 F_{sta} &= \int_L f_b d\xi
 \end{aligned} \tag{4.2}$$

in which f_l represents the sectional hydrodynamic lift and f_b the sectional buoyancy. The Froude-Krylov force is incorporated in the sectional forces.

The body fixed vertical acceleration can be written as:

$$A_{z_{bow}} = \ddot{\zeta}_{CG} - \xi_{bow} \cdot \ddot{\theta} \quad (4.3)$$

The current surge equation of motion does not include horizontal oscillations due to a surge force in waves (similar to the surge equation of motion of the elementary model, see Equation 3.6). Using a 2-dimensional theory, horizontal forces are difficult to model. A surge force will alter the path of the deceleration and consequently it may alter the speed reduction within the prediction window, but this has been disregarded (see Section 2.2.2).

4.3 Calculation input

Thrust control is effectively applied by operators on the SAR boat of the Arie Visser class (see Chapter 2). This ship is able to reduce speed quickly. Furthermore, research in to the hydromechanics has been carried out in the past at department of ship hydromechanics and structures at the Delft University of Technology. Much information about the hydromechanics of this ship is available. This makes the SAR boat of the Arie Visser class a good benchmark ship for the simulations. Table 4.1 presents the main dimensions and Figure 4.7 the linesplan (a photo was depicted in Figure 2.1).

Table 4.1: Specifications of the SAR boat of Arie Visser class

Designation	Symbol	Value	Unit
Length overall	L_{oa}	18.8	m
Length waterline	L_{wl}	14.5	m
Breadth overall	B_{oa}	6.1	m
Breadth waterline	B_{wl}	4.14	m
Draft	T	1.04	m
Displacement	∇	27.317	m^3
Mass	m	28	t
Longitudinal Centre of Gravity	LCG	6.10	m
Vertical Centre of Gravity	VCG	1.25	m
Radius of gyration y-axis	k	4.50	m
Moment of gyration y-axis	I	567	tm^2

A typical calm water resistance of the Arie Visser is depicted in Figure 4.8. The dashed curve (Rt_{meas}) was obtained during model tests. The calm water resistance

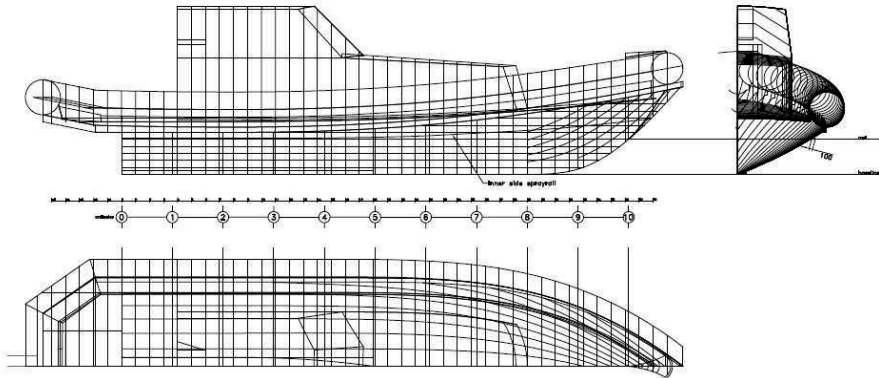


Figure 4.7: Linesplan SAR boat of Arie Visser class

for this ship is dependent on the displacement and the position of LCG , which for the curve depicted here were different than the values given in Table 4.1. For this study, however, a 3rd degree polynomial function for the calm water resistance, that approximates the typical shape of the calm water resistance curve, suffices. Therefore, the measured curve has been approximated by a 3rd degree polynomial function (solid line, Rt_{appr}) The minimum speed for which the calm water resistance was measured was 10 kts ($\sim 5 \text{ m/s}$). For this study, the resistance between 0 and 5 m/s is of minor importance and was therefore assumed to be linear. For a displacement of 27 t the effective specific power is 33 kN/t displacement.

In the present setup the moment in time is frozen, while the response is predicted and the presumed actual motions are calculated. In reality, the response predictions take time, which imposes a limit to the number of predictions that can be carried out before impact. It is believed that if automated proactive thrust control functions in reality only a few predictions could be carried out consuming little calculation time. Hence, in the present setup the discretization of the bridge handle positions used for the predictions was chosen to be 20%, instead of the 5% used in the conceptual model (see Section 3.3). So, the relation between thrust force and predicted vertical peak acceleration is based on 6 response predictions (see Figure 4.4). The time interval between two predictions was 0.5 s .

For the simulations in this chapter the criterion is set to 20 m/s^2 . The lengthwise position where the vertical accelerations were considered was 65% of the ship's length (at 9.6 m from the stern at the same height as the centre of gravity). A body fixed vertical acceleration is considered. Figure 2.5 presented the distributions of the vertical peak accelerations measured at 65% of the ship's length during the full scale trials with the

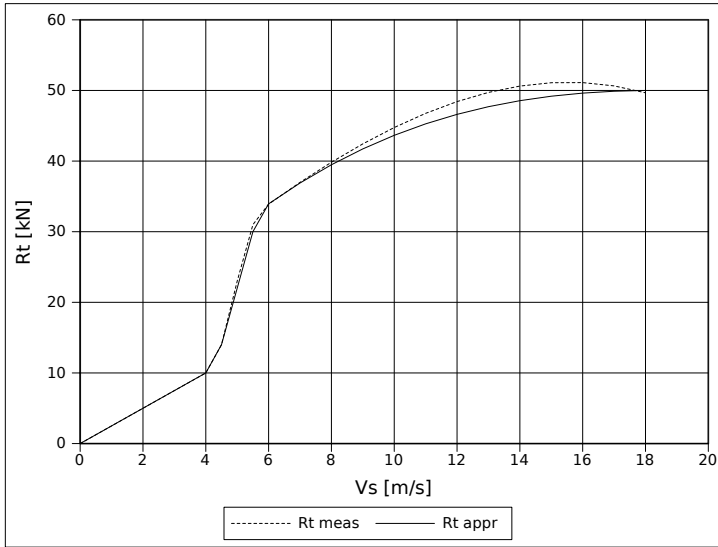


Figure 4.8: Typical calm water resistance SAR boat of Arie Visser class

SAR boat of the Arie Visser class. For the crew on board of the SAR boat of the Arie Visser class the maximum vertical peak acceleration lied somewhere between 15 to 30 m/s^2 at 65% of the ship's length, based on the limited number of trials.

The area of operation of the SAR boat of the Arie Visser class is the North Sea. Two combinations of a peak period, significant wave height and average forward speed were chosen:

1. A moderate sea state and high forward speed: $T_p = 5.0$ s, $H_s = 1.25$ m, 28 kts;
2. A rougher sea state and a moderately high forward speed: $T_p = 7.5$ s, $H_s = 2.15$ m, 20 kts;

The two sea states are typical for the North Sea (Hogben and Lumb 1967). The combinations of sea state and forward speed have been termed Condition 1 and 2.

A calmer sea state, where the ship is able to sail most of the time at its design speed and where most likely just a few thrust reductions will occur, is not very interesting. During full scale trials with the SAR boat of the Arie Visser class in calm sea states (not reported in Chapter 2) thrust control was not applied. The ship could sail safely at a high forward speed. Rougher sea states are interesting, but cannot be simulated in the present setup due to the limitations of the computational model. In the first place, short and/or steep waves cannot be simulated, as explained in Section 4.2.1. Secondly, in a rougher sea state the average forward speed will drop. Using thrust control, the

speed will probably fall below the lower speed boundary of the computational model ($F_{N\varphi} \approx 1.5$) too often. The generated results will become unreliable.

If results of simulations carried out with thrust control show that a lower level of accelerations could be realised using thrust control it may be concluded that this is valid for any moderate or rough sea state similar to the two simulated sea states. Automated proactive thrust control functions optimally if (nearly) no vertical accelerations smaller than -20 m/s^2 occur.

The influence of the desired forward speed has been addressed as well. For Condition 1, the range of desired forward speeds was equal to 28, 30, 32 and 34 *kts* and for Condition 2 20, 22, 24 and 26 *kts*. It is expected that the desired forward speed affects the number of thrust reductions, the level of accelerations and the average forward speed.

The wave spectrum was irregular, built up out of 100 components with random phases ($d\omega = 0.025 \text{ rad/s}$). A Jonswap spectrum was used. Using various sets of random phases a number of wave realisations was generated. The repetition time of the wave train for a ship sailing in head seas is dependent on the forward speed (see Appendix B). For a forward speed of 30 *kts* (15.43 *m/s*) and a frequency step of 0.025 *rad/s* the wave train the ship encounters is unique for 6500 *s*; for a forward speed of 20 *kts* (10.28 *m/s*) it is unique for 9500 *s*. This is true provided that the forward speed is constant. The corresponding repetition distance is for both conditions nearly equal to 100 *km*.

The distribution of the vertical peak accelerations depends on the chosen simulation time and on the encountered wave train. The encountered wave train depends on the chosen wave realisation and the travelled path of ship. When using thrust control, this path depends on the chosen thrust reductions. For an accurate determination of the distribution of the vertical peak accelerations for the chosen simulation time, especially at low probabilities of exceedance (less than 5%), simulations in a number of wave realisations were required.

The run length was 2500 *s* (42 minutes) for Condition 1 and 4000 *s* (67 minutes) for Condition 2, corresponding with a total number of approximately 2000 counted peaks for the vertical acceleration at the bow for both conditions.

The calculation time step was equal to 0.025 *s*, except for the simulations where the influence of the time step was analysed. A convergence study showed that results generated with a smaller time step (0.01 *s*) were equal to the results generated with a time step of 0.025 *s* for both conditions. Figure 4.9 shows the influence of the calculation time step on the calculated response. These distributions were generated using a constant forward speed of 28 and 20 *kts* respectively.

A range of maximum speed reductions was realised using a range of prediction windows. Table 4.2 depicts the maximum speed reduction within the prediction window, starting from the desired speeds of 30 and 20 *kts* respectively, assuming a 100%

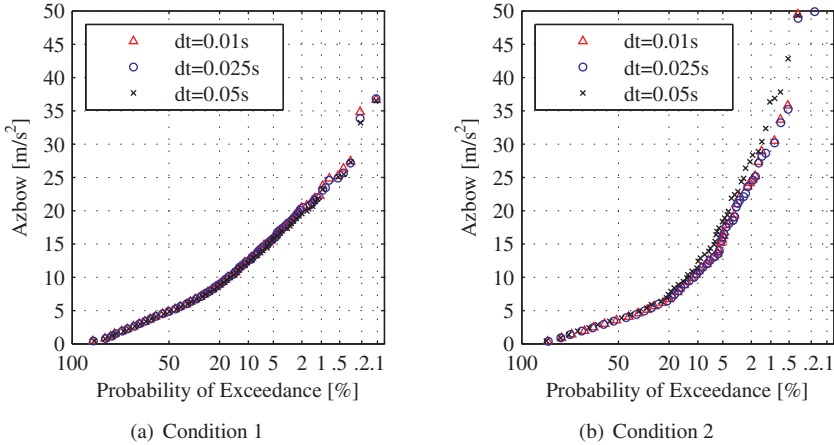


Figure 4.9: Rayleigh plots of the vertical accelerations, showing the influence of the calculation time step on the calculated response

thrust reduction and $T_{dw} = T_{pw}$). The maximum decelerations (\ddot{x}_{max}) are also given. The maximum speed reduction is greater when the deceleration starts from 30 *kts* due to larger maximum deceleration and specifically due to the low gradient of the calm water resistance curve at that speed (see Section 2.2.2). The maximum speed reductions before impact cover a realistic range. The speed reductions observed during the full scale trials on this ship varied between 2 to 10 *kts* (see Section 2.1.2). Larger speed reductions have also been simulated in this chapter in order to show the effect of a sufficiently large speed reduction. A prediction window of 1 *s* has been omitted, because the time interval for deceleration becomes too small ($T_{pw} - t_p \leq T_{dw} \leq T_{pw} \Rightarrow 0.5 \leq T_{dw} \leq 1$). This yields a negligible speed reduction before impact.

Table 4.2: Maximum possible speed reduction within prediction window

Condition	P_e/m [kW/t]	V_o [kts]	\ddot{x}_{max} [m/s ²]	T_{pw} [s]:					
				2	3	4	5	6	
1	33	30	-1.8	5.1	8.4	11.4	14.3	16.9	[kts]
2	33	20	-1.6	4.6	7.2	9.5	11.0	11.9	[kts]

To establish the reduction of the vertical acceleration level using automated proactive thrust control set of two simulations are carried out for each simulated condition:

1. A simulation with thrust control;

2. A simulation at a constant forward speed equal to the average forward speed found during the simulation with thrust control;

The generated results are compared with respect to the percentage of vertical peak accelerations above the criterion and the level of accelerations (visualised using a Rayleigh plot).

To show whether automated proactive thrust control reduces the vertical accelerations the level of accelerations has been compared between 5 and 0.5% probability of exceedance. A probability of 5%, the higher boundary of the probability range of interest, corresponds with the 100 largest peaks. A probability of 0.5%, the lower boundary, corresponds with the 10 largest peaks, occurring on average approximately each 5-6 minutes. The occurrence of a limited number of very large peaks does not prove whether or not the vertical accelerations were reduced using automated proactive thrust control. The reduction of the vertical accelerations between 5 and 0.5% provide sufficient information to what extent the level of accelerations was reduced. Although extreme values are considered the limiting factor for the operability of a planing monohull sailing in head seas, they were not used to compare the outcome of the simulations with the idealised model of automated proactive thrust control.

4.4 Applicability idealised model

The equations of motion in the computational model should describe the nonlinear seakeeping behaviour of a planing monohull sailing in head seas. The relation of the vertical accelerations with the amplitude of the incoming wave should be nonlinear, yielding large vertical peak accelerations. Their magnitude should be speed dependent. Thrust reductions should yield realistic speed reductions and reduced vertical peak accelerations.

Typical time-traces of the calculated motions and accelerations using thrust control are given in Figure 4.10 (for comparison with the time-traces generated with the conceptual model, see Figure 3.13). The calculated vertical peak accelerations show the typical short duration of the vertical peak accelerations. It also that it takes significantly more time to accelerate than to decelerate. This is because of the low gradient of the resistance curve (see Section 2.2.2, Figures 2.11 and 2.13). Two thrust reductions were required in the first 100 s. The speed reductions were 10 and 7 *kts* respectively, one with a 100% thrust reduction, the other with a 60% reduction. The two vertical peak accelerations were diminished to a value less than the criterion of 20 m/s^2 . The thrust reduction between 80 and 86 s is probably a sequence of two reductions for two peaks. Figure 4.11 shows the peaks when the ships would have sailed at a constant speed of 28 *kts*. The effect of temporary speed reductions on the magnitude of the vertical peak accelerations is distinguishable.

Figure 4.12 shows the distributions of the vertical peak accelerations of simulations carried out at a constant forward speed. In the first sea state the simulated speeds

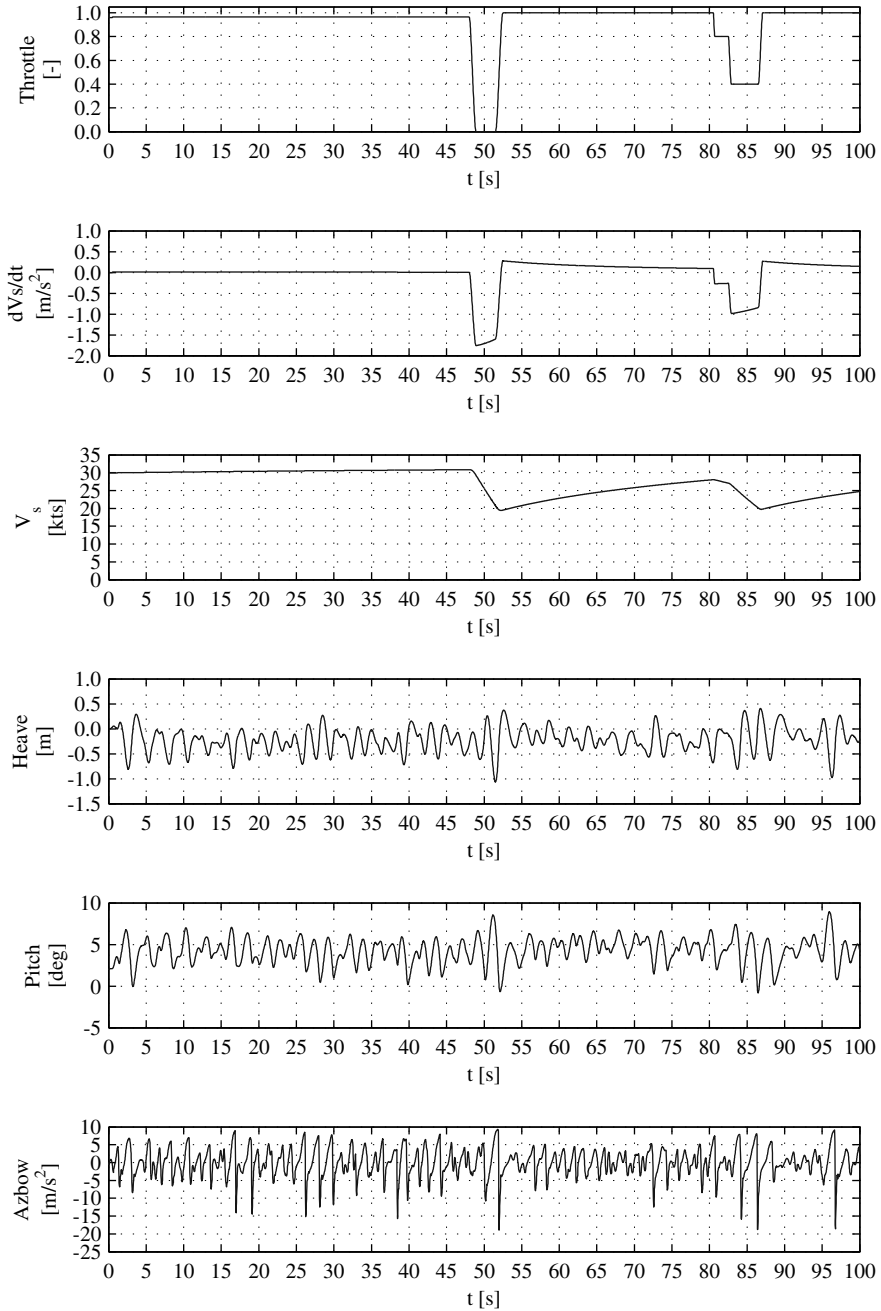


Figure 4.10: Typical time-traces of the calculated response using thrust control (Condition 1, $T_{pw} = 4$ s)

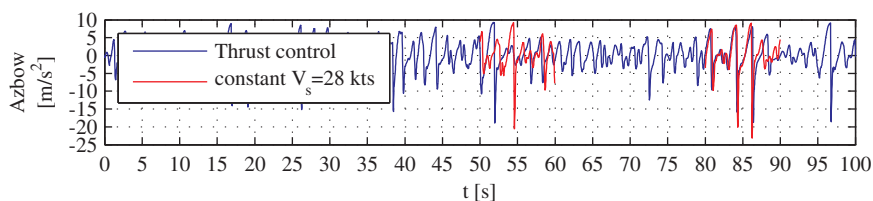


Figure 4.11: Comparison vertical accelerations at the bow

were 24, 28 and 32 *kts*, in the second 16, 20 and 24 *kts*. The positive peaks of the calculated signal were omitted in this figure since only the troughs (vertical accelerations upwards) were considered. The wave amplitudes were Rayleigh distributed. The straight lines, representing a linear relation with the amplitude of the incoming wave, correspond with a forward speed of respectively 28 and 20 *kts*. The nonlinearity of the response, as well as the speed dependency of the level of accelerations, is visible. The response of the ship in Condition 2 was more nonlinear to the amplitude of the incoming wave due to the larger relative motions in the higher sea state.

The time-traces given in Figure 4.10 and the Rayleigh plots depicted in Figure 4.12 show that the computational model represents the nonlinear seakeeping behaviour of a planing monohull very well. It is a valid approach for estimating to what extent the vertical accelerations can be reduced if automated proactive thrust functions in reality on board of a planing monohull.

The time-traces given in Figure 4.10 shows that the computational model calculates vertical peak accelerations. Figure 4.11 shows that a temporary speed reduction yields a diminished vertical peak acceleration. The Rayleigh plots depicted in Figure 4.12 shows that the calculated response is nonlinear to the amplitude of the incoming wave. It is also speed dependent. The idealised model of automated proactive thrust control, using the computational model developed by Zarnick (1978) and Keuning (1994) as a representation for the response of a planing monohull sailing in head seas, is therefore an applicable approach to show to what extent the vertical accelerations can be reduced when automated proactive thrust control is applied on board.

4.5 Influence of automated proactive thrust control in ideal situation

4.5.1 Influence wave realisation

At low probabilities of exceedance (less than 5%) the magnitude of the vertical acceleration may show a large dependency on the encountered wave train. Using a number of wave realisations the bandwidth of the distributions for the chosen simulation time

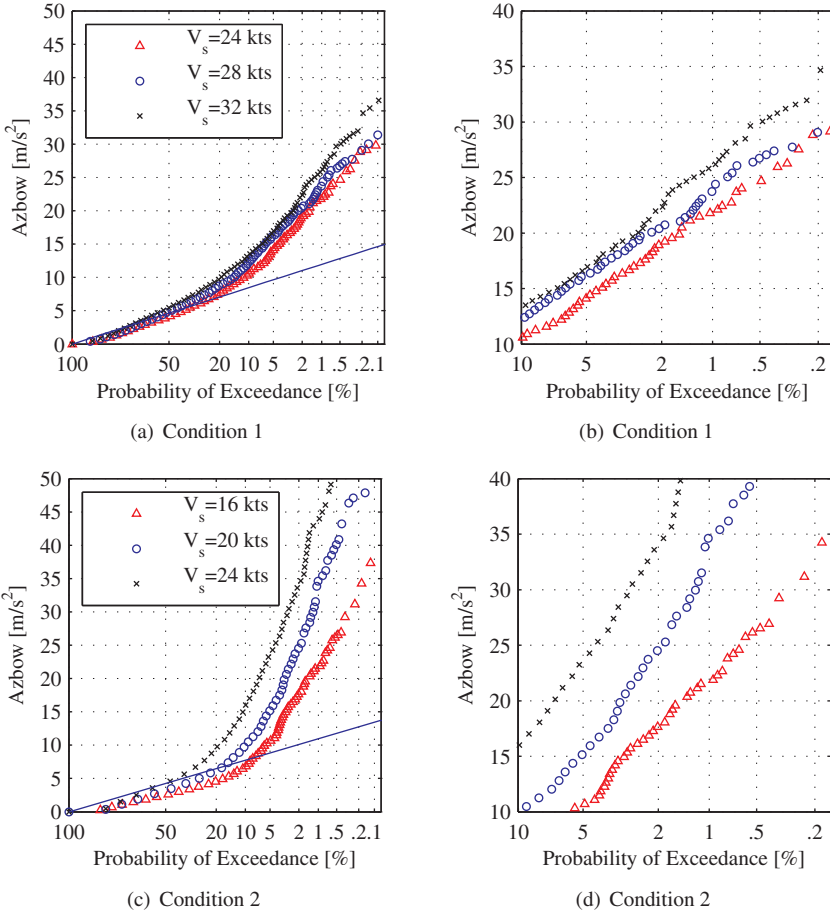


Figure 4.12: Rayleigh plots of the vertical accelerations at the bow, showing the influence of different constant forward speeds

can be determined. Distributions of the vertical accelerations have been generated for an increasing number of wave realisations. The range of values found at a probability of exceedance of 5 and 0.5% have been used to determine the minimum required number of wave realisations for which a fair comparison with the results generated using thrust control can be made. The largest differences between distributions based on various realisations may be expected when the simulation has been carried out at a constant forward speed. Large vertical peak accelerations are counteracted using thrust control.

The values of the vertical peak accelerations corresponding with a probability of

5 and 0.5% have been determined 6, 11 and 16 wave realisations for Condition 1 and 2. Throughout the rest of this chapter, if not stated otherwise, results based on wave realisation 1 have been plotted.

Tables 4.3 and 4.4 show the mean, minimum and maximum value at a probability of exceedance 5% and 0.5% based on 6, 11 and 16 wave realisations for both conditions. The results show that neither the mean values, nor the minimum and maximum peak value showed a large variation if more realisations were considered. The difference at a probability of 5% was small. 5% probability of exceedance corresponds with the largest 100 peaks. Statistically, another wave realisation has more effect on the extreme values, the largest 10 peaks (corresponding with a probability of exceedance less than 0.5%). The difference between the minimum and maximum value at 0.5% probability increased slightly, from 2.8 to 4.5 m/s^2 for Condition 1 and from 7.2 to 9.4 m/s^2 for Condition 2. The difference was larger for Condition 2, because the response of the ship was more nonlinear to the amplitude of the incoming wave (see Section 4.4). By coincidence, the minimum value for Condition 1 and the maximum value for Condition 2 remained equal for an increasing number of wave realisations. Adding up the simulated results based on more realisations implies that it is more likely that a smaller minimum or a higher maximum will be found.

Table 4.3: Minimum, mean and maximum vertical peak acceleration Condition 1 at 5% and 0.5% probability (constant forward speed of 28 kts)

$A_{z_{bow}}$ [m/s^2]	5%			0.5%		
	1-6	1-11	1-16	1-6	1-11	1-16
minimum	15.3	15.2	15.1	24.9	24.9	24.9
mean	15.9	15.7	15.7	26.8	26.5	26.8
maximum	16.3	16.3	16.3	27.7	28.2	29.4

Table 4.4: Minimum, mean and maximum vertical peak acceleration Condition 2 at 5% and 0.5% probability (constant forward speed of 20 kts)

$A_{z_{bow}}$ [m/s^2]	5%			0.5%		
	1-6	1-11	1-16	1-6	1-11	1-16
minimum	15.2	14.5	14.5	36.7	36.0	34.5
mean	16.0	16.0	15.9	40.5	40.1	39.7
maximum	16.3	17.4	17.4	43.9	43.9	43.9

Figure 4.13 shows the distributions of the vertical peak acceleration in Condition 1 and 2 at a constant forward speed of 28 and 20 kts respectively. The distributions calcu-

lated using three wave realisations are plotted, corresponding with the first realisation, the one yielding the lowest and the one yielding the highest level of accelerations. The minimum, mean and maximum peak value at a probability of 5 and 0.5% are plotted as well.

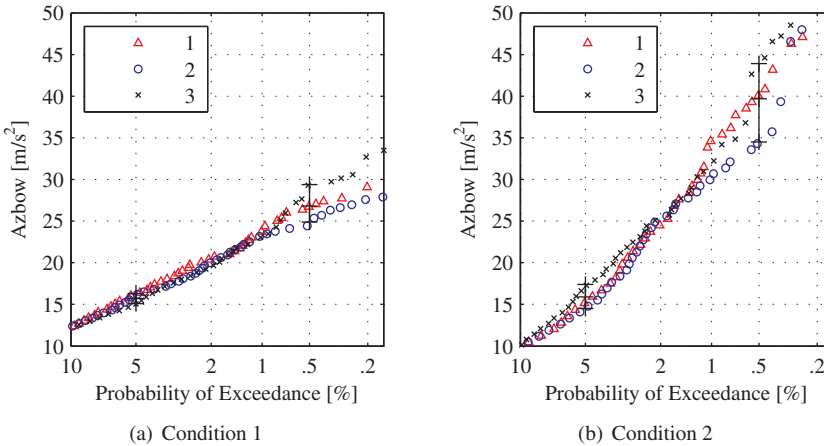


Figure 4.13: Rayleigh plots of the vertical accelerations at the bow, showing the influence of various wave realisations at a constant forward speed

The difference between the minimum and maximum peak value at a probability of 5% is negligible. The used number of wave realisations is of minor importance. The difference between the mean, minimum and maximum peak value at a probability of 0.5% for 6, 11 and 16 wave realisations was minimal (see Table 4.4). For a fair comparison between simulations at a constant forward speed and simulations using thrust control it is therefore save to use results of only 6 different wave realisations for the chosen simulations lengths.

4.5.2 Influence maximum speed reduction before impact

Figure 4.14 shows that the number of vertical peak accelerations greater than 20 m/s^2 decrease with increasing prediction window and thus with increasing maximum speed reduction before impact. The number is given as a percentage of the total number of peaks. The percentage found when simulating at a constant speed of 28 kts for Condition 1 and 20 kts for Condition 2 are depicted as well. The average forward speeds using thrust control, despite the duration of the prediction window, were nearly equal to these values. This figure is based on the first wave realisation. It is given to show that generally the number of vertical peak accelerations greater than the criterion decrease with increasing maximum speed reduction before impact.

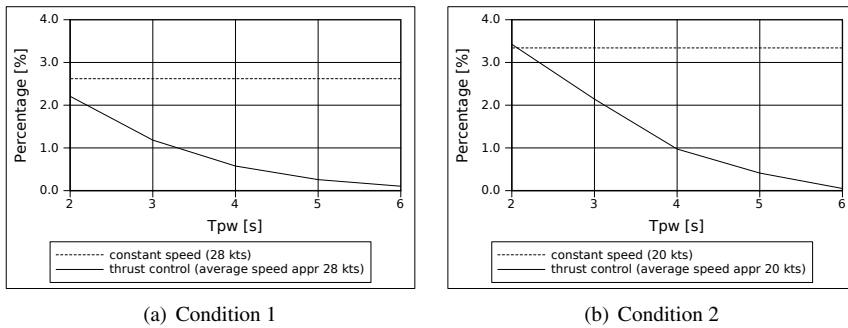


Figure 4.14: Percentage of vertical accelerations at the bow exceeding the criterion, dependent on prediction window

Automated proactive thrust control functioned optimally for a prediction window of 6 s for both conditions. All unacceptable vertical peak accelerations were counteracted using thrust control. The maximum speed reduction within the prediction window, however, starting from an initial speed of 30 *kts* was 16 *kts*; starting from 20 *kts* it was equal to 12 *kts*. The maximum speed reduction observed during full scale trials on this boat was 10 *kts*. A speed reduction more than 10 *kts* was often observed during simulations using a prediction window of 6 s. A prediction window less than or equal to 4 s corresponds values for the maximum speed reduction within the prediction window more in line with what was observed during the full scale trials. The maximum speed reduction is approximately 11 *kts* (see Table 4.2). For $T_{pw} = 2$ s the decrease of the number of unacceptable vertical peak accelerations was nil, but for $T_{pw} = 3$ and 4 s the percentage of vertical peak accelerations at the bow exceeding 20 m/s^2 has been decreased substantially.

The relative velocity between ship and incoming waves was approximately 20-25 m/s for both conditions. This implies that the wave should be measured over 120-150 m at the start of the response prediction to realise a prediction window of 6 s (excluding any time delays or lags). Over such a distance and time the dispersion of the wave might become an issue. To realise a prediction window of 4 s the wave should be measured over 80-100 m, for a prediction window of 3 s 60-75 m.

Figure 4.15 shows the distributions of the vertical peak accelerations for Condition 1 for various prediction windows. The distribution found using an equal constant speed of 28 *kts* is plotted as well. For a prediction window of 2 s the level of accelerations was comparable to the level found during a simulation at a constant forward speed of 28 *kts*. The reduction of the vertical accelerations was limited. For a prediction window of 3 s (not depicted) the level of accelerations was reduced more, approximately 1.5% of the peaks were greater than 20 m/s^2 . For a prediction window of 4 s the level of accelerations was decreased further; more or less 0.5% of the peaks

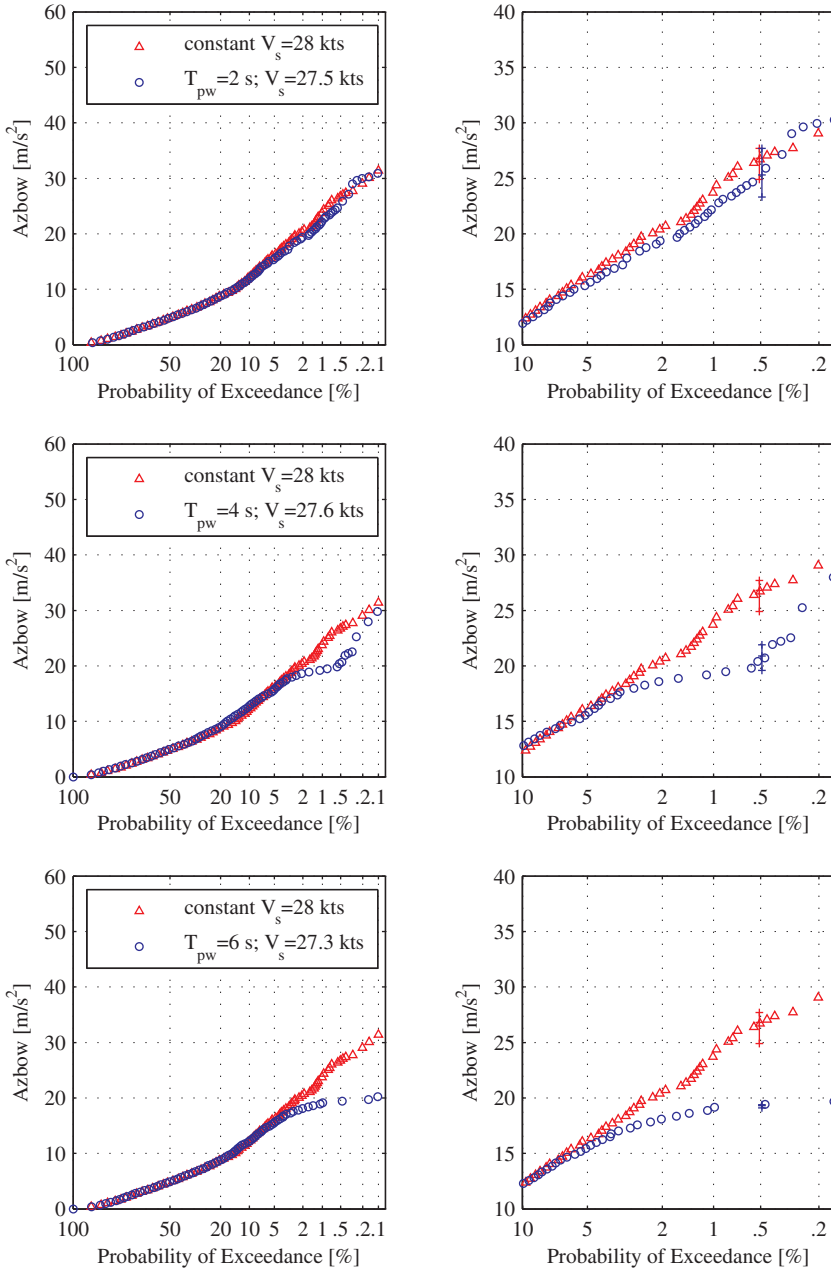


Figure 4.15: Rayleigh plots of the vertical accelerations at the bow, showing the influence of the prediction window (Condition 1)

were unacceptable. Comparing the distributions found at a constant speed of 28 *kts* and using thrust control, taking into account the influence of the wave realisation, it is clear that the level of accelerations has been decreased significantly. Automated proactive thrust control functioned optimally for a prediction window of 6 *s*. The difference between the minimum and maximum value found based on 6 wave realisations decreased for increasing prediction window. Large vertical peak accelerations are counteracted using thrust control. Hence, the chosen wave realisation has less effect on the distribution.

The vertical acceleration level for Condition 1 could be reduced significantly for a prediction window greater than or equal to 4 *s* (equivalent to a maximum speed reduction greater than 11 *kts*). For a prediction window of 3 *s* (equivalent to a maximum speed reduction of approximately 8 *kts*) the reduction was sufficient.

Figure 4.16 shows the distributions of the vertical peak accelerations for Condition 2 for various prediction windows. The distribution found using an equal constant speed of 20 *kts* is plotted as well. For a prediction window of 2 *s* no decrease of the level of accelerations was realised. The level of accelerations was approximately equal to the one found during a simulation at a constant forward speed of 20 *kts*. For a prediction window of 4 *s* the level of accelerations was reduced more significantly, approximately 1% of the peaks were greater than 20 m/s^2 . The variation of the peak value at a probability of 0.5% due to various wave realisations was large, but the values found at 1% were nearly equal. All unacceptable vertical peak accelerations were also counteracted using thrust control for a prediction window of 6 *s*.

The vertical acceleration level for Condition 2 could be reduced significantly for a prediction window greater than or equal to 4 *s* (equivalent to a maximum speed reduction greater than 9 *kts*).

In this condition the required prediction window was 4 *s* compared to 3 *s* for Condition 1, before a significant reduction of the vertical acceleration level was found. Using the current modelling of the surge equation of motion, the corresponding required time interval available for deceleration depends on the desired forward speed. The desired forward speed in Condition 2 is lower than in Condition 1. The absolute magnitude of the resistance force at a desired forward speed of 20 *kts* is less than at 30 *kts*, yielding a smaller deceleration once the thrust has been reduced. Moreover, the gradient of the calm water resistance curve at a desired forward speed of 20 *kts* of this particular boat is high; the deceleration diminishes quickly once the speed reduces. Therefore, the required time to decelerate increases. The required speed reduction before impact for Condition 2 was in the same order of magnitude as for Condition 1 (approximately 9 *kts*).

If a significant time delay exists (eg. calculation time), the time to decelerate may quickly reduce to 2 *s*. The reduction of the vertical accelerations for a prediction window of 2 *s* was nil for both conditions. The level of accelerations found is comparable to the level found at an equal constant forward speed. Short, temporary speed

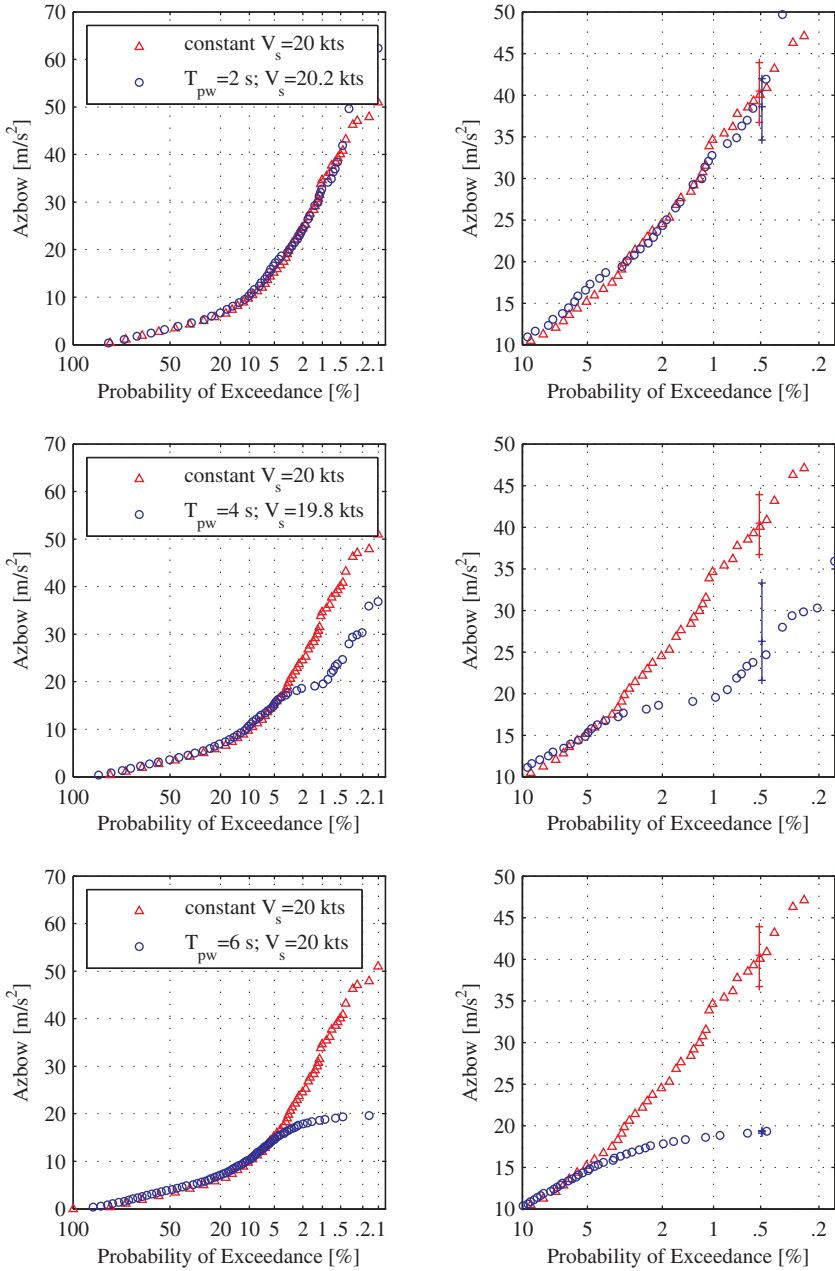


Figure 4.16: Rayleigh plots of the vertical accelerations at the bow, showing the influence of the prediction window (Condition 2)

reductions have no effect on the magnitude of the next vertical peak acceleration. The maximum peak value found at a probability of 0.5% based on 6 wave realisations was not larger when thrust control has been applied (see top of Figures 4.15 and 4.16). The mean value at a probability of exceedence of 0.5% was lower if thrust control was used. The extreme values at probability less than 0.5%, however, were larger. The encountered wave train may have been different. Or in some occasions the instantaneous heave and pitch motion were unfavourable and yielded high peaks. Top of Figures 4.15 and 4.16) do suggest that automated proactive thrust control does not increase the level of accelerations when the time to decelerate is limited. A few extreme values, however, may be increased. If the time to decelerate is small or even close to zero, the simulation is nearly equal to a simulation carried out at a constant forward speed.

The simulations in two conditions have shown that a reduction of the vertical accelerations can be realised using automated proactive thrust control. If the time to decelerate is 6 s or more all peaks could be kept below the predefined criterion of 20 m/s^2 .

In calmer sea states a significant reduction of the vertical accelerations is not to be expected. The ship is able to sail most of the time at close to its design speed. The relative motions are small. The number of unacceptably large vertical peak accelerations occurring during a trip is limited. Consequently, the number of required thrust reductions is limited. Temporary speed reductions are effective (the hydrodynamic lift is large due to the high forward speed), but since the number of thrust reductions is limited the possible reduction of the vertical acceleration level is probably limited.

A rougher sea state was not simulated due to the limitations of the computational model. The reduction of the vertical acceleration level is expected to diminish. The forward speed in such a sea state is not high, meaning that the hydrodynamic lift is relatively small. The magnitude of the lift is not expected to be decreased significantly, if the speed has been reduced. Consequently, the rate of change of the hydrodynamic lift has not been changed that much. Temporary speed reductions may have a limited effect on the next occurring vertical peak acceleration in very rough sea states.

Based on the calculated results for the SAR boat of the Arie Visser class in a moderate and rough sea state and based on the aforementioned reasoning an estimate of the expected reduction of the vertical peak accelerations dependent on sea state may be given. Figure 4.17 depicts a sketch of the relation between the expected reduction of the vertical peak accelerations and the sea state if automated proactive thrust control functions in reality. The dots on the solid lines represent the simulated conditions (Condition 1 and 2) for the Arie Visser. The reduction is measured against the vertical acceleration level at an equal constant forward speed (respectively 28 and 20 *kts*). The reduction of the vertical accelerations is dependent on the prediction window as depicted in Figures 4.14 to 4.16. The largest reduction may be expected in moderate to rough seas where the forward speed is high and where thrust reductions are applied frequently.

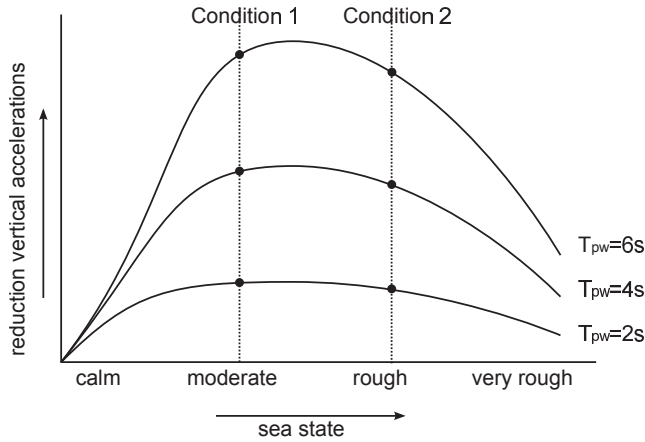


Figure 4.17: Expected relation between sea state and possible reduction of vertical acceleration level using automated proactive thrust control

Note to effect desired forward speed

The initially chosen desired forward speed is an important parameter regarding the performance of automated proactive thrust control. It is expected that the desired forward speed affects the number of thrust reductions, the level of accelerations and the average forward speed.

The results for Condition 1 and 2 showed that the number of thrust reductions depended on the condition and the prediction window. In Condition 1, the frequency of applying thrust control was one each 50 s, for all predictions windows. In Condition 2 it varied between one each 80 s to one each 60 s.

Table 4.5: Average forward speed and number of thrust reductions for a range of desired forward speeds

Condition						
1	$V_{s_{des}}$	28	30	32	34	[kts]
	\bar{V}_s	27.5	27.7	28.7	30.7	[kts]
	no.reductions	1/70	1/50	1/50	1/50	[1/s]
2	$V_{s_{des}}$	20	22	24	26	[kts]
	\bar{V}_s	19.8	21.7	22.3	22.7	[kts]
	no.reductions	1/80	1/45	1/40	1/30	[1/s]

Simulations in both sea states were also carried out for a range of desired forward speeds. The prediction window was equal 3 s for Condition 1; 4 s for Condition 2. For these prediction windows a significant reduction of the vertical accelerations was

realised, while the maximum speed reduction within the prediction window correspond with realistic values (maximum speed reduction approximately 9 *kts*, see Table 4.2). Table 4.5 shows the average forward speed found for both conditions, dependent on the desired forward speed. Figure 4.18 shows the distributions of the vertical peak accelerations for increasing desired forward speeds.

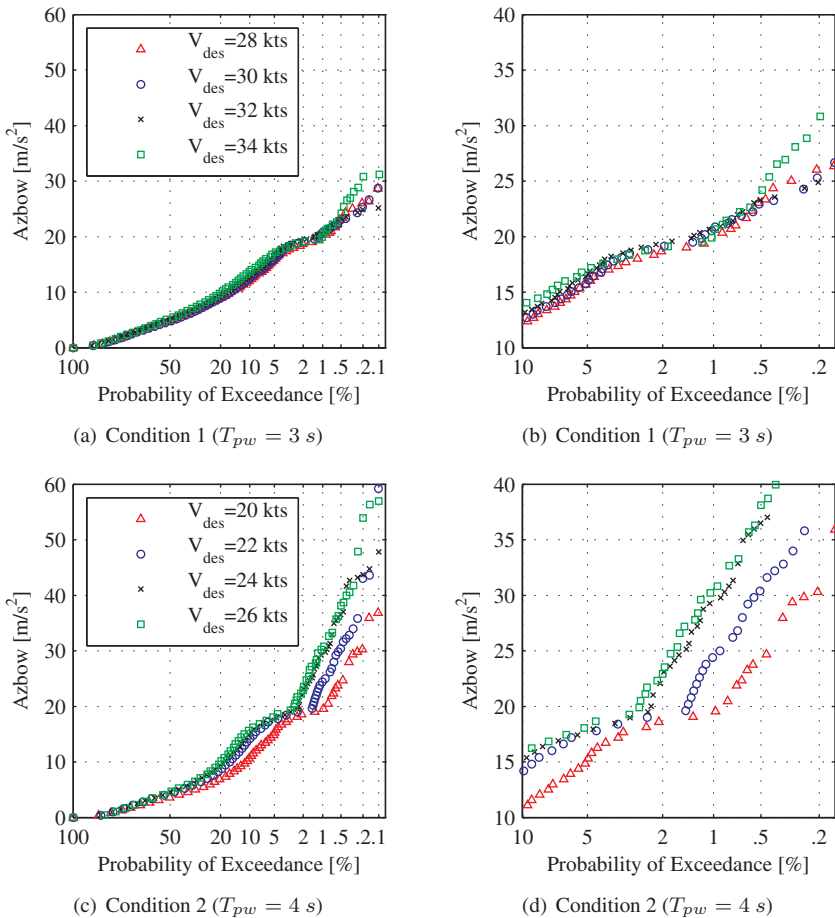


Figure 4.18: Rayleigh plots of the vertical accelerations at the bow, showing the influence of an increasing desired forward speed

The results show that the number of thrust reductions during the simulation increase for increasing desired forward speed. The average forward speed also increased with increasing desired forward speed. The difference between the desired forward speed and the average forward speed, however, becomes larger. The reduction of the vertical

accelerations becomes less compared to the initial situation. For higher desired forward speeds it is less likely that the required speed reduction before impact can be realised.

It can be concluded that the combination of sea state and desired forward speed is important and determines the frequency of the thrust reductions during a trip, the average forward speed and the final level of accelerations. For increasing desired forward speeds the number of thrust reductions, the average forward speed and the level of acceleration increase compared to the initial situation. The increased number of thrust reductions, however, puts a limit to the maximum average forward speed that can be attained during a trip.

The magnitude of the desired forward speed, however, can be considered an input parameter when automated proactive thrust control is applied in reality. Based on the experience and motivation of the crew an initial desired forward speed can be chosen. If during the trip it appears that in a certain sea state the level of accelerations is considered too high, reducing the desired forward speed would reduce the level of accelerations. If it appears that the trip is too comfortable an increase of the desired forward speed is possible. This measure, however, has a limited effect since a maximum average forward speed will be reached. If in that case it is still desired to sail faster larger value for the vertical acceleration can be chosen as criterion.

4.6 Influence of inaccurate response predictions

4.6.1 Influence accuracy of the predicted vertical accelerations

Real-time response predictions will most likely not provide results that are 100% accurate. For these simulations in this section the magnitude of the predicted vertical peak accelerations were multiplied by a constant factor, yielding either over- or underestimated peaks throughout the simulations. For overestimated vertical accelerations all predicted peaks were multiplied by 1.25; for underestimated vertical peak accelerations by 0.75. The results indicate the relation between the degree of accuracy of the predicted vertical peak accelerations and the reduction of the vertical accelerations and the average forward speed.

If peaks were overestimated the control system acted more often and the speed reductions were more (the amount of thrust reduction was more). The average speed dropped. For Condition 1 the average forward speed was reduced from 28 *kts* in the ideal situation (for all prediction windows) to 25.5 *kts* for $T_{pw} = 3$ s, 25.0 *kts* for $T_{pw} = 4$ s and to 24.5 *kts* for $T_{pw} = 6$ s. The number of thrust reductions was increased to nearly 1/30 s for all prediction windows (compare with Table 4.5). For Condition 2 the effect on the forward speed was nil; it remained 20 *kt*. The resistance at 20 *kts* and the gradient of the resistance curve were favourable to accelerate quicker than at a speed of 28 *kts*. Therefore, the speed loss due to more frequently applied

thrust reductions in case of overestimated peaks could be more easily counteracted. The speed was quicker restored to the desired speed. The number thrust reductions was increased to $1/40$ s for all prediction windows. If the peaks were underestimated the control system acted less often and the amount of thrust reduction was less. The number of thrust reductions was reduced significantly to less than once per 2 minutes for both conditions. The average forward speed was equal to the desired forward speed for both conditions.

The Rayleigh plots depicted in this section show what can be expected if the response predictions provide either over- or underestimated values for the next occurring vertical peak acceleration. It may also be that the accuracy of the response predictions show a certain randomization. The magnitude of the vertical peak accelerations is sometimes overestimated, sometimes estimated quite accurately and sometimes underestimated. The given distributions, therefore, mark the outer limits of the level of accelerations if an inaccuracy of 25% may be expected. The level of accelerations, if the peaks were sometimes overestimated, sometimes underestimated by 25%, would lie between the given distributions. The corresponding average forward speeds found also mark the lower and upper boundary of the average forward speed that may be expected. The actual average forward speed, if the peaks were sometimes overestimated, sometimes underestimated, would be somewhere in between.

These results were generated using one wave realisation (first realisation). A dependency of the given distributions on the encountered wave still exists. The results, however, are meant to show the general trend if the response predictions prove to be inaccurate.

Figure 4.19 shows the distributions of the vertical peak accelerations for both conditions for $T_{pw} = 4$ s. In each plot the distribution found in the previous section for that particular prediction window has been plotted together with the distributions when the vertical accelerations were 25% under- and overestimated. The difference is especially noticeable between the probability range of interest. If the vertical peak accelerations were overestimated, the level of accelerations for a probability between 5 and 0.5% decreased. If the vertical peak accelerations were underestimated, it increased. The upper limit for the latter case is the level of acceleration found during a simulation with an equal constant forward speed (no unacceptable vertical peak accelerations were predicted, so thrust control was not applied).

Figure 4.20 depicts the distributions of the vertical accelerations for $T_{pw} = 6$ s. The effect of inaccurate predicted vertical peak accelerations on the level of accelerations is even clearer here. Overestimation caused that the level of accelerations was reduced to approximately 16 m/s², as if that was a new criterion. Vice versa, for underestimated vertical peak accelerations the level of accelerations was increased to approximately 27 m/s².

The fact that a new upper limit for the level of accelerations was found if the vertical peak accelerations were assumed to be under- or overestimated can be explained as

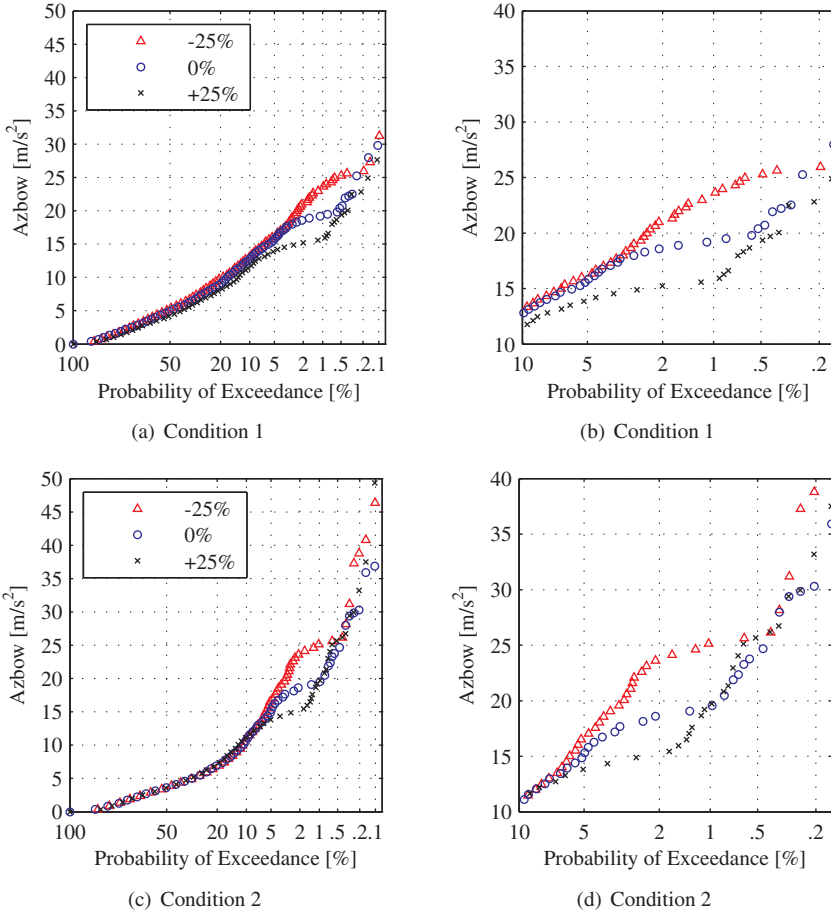


Figure 4.19: Rayleigh plots of the vertical accelerations at the bow, including the effect of inaccurate response predictions ($T_{pw} = 4$ s)

follows. The control system strives at keeping the vertical accelerations below the preset criterion of 20 m/s^2 . The 'new' criterion has an inverse relation with the assumed under- or overestimation of the vertical peak accelerations. If the assumed under- or overestimation of the vertical accelerations is equal to a , then the upper limit is equal to $1/(1+a) \cdot 20 \text{ m/s}^2$. So, a 25% overestimation yields a new criterium of 16 m/s^2 ($1+a = 5/4 \Rightarrow 4/5 \cdot 20 = 16 \text{ m/s}^2$). A 25% underestimation yields a new criterium of 27 m/s^2 ($1+a = 3/4 \Rightarrow 4/3 \cdot 20 = 27 \text{ m/s}^2$). Hence, the lower and upper limit if the peaks are predicted with a 25% degree of accuracy is respectively 16 and 27 m/s^2 . Consequently, it may be assumed that if the vertical accelerations are predicted with

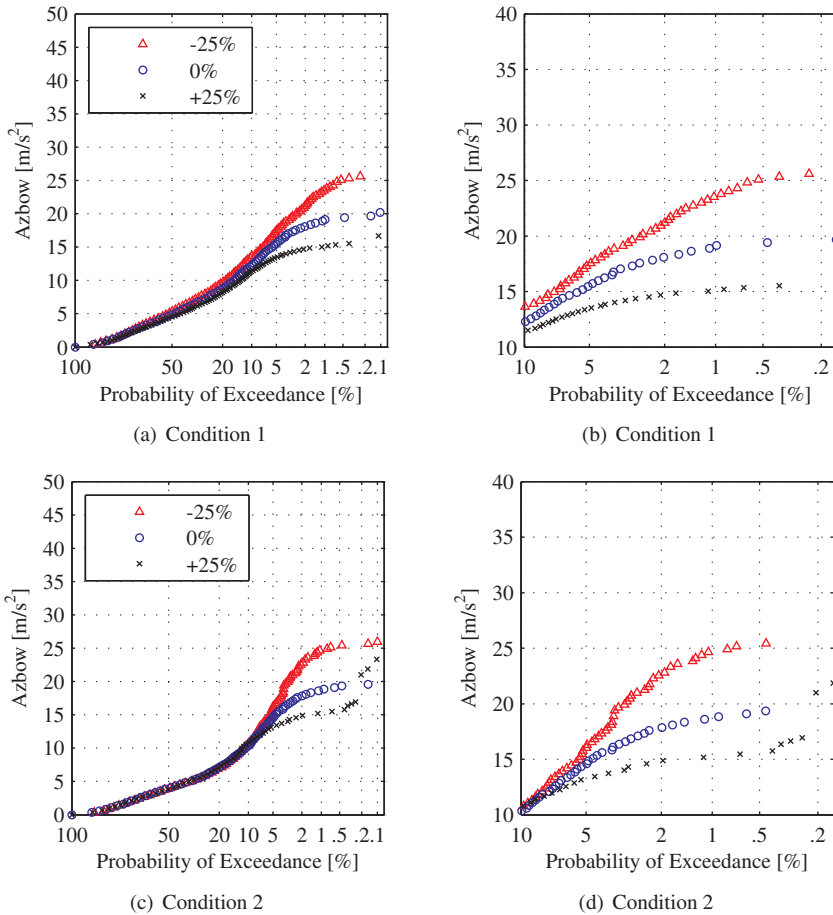


Figure 4.20: Rayleigh plots of the vertical accelerations at the bow, including the effect of inaccurate response predictions ($T_{pw} = 6 s$)

another degree of accuracy, the upper and lower limit of the distribution of the vertical peak accelerations may be found as explained (e.g. for 50% degree of accuracy: 13 and 40 m/s^2).

It appears that overestimated peaks yield larger and more frequently applied thrust reductions. Consequently the average forward speed drops. Underestimated peaks yield smaller and less frequently applied thrust reductions. Consequently the level of accelerations for a probability between 5 and 0.5% lies above the criterion. In both cases, the performance of automated proactive thrust control diminished compared to

the ideal situation, where the response predictions were 100% accurate (see Section 4.5.2). Either the level of accelerations for a probability between 5 and 0.5% lies above the criterion or the average forward speed decreases significantly.

4.6.2 Influence calculation time step

The chosen calculation time step influences the accuracy of the predictions. The influence hereof on the reduction of the vertical acceleration level was addressed using larger time steps for the response predictions than for the calculations of the presumed actual response. The presumed actual motions were calculated using a time step of 0.025 s. The results generated in this section show the effect if due to limited available calculation time a large time step is required. In the future, it might be that for a small calculation time step, say 0.01 s, the calculation time is sufficiently small. At present, this not yet the case.

Figure 4.21 shows the distribution of the vertical peak accelerations for a prediction window of 4 s for both conditions. For this duration a reduction of the vertical acceleration level may be expected if the predicted response is equal to the presumed actual response (see Section 4.5.2). For Condition 1, the difference between using a calculation time step of 0.025 and 0.05 s for the prediction of the response was small. The difference, if a time step of 0.10 s was used, however, was much greater. Many unacceptably large vertical peak accelerations were 'missed'. The time step used for the response predictions is in the same order of magnitude as the duration of the vertical peak accelerations. The frequency of thrust control was reduced to one each 80 s, compared to one each 50 s found previously. The average forward speed during this simulation was close to the desired forward speed of 30 *kts*. The reduction of the vertical acceleration level diminished. This Rayleigh plot is representative for all $T_{pw} \geq 3$ s in Condition 1. The effect of a large time step (peaks were 'missed') could not be counteracted by a larger prediction window.

The results for Condition 2 were similar. Using a time step of 0.05 s, the level of accelerations was increased slightly, but using a time step of 0.10 s for the response predictions, the level of accelerations was increased significantly compared to the ideal situation. The average forward speed was equal to the desired forward speed of 20 *kts*. This Rayleigh plot is also representative for all $T_{pw} \geq 4$ s in Condition 2. It can be concluded that the reduction of the vertical accelerations, as was estimated in Section 4.5.2, still may be expected if a time step smaller than 0.05 s would be used for the response predictions. Using greater time steps, the prediction of the vertical peak accelerations might be significantly incorrect. Many unacceptable peaks are 'missed'. As a result, the number of thrust reductions decreases, the average forward speed increases to the desired speed and the reduction of the level of accelerations quickly diminishes.

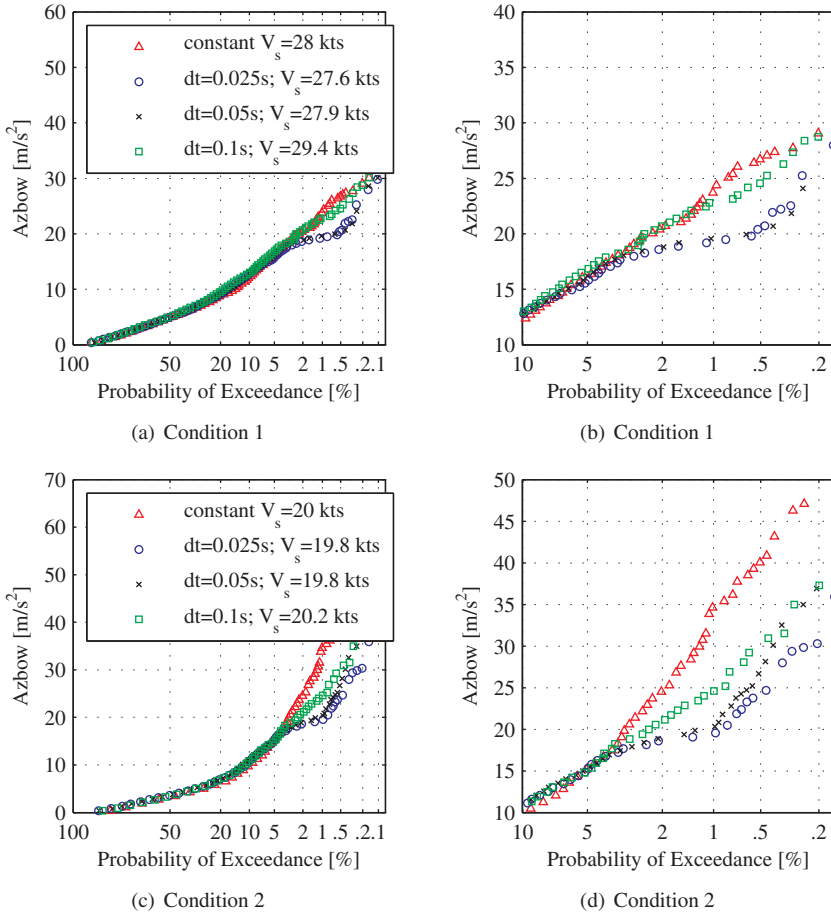


Figure 4.21: Rayleigh plots of the vertical accelerations at the bow, including influence calculation time step ($T_{pw} = 4$ s)

4.7 Conclusions

The simulations carried out in this chapter illustrate what the expected reduction of the vertical accelerations may be when automated proactive thrust control has been applied on the SAR boat of the Arie Visser class, having a specific power of 33 kN/t displacement. An idealised model of automated proactive thrust control has been used. An adequate computational model has been used for calculating the response of the Arie Visser in head seas. A time delay was not considered. The waves are assumed to be known. The reduction of the vertical acceleration level is dependent

on the time interval available for deceleration, the corresponding maximum speed reduction before impact, the sea state and the desired forward speed. The accuracy of the response predictions, also dependent on time step, also have an influence.

The generated results have shown that if sufficient time to decelerate to a sufficiently low speed, provided that the response is predicted accurately, a significant reduction of the vertical acceleration level can be realised using automated proactive thrust control (see also conclusions Chapter 3). Based on the ideal situation, a significant reduction of the vertical accelerations may be expected if automated proactive thrust control is applied on board of the SAR boat of the Arie Visser class if a speed reduction within the prediction window greater than 9 *kts* can be realised. The required time interval for deceleration is at least 3 *s*. For the simulated wave conditions this corresponds with a distance of 60-75 *m* over which the waves should be measured. For large prediction windows (6 *s* or more) automated proactive thrust control functions optimal. All vertical accelerations are kept below the predefined criterion of 20 m/s^2 at the bow. For smaller prediction windows the reduction of the vertical acceleration level quickly diminishes. Thrust control, however, does not increase the level of accelerations between 5 and 0.5% probability of exceedance.

An influence of the sea state on the reduction of the vertical accelerations exists. A moderate and rough sea state have been simulated. In moderate to rough sea states the reduction of the vertical acceleration level is significant, if sufficient time to decelerate is available. The number of thrust reductions increases. The forward speed is high. A significant hydrodynamic lift exists. By a temporary speed reduction, the magnitude of the hydrodynamic lift has been decreased, and so its rate of change when the fore ship submerges coming down behind the crest of the wave. In a calm sea state the reduction is expected to be limited due to the limited number of thrust reductions. The ship can sail safely at a high forward speed. Thrust control is not really necessary. In rough sea states high forward speeds cannot be attained. The hydrodynamic lift is small and so its rate of change. Temporary speed reduction have a limited effect on the vertical accelerations. It is expected that the reduction of the vertical acceleration level is limited when using thrust control in very rough sea states.

The chosen desired forward speed has an effect on the number of thrust reductions during a trip, the average forward speed and the final level of accelerations. The magnitude of the desired forward speed, however, can be considered an input value when automated proactive thrust control is applied in reality.

Based on the generated results, the vertical peak accelerations should be predicted with a degree of accuracy of approximately 25%, with a maximum up to 33% (either over- or underestimated). A 33% underestimation yields a new criterion of 30 m/s^2 . It may be expected that vertical peak accelerations greater than 30 m/s^2 , using a criterion of 20 m/s^2 , are not desired. For an overestimation greater than 33% the speed gain is limited. In both cases, if the peaks were to be predicted less accurate, the performance of automated proactive thrust control diminished compared to the ideal situation.

The results generated using the present computational model suggests that the maximum time step for which the reduction of the vertical accelerations remains sufficient, provided that sufficient time to decelerate to a sufficiently low speed is available, is equal to 0.05 s using the present computational model (Zarnick 1978, Keuning 1994).

Chapter 5

Proof of concept

The previous chapter showed that a reduction of the acceleration level can be realised if automated proactive thrust control has been applied on board of the SAR boat of the Arie Visser class sailing in head seas. The study presented in the previous chapter was solely based on applying a computational model. The current chapter presents a proof of concept based on the implementation of the control scheme in model experiments in order to study the scheme in a more realistic setting.

Section 5.1 explains the limitations of the experimental setup compared to the idealised model. Section 5.2 continues with the implementation of the control scheme in the model experiments. More background to the wave prediction method and the deceleration capacity of the towing carriage are given as well. In Section 5.3 the experimental setup is explained. Section 5.4 presents the results of the model tests. Section 5.5 finalises this chapter with conclusions based on the model tests.

5.1 Limitations experimental setup

For the simulations carried out with the idealised model of automated proactive thrust control (Chapter 4) the chosen benchmark ship was also the SAR boat of the Arie Visser class. The simulations were carried out in irregular head waves. The waves were assumed to be known. The response predictions did not consume time (no time delay). The response was predicted for a number of thrust reductions. A relation between the amount of thrust reduction and the predicted magnitude of the vertical acceleration was determined. The largest possible thrust (minimum speed loss) was chosen (see Figure 2.21).

When automated proactive thrust control for this planing boat sailing in irregular head seas is implemented in model experiments, the test setup should meet the following requirements:

1. The irregular waves should be measured real-time during a test providing wave information for a prediction window equivalent to 3 s or more (excluding the time-lag) on full scale;
2. It should be possible for the model of the benchmark ship to decelerate at -1.5 to -2.0 m/s^2 and realise a speed reduction equivalent to 9 *kts* or more on full scale;
3. It should be possible to predict the response for a number of control settings (3 to 5) with little calculation time;

Using the present state of technology it is difficult to meet these requirements. Real-time wave measurements of long-crested irregular waves under high forward speed conditions, even in a towing tank, is still very much difficult. Another approach to measure an irregular wave is to determine the water elevation in the towing tank on forehand. This implies separate experiments. It should also be checked if it is possible to reproduce the previously generated wave train exactly. Moreover, the timing during the experiments with a model of a ship becomes very critical. If there is a spatial offset between the measured and actual position of the towing carriage (for example due to an offset at the start of a run), or if a time offset exists (for example if the towing carriage departs too early or too late), a difference between the actual encountered wave and the water elevation that has been presumed exists. Experiments with thrust control will fail, since control is based on an incorrect predicted wave profile in front of the ship.

Most towing carriages cannot reach a deceleration in the order of magnitude of -1.5 to -2.0 m/s^2 . The maximum deceleration is limited due to the friction between steel wheels on a steel rails. It will also take time before it reaches the maximum deceleration. The deceleration could be increased using a free sailing model or a model that is fixed to the towing carriage but is free to surge, heave and pitch. This requires a control system of the towing carriage. It should follow the model at all times, because the wave, ship motion and other measurement equipment, the computer with the control system, etc. are situated on the carriage and need to be in the vicinity of the current position of the model.

The time is scaled with the square root of the scale of the scale ratio (using Froude's law of similitude). A time delay does not scale, so it is relatively larger on model scale than on full scale. It consumes a bigger portion of the available prediction window, leaving relatively less time to decelerate. The available calculation time is therefore limited, reducing the possibility to carry out a number of response predictions before impact.

The model tests presented in this chapter, based on the implementation of the control scheme in a more realistic setting, are therefore carried out in regular and bichromatic waves because of the aforementioned practical limitations. It has been assumed that if automated proactive thrust control functions in reality the wave profile in front of the ship can be measured using state-of-the-art measurement techniques (see Section

2.3). A setup, where the wave in front of the ship is measured during the run, resembles what would be the future scenario. It is assumed to be a robust setup. Using one wave probe, mounted on the towing carriage on a sufficient distance in front of the model, the wave profile of the regular and bichromatic waves can be computed for a sufficiently large time interval. The model has been fixed to the towing carriage. The control variable concerning automated proactive thrust control is the forward speed. During these tests direct control of the forward speed has been applied. The deceleration properties of the towing carriage determine the speed reduction ability over time. In the current setup, the number of response predictions had to be reduced to one due to the limited available calculation time. The response is predicted using the current desired forward speed.

5.2 Implementation control scheme

Figure 5.1 depicts an overview of the proactive control system in the test setup. The dashed frame represents the control system. The elements outside the frame are elements in the real world. The specifications of the ship under consideration are incorporated in the computational model. The computational model that will be used for the response predictions is the model developed by developed by Zarnick (1978) and Keuning (1994) (see also Section 4.2.1). The control strategy is that the response is predicted for a certain time interval, called the prediction window (T_{pw}), for the current forward speed.

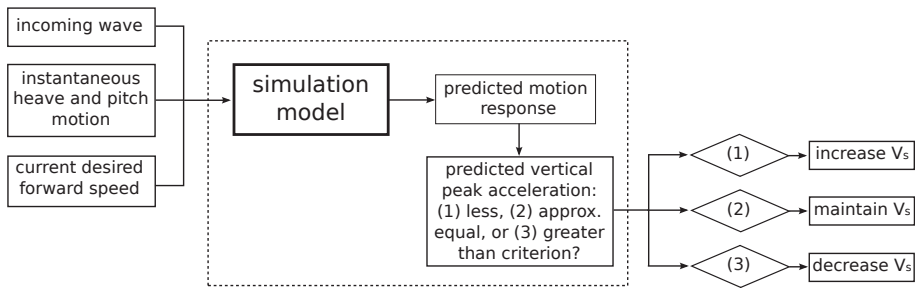


Figure 5.1: Overview proactive control system during model tests

A bandwidth in which the vertical accelerations are considered acceptable is defined and used to determine if speed reductions is required. At the start of the test the towing carriage accelerates to an initial forward speed. On time t_i , the response will be predicted for the duration of the prediction window for this initial forward speed. If the predicted vertical acceleration falls in between the lower and upper limit of a predefined bandwidth for the vertical accelerations, the speed used for the prediction

may be maintained. If the predicted vertical acceleration was smaller than the lower limit, speed increase is possible. If it exceeds the upper limit, speed reduction is necessary. If an alteration of the speed is required, the next response prediction will be carried out using the altered desired forward speed.

The response predictions are performed sequentially (see Figure 5.2). The time interval between two predictions (t_p) is now equal to the calculation time (Δt_c). The time interval between two predictions is therefore not constant. The time interval available for speed reduction is due to the calculation time always smaller than the prediction window: $T_{dw} < T_{pw} - \Delta t_c$.

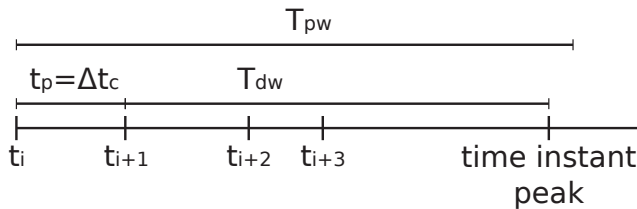


Figure 5.2: Time line with respect to response predictions during model tests

Wave prediction method

During a test run the water elevation was measured at a certain distance in front of the model. A wave probe has been mounted on the towing carriage at distance L_{probe} from the centre of gravity of the ship. Discrepancies between actual and predicted water elevation have been minimized using a setup where the wave probe has been mounted a limited distance from the model. The time-trace of the measured water elevation has been used to derive time dependent snapshots of the wave profile. These snapshots were used to determine to sectional submergence of the cross sections defined in the computational model.

Figure 5.3 depicts a time-space plot of the model of the ship and the wave probe. The water elevation has been measured including its moment in time and position in the towing tank ($r(x(t), t)$). A regular wave with a constant amplitude propagates with the phase velocity. Each time a response prediction is carried out (on t_i), the last T_s s of the measurement of the water elevation, the position of the model and the corresponding time instant it was measured are used to derive the water elevation at and in front of the current position of the model. This yields n measured water elevations (depending on the sample rate and duration). Each measured water elevation is translated in time and space using the wave celerity: $x_{CG}(t_n) + L_{probe} - c \cdot (t_i - t_n)$, where $c = g/\omega$ m/s (assuming deep water). The wave celerity is determined using the wave frequency, that has been provided to the wave flap. This is in fact an input parameter. Time instant t_n represents the time instant that the water elevation was measured; time instant t_i to $t_i + T_{pw}$ represents the time for which the response will

be predicted. The measured hindcast data of the water elevation can now be used to derive snapshots for the duration of the prediction window (see Figure 5.3).

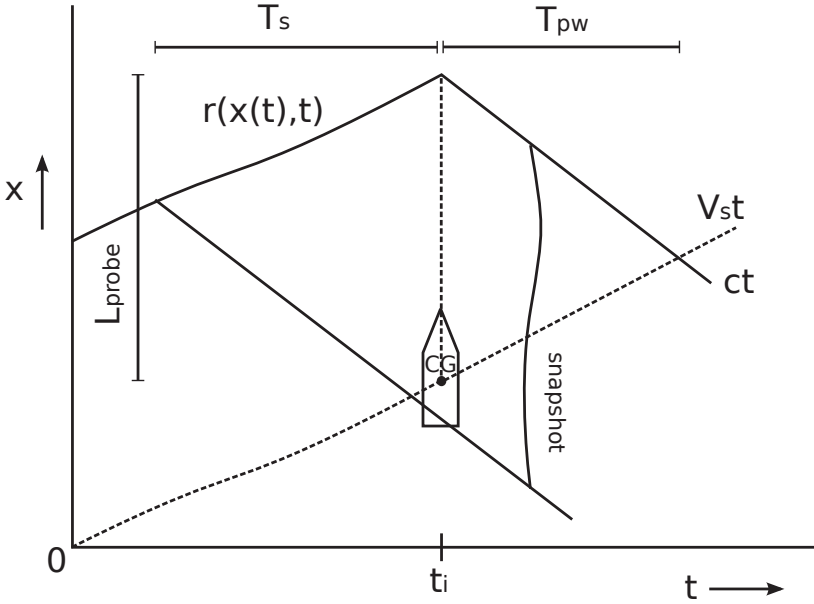


Figure 5.3: Wave prediction method

The computational model also requires an input for the orbital velocity at the undisturbed water line (see Section 4.2.1). The orbital velocity has been found taking the derivation in time of the time-trace of the measured water elevation. The water elevation has been measured at approximately the encounter frequency.

A sine fit has been created of the water elevation. The derivation of the sine fit over the time-trace of the water elevation yields a time dependent expression for the orbital velocity:

$$\begin{aligned} r(x(t), t) &= r_{1a} \cdot \sin(\omega_{1e}t + \epsilon_1) + r_{2a} \cdot \sin(\omega_{2e}t + \epsilon_2) \\ w(x(t), t) &= \frac{dr}{dt} = w_{1a} \cdot \cos(\omega_{1e}t + \epsilon_1) + w_{2a} \cdot \omega \cdot \cos(\omega_{2e}t + \epsilon_2) \end{aligned} \quad (5.1)$$

in which: $w_{1a} = r_{1a} \cdot \omega$ and $w_{2a} = r_{2a} \cdot \omega$.

The wave frequency ω was determined using:

$$\frac{V_s}{g} \omega^2 + \omega - \bar{\omega}_e = 0$$

in which $\omega_e = \frac{\omega_{1e} + \omega_{2e}}{2}$.

The position of the vertical orbital velocities is equal to the position of the corresponding water elevation. Using the same translation in time and space as explained above 'snapshots' of the vertical orbital velocity at the current position of the model can be found.

Deceleration towing carriage

The towing carriage at the Delft University of Technology is able to attain a maximum speed of 7 m/s . The maximum deceleration of the carriage is -1.0 m/s^2 . This is, however, the absolute maximum deceleration. Using a maximum deceleration of -0.8 m/s^2 the risk of damaging the engines on the carriage has been reduced to an acceptable level. The towing carriage has its own speed control system. If the desired forward speed has been altered, its control system will see to it that the speed changes to the new desired speed.

Deceleration tests were carried out to determine the path of the deceleration. Of course the maximum deceleration cannot be attained instantly. A time delay between the moment that the chosen speed reduction has been communicated with the control system of the carriage and the start of the deceleration exists. Figure a in Figure 5.4 depicts the path of the speed of the carriage, once the desired forward speed has been changed. The time the control system of the towing carriage needs to react has been defined as Δt_{tc} (tc : towing carriage). The total time delay between the start of a response prediction and the start of a speed reduction is therefore equal to: $\Delta t = \Delta t_c + \Delta t_{tc}$ (Δt_c : calculation time).

The forward speed changes gradually. It shows a S-shape. The reaction time of the carriage is typically 0.4 to 0.5 s . If sufficient time is available the deceleration reaches its maximum value of -0.8 m/s^2 . The average deceleration is therefore less than the maximum value.

If an alteration of the forward speed is required the change of desired forward speed goes in steps of 0.25 m/s . A speed step of 0.25 m/s is considered an optimum between a sufficiently small discretization of the speed reduction and a sufficiently large speed reduction. For larger speed steps the discretization of the speed may become too coarse. Where the magnitude of the predicted vertical peak accelerations is larger than the upper limit of the predefined bandwidth for the current desired forward speed, it might jump below the lower limit for the reduced forward speed. The speed of the towing carriage might start to oscillate. For smaller speed steps the deceleration becomes limited (see Figure b in Figure 5.4). Here the signal the control system receives is in steps of 0.25 m/s . As a result, the average deceleration has been decreased. Each prediction takes about 0.3 to 0.5 s . The resulting average deceleration (including reaction time of the carriage) is in the order of magnitude of -0.40 to -0.45 m/s^2 . For smaller speed steps this will be decreased even further.

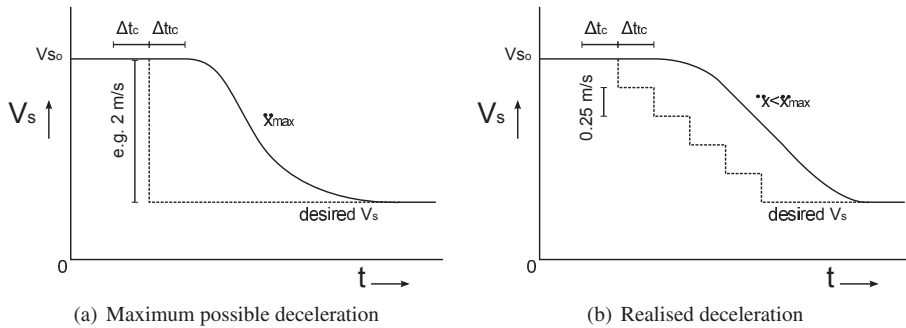


Figure 5.4: Deceleration towing carriage

5.3 Experimental setup

5.3.1 Aim and objectives

The aim of this study is to proof that it is possible to control the vertical acceleration level by means of proactive control of the forward speed.

Two sets of model tests were carried out:

1. Model tests in regular waves to check the implementation of the control scheme (Figure 5.1);
2. Model tests in bichromatic waves to shows that the speed is adjusted according to the in- and decrease of the vertical peak accelerations;

If the speed has been altered so that the measured vertical accelerations are kept within the predefined bandwidth it can be concluded that it is possible to control the level of accelerations by means of proactive control of the forward speed.

5.3.2 Experimental setup

The experiments were carried out in the towing tank of the Ship Hydromechanics Laboratory of the Delft University of Technology. The towing tank has a total length of 142 m and a width of 4.25 m. The water depth during the experiments was equal to 2.34 m. The towing tank is fitted with a hydraulically actuated flap type wave generator.

Figure 5.5 depicts a sketch of the experimental setup. The model was fitted underneath the towing carriage using a strut. The strut could move frictionless in a guide bearing. It was fixed to the model using a support hinge. The model was free to heave and pitch, but it was fixed in all other directions. A guide bearing at the stern prevented the model to yaw.

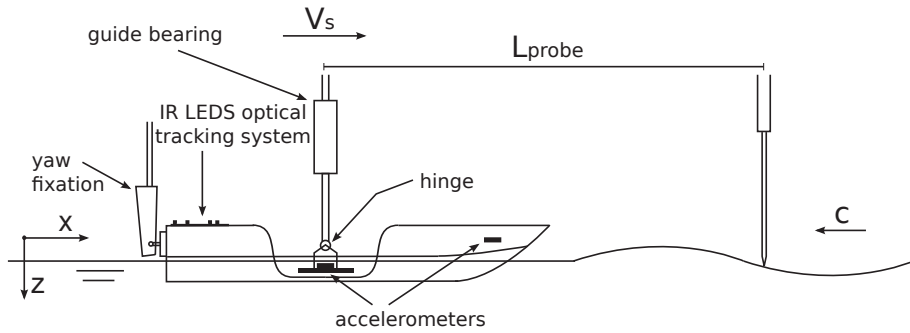


Figure 5.5: *Experimental setup*

The used ship was the SAR boat of the Arie Visser class. The model was fabricated out of carbon fibre. It was ballasted to a typical weight, mass moment of inertia, longitudinal and vertical location of the centre of gravity. In Table 5.1 these values are given on model scale. Throughout the rest of this chapter all dimensions are given on model scale. Figure 5.6 depicts a photo of the model beneath the carriage.

A scale of 1/16 was chosen leading to a model length of 1.18 m (18.8 m on full scale). The time scale, using Froude law of similitude, was equal to 1/4. The resistance was not of interest during these tests, so a large model was not required. A small scale limits the speed of the carriage. A low forward speed implied more measurement time for the given length of the towing tank. Moreover, since these model tests, where the speed of the carriage is controlled real-time during the tests, is a new concept, it was preferred to limit the speed due to safety reasons. The design speed of the SAR of the Arie Visser class is 35 *kts*, which becomes 4.5 *m/s* on model scale.

During the tests the following quantities were measured:

- The travelled distance from the starting point;
- The forward speed;
- The heave and pitch displacement;
- The vertical accelerations at the centre of gravity and the bow;
- The water elevation in front of the model;

The motions were measured in an earth fixed coordinate system with the x -axis lying at the centre of gravity of the ship at zero forward speed, pointing in the direction of the forward speed (see Figure 5.5). The z -axis is pointing down, implying a positive pitch bow up.

The travelled distance was measured by counting the pulses given by the measurement wheel on the carriage. Each time the wheel made a complete circle 10000 pulses were counted. The forward speed was read from the control system of the

Table 5.1: Loading condition of SAR boat of Arie Visser class

Designation	Symbol	Value	Unit
Length over all	L_{oa}	1175	mm
Length between perp.	L_{pp}	906	mm
Beam over all	B_{oa}	381	mm
Beam over waterline	B_{wl}	259	mm
Draft	T	68.5	mm
Mass	m	7.40	kg
Displacement	∇	7.40	dm^3
Longitudinal Centre of Gravity	LCG	380	mm
Vertical Centre of Gravity	VCG	102	mm
Radius of gyration y-axis	k	303	mm
Moment of gyration y-axis	I	0.6794	kgm^2

**Figure 5.6:** Model beneath towing carriage

towing carriage. The sample rate was 5 Hz . The heave and pitch motion were measured using an optical measurement system, called Krypton. IR LEDs were positioned on the model to enable optical motion tracking with a dedicated IR camera system. The sample rate was 200 Hz . The heave and pitch velocity were derived from their measured displacements.

The vertical accelerations were measured using accelerometers. One was positioned at the lengthwise position of the centre of gravity, at the same height as the hinge (which is 29 mm below the centre of gravity). The other was positioned at the

bow. This was at 855 mm from the stern of the ship at the same height as the centre of gravity. This corresponds with 13.68 m from the stern on full scale (equal to 87% of the total length, measured from the aft). The vertical accelerations were measured at a frequency of 99 Hz and filtered at 40 Hz (low pass filtering). The vertical peak accelerations were measured body fixed. Upward vertical peak accelerations appear as negative peak values due to the z -axis pointing downwards.

A wave probe was mounted at the front of the towing carriage, at 6.38 m from the centre of gravity of the model. This wave height meter was a servo controlled instrument, capable to measure wave heights with high accuracy and frequency. This wave probe was selected for its capability to measure the water elevation at high forward speeds. The mechanical part consisted of a guided rod at the end of which a needle was mounted. An electronic circuit detected the contact of the needle with the water surface. A servo motor moved the rod up and down. The electronic circuit controlled the servo motor in such a way that the needle was in continuous contact with the water surface. In this way the needle followed the wave profile. The sample frequency was equal to 15 Hz. Note that a wave crest has a negative value due to the z -axis pointing downwards.

A computer mounted on the carriage acted both as a measurement and control computer. For a response prediction the incoming wave and the instantaneous heave and pitch displacement and velocity were input for the computational model. On t_i s, the data acquisition card of the computer got the current output the measurement wheel and the data of the wave probe, the speed of the carriage and the heave and pitch displacements measured by the Krypton for the past 3 s at a sample rate of 200 Hz. The heave and pitch velocity were derived from the displacements. By taking the average over the last 10 samples the instantaneous heave and pitch displacement and velocity on t_i s were approximated. The position was determined using the measurement wheel. The hindcast data of the water elevation was converted to time dependent snapshots of the wave profile and the vertical orbital velocity, as explained in Section 5.2. The response was predicted for the duration of the prediction window at the current desired forward speed. If the response predictions implied a speed in- or decrease the computer communicates the new desired forward speed with the control system of the towing carriage. The measured vertical accelerations were not used for the response predictions. They were used for comparison after the run.

The time step was equal to 0.01 s. The peak value was found by averaging the values belonging to the neighboring samples of the maximum value found. This yielded a peak width of 0.02 s. The corresponding calculation time varied between 0.3 and 0.5 s.

5.3.3 Test program

The initial speed of the towing carriage was equal to 4 m/s. Once the towing carriage attained a constant forward speed, the proactive control system was activated. Based

on the predicted vertical peak accelerations the speed was reduced. In case of a bichromatic wave the speed was also increased again, once the wave amplitude started to decrease. The minimum speed was set to 1.75 m/s . This implies a speed range of 7 to 16 m/s (13.6 to 31.1 kts) on full scale, well in the middle to high speed range of the SAR boat of the Arie Visser class.

The bandwidth, between which the control system should keep the vertical accelerations, was chosen to -17.5 to -12.5 m/s^2 (the z-axis is defined positive downwards). These values are independent of the chosen scale when using Froude law of similitude.

Model tests have been carried out in regular waves at a constant forward speed in order to compare the measured and calculated vertical peak accelerations beforehand. The wave frequency range was 3.5 to 6.0 rad/s and the wave amplitude was 4 and 6 cm. The forward speed range was 2.0 to 3.5 m/s . Comparison between measured vertical accelerations (filtered at 20 Hz) and calculated ones (time step equal to 0.01 s) showed that the vertical peak accelerations were sufficiently accurately predicted for wave frequencies between 5.0 and 6.0 rad/s , but for lower frequencies ($\omega < 5.0\text{ rad/s}$) the peaks were significantly overestimated. Figure 5.7 depicts the measured and calculated vertical peak accelerations at a range of constant speeds in regular waves.

The chosen wave frequency range was therefore 5.0 , 5.5 and 6.0 rad/s for the tests in regular waves. The wave amplitude was 4 cm. The mean wave frequency of the bichromatic waves was 5.5 rad/s . The wave amplitude increased from 2 to 4 cm and 3 to 5 cm. Two different durations of the wave envelope were chosen: 62.8 and 125.7 s (ω was equal to 0.10 and 0.05 rad/s). It is expected that for a short duration of the envelope the peaks might exceed the bandwidth due to the limited deceleration capacity of the carriage. For the longer wave envelope it is expected that the peaks can be kept between the predefined bandwidth.

5.4 Results

5.4.1 Results model tests in regular waves

Figure 5.8 to Figure 5.10 show the measured water elevation (translated to the CG of the model), the speed of the carriage and the vertical peak accelerations at the bow for the experiments in regular waves. The predicted vertical peak accelerations are displayed as green triangles. These figures show that only after 5 s after the control system had been activated, the speed was reduced. After 3 s the data required for a response prediction was available. The wave prediction method required hindcast data of the water elevation. The first calculation time was considerably larger than the time delays throughout the rest of the run (approximately 1.5 s). Adding the reaction time of the towing carriage the start of the speed reduction was at approximately 5 s after the control and measurement system was activated.

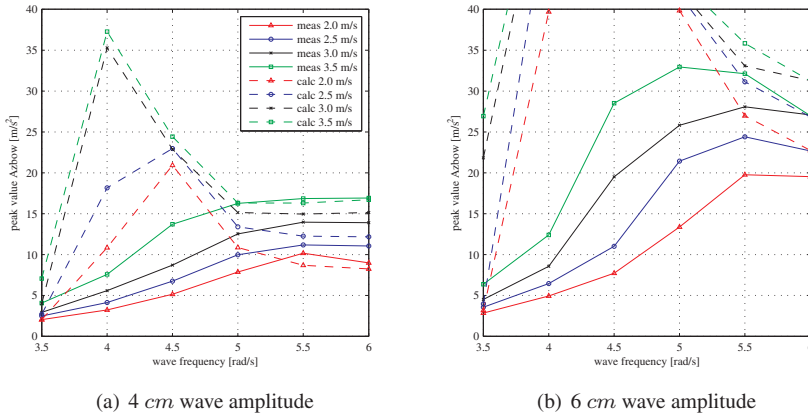


Figure 5.7: Amplitude vertical acceleration in regular waves

For a wave frequency of 5.0 rad/s the required speed reduction was little; approximately 0.25 m/s . The first and last peaks of the run were underestimated. The speed was therefore reduced somewhat late. The control system could not react on the last predicted peaks, because the end of the towing tank was reached. Generally speaking, the vertical accelerations could be kept within the bandwidth of -17.5 to -12.5 m/s^2 . For a wave frequency of 5.5 rad/s the vertical peak accelerations were overestimated by 2 to 5 m/s^2 . The measured peaks, however, were kept within the bandwidth of -17.5 to -12.5 m/s^2 . The speed varied due to the slowly varying wave amplitude. For waves having a high frequency a constant wave amplitude could not be generated. The final forward speed was therefore not constant.

For the shortest waves (6.0 rad/s), however, the variation of the wave amplitude was large. At the start of the run the control system did not decrease the speed in time. The wave amplitude and thus the vertical accelerations varied quickly. The acceleration capacity of the carriage was insufficient to follow these changes. The vertical peak accelerations were overestimated by 2 to 5 m/s^2 , causing that sometimes the actual peaks were greater than -17.5 m/s^2 .

The presented time-traces show that proactive control of the forward speed based on predicted vertical peak accelerations is possible. It is, however, essential that the peaks are predicted with a certain degree of accuracy. The relation between the forward speed and the vertical peak accelerations should be captured accurately in the computational model.

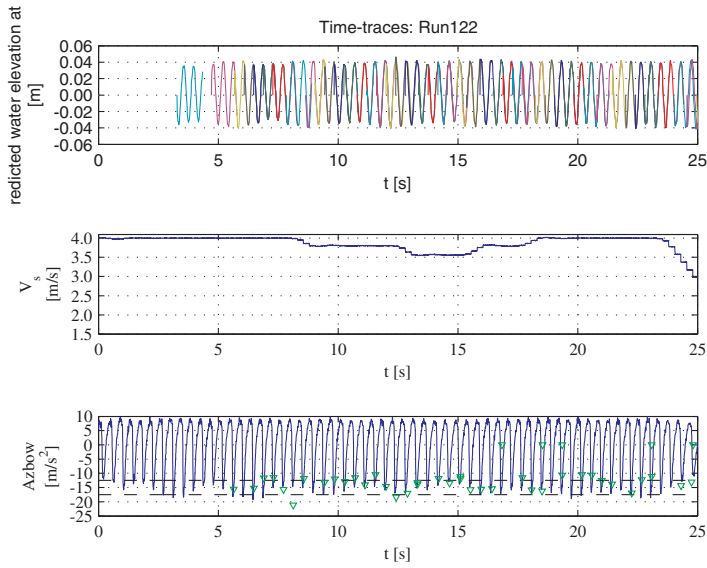


Figure 5.8: Time-traces of the translated water elevation, speed carriage and vertical peak accelerations at the bow in a regular wave of 5.0 rad/s

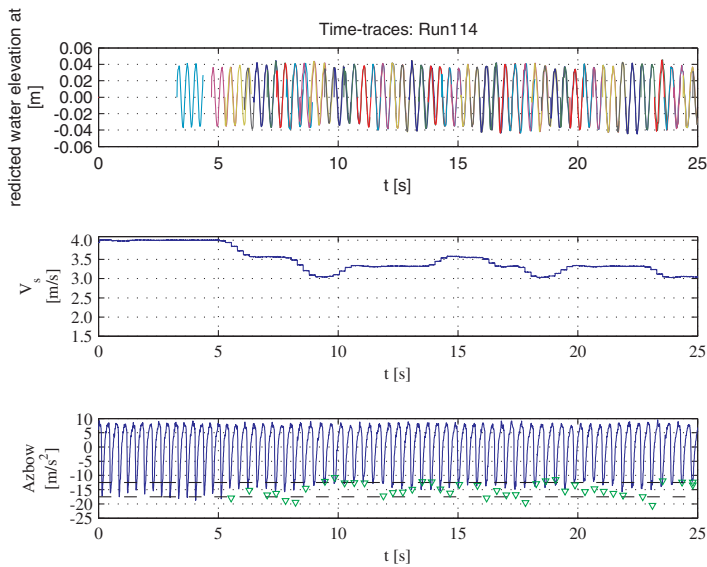


Figure 5.9: Time-traces of the translated water elevation, speed carriage and vertical peak accelerations at the bow in a regular wave of 5.5 rad/s

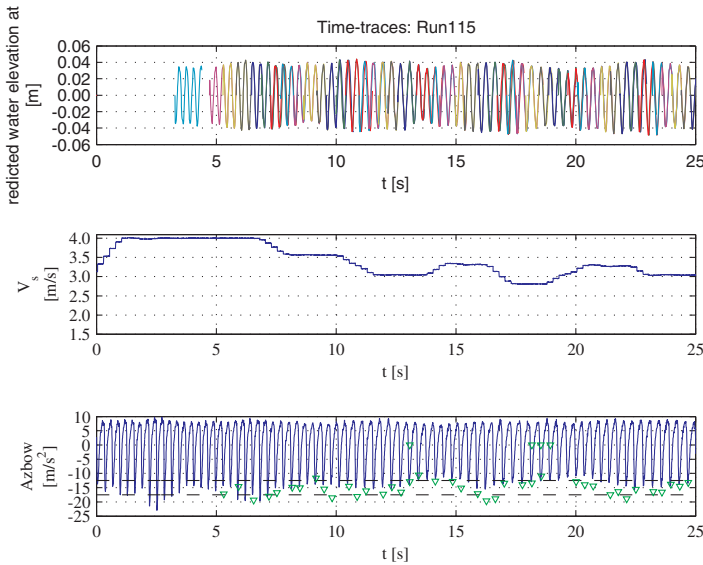


Figure 5.10: Time-traces of the translated water elevation, speed carriage and vertical peak accelerations at the bow in a regular wave of 6.0 rad/s

5.4.2 Results model tests in bichromatic waves

Figure 5.11 and Figure 5.12 display the time-traces of the measured water elevation (translated to the CG of the model), the speed of the carriage and the vertical accelerations at the bow for a bichromatic wave with a mean frequency of 5.5 rad/s and an envelope duration of 62.8 s . The predicted peaks are also displayed. The wave amplitude was increased from 2 to 4 cm and 3 to 5 cm respectively. The shape of the bichromatic wave is clearly visible. The first unacceptable vertical peak acceleration was detected early. For an increase of wave amplitude from 2 to 4 cm the increase of the magnitude of the vertical acceleration could still be counteracted by reducing the speed. The speed reduction, chosen based on the predicted response, was sufficient. If the wave amplitude was increased to 5 cm, the speed reduction was not in time. The increase of the vertical peak acceleration due to the increase of wave amplitude was too quick in relation to the deceleration of the towing carriage. Besides, not all peaks were predicted at the beginning of the run, causing a late reaction of the control system.

Figure 5.13 and Figure 5.14 display the time-traces of the measured water elevation (translated to the CG of the model), the speed of the carriage and the vertical accelerations at the bow for a bichromatic wave with a mean frequency of 5.5 rad/s and an envelope duration of 125.7 s . The wave amplitude was increased from 2 to 4 cm

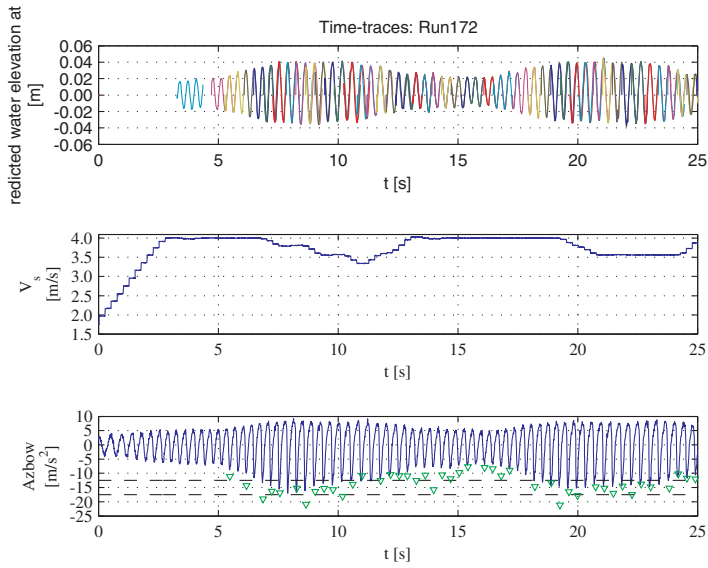


Figure 5.11: Time-traces of the translated water elevation, speed carriage and vertical peak accelerations at the bow in a bichromatic wave of $T_{env} = 63$ s, wave height 2 to 4 cm

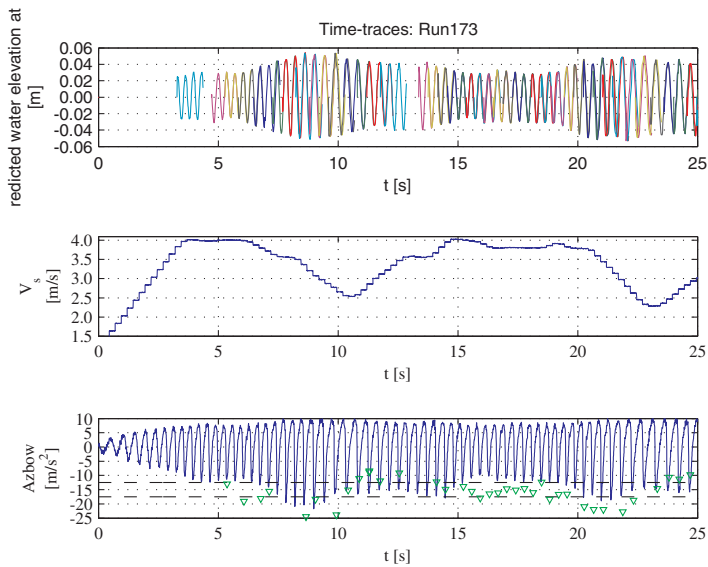


Figure 5.12: Time-traces of the translated water elevation, speed carriage and vertical peak accelerations at the bow in a bichromatic wave of $T_{env} = 63$ s, wave height 3 to 5 cm

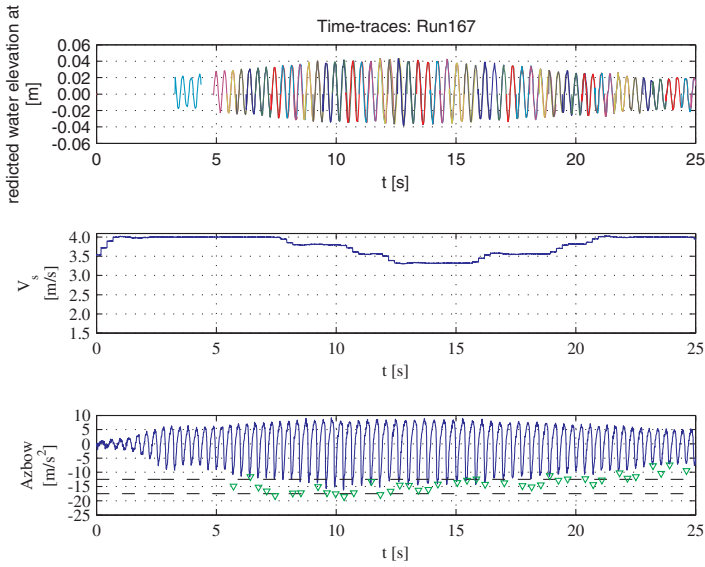


Figure 5.13: Time-traces of the translated water elevation, speed carriage and vertical peak accelerations at the bow in a bichromatic wave of $T_{env} = 126$ s, wave height 2 to 4 cm

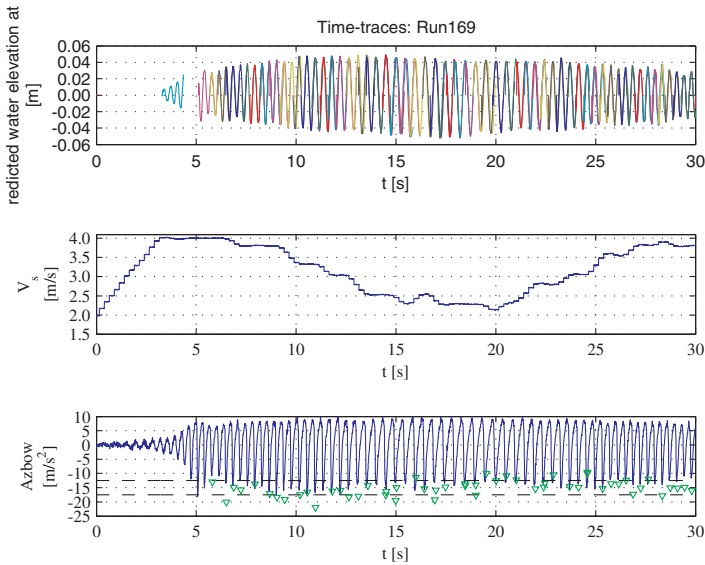


Figure 5.14: Time-traces of the translated water elevation, speed carriage and vertical peak accelerations at the bow in a bichromatic wave of $T_{env} = 126$ s, wave height 3 to 5 cm

and 3 to 5 *cm* respectively. For both increases of wave amplitude was detected in time and the corresponding speed reduction was sufficient. The predictions of the vertical peak accelerations were more consistent than for the shorter bichromatic waves. They were, however, slightly overestimated. Overall, the vertical accelerations were kept within the predefined bandwidth.

5.5 Conclusions

A proof of concept of proactive control of the forward speed has been presented in this chapter. Real-time proactive control for one variable (the forward speed) for a planing monohull in head seas, based on predicted vertical peak accelerations, is possible. The model tests in regular waves have shown the applicability of the control scheme. If the vertical peak accelerations were predicted accurately the vertical accelerations were kept within the predefined bandwidth. The model tests in bichromatic waves have shown the relation between the increase of wave amplitude over time (and thus the increase of vertical accelerations) the corresponding speed reduction and the actual measured vertical accelerations. The results have shown that the speed was adjusted according to the predicted vertical peak accelerations. For gradual increases of the wave amplitude the speed was adjusted in time as well; (most of) the vertical peak accelerations were kept within the predefined bandwidth.

Chapter 6

Conclusions and recommendations

6.1 Conclusions

The main limiting factor for operability for planing monohulls in head seas is the occurrence of large vertical peak accelerations. The operability of planing monohulls sailing in head seas may be increased if the vertical acceleration levels can be reduced. In this dissertation a solution to reduce the vertical acceleration level has been found in automated proactive thrust control.

The purpose of this study was to show the level of reduction of the vertical accelerations possible with automated proactive thrust control. A reduction of the vertical accelerations implies that it is possible to sail faster without increasing the discomfort on board. This means an improvement of the operability.

The results presented in this dissertation have proven that reduce the vertical acceleration level using automated proactive thrust control on board of a planing monohull sailing in head seas.

Operators on board of Dutch Search and Rescue vessels were able to sail at a 20% higher average forward speed when they were allowed to use thrust control, compared to a trial where the operator had to choose a constant thrust on forehand. This suggested that thrust control has a beneficial effect. Based on a limited number of full scale trails on board of Dutch Search and Rescue vessels it was, however, not possible to conclude whether the vertical acceleration level was reduced using thrust control. For this, the acceleration level should be compared at an equal forward speed.

The conceptual simulation model of automated proactive thrust control has shown that a significant reduction of the vertical acceleration level can be realised using auto-

mated proactive thrust control. In the conceptual model the response of a planing monohull sailing in head seas has been mimicked by an elementary response model. The level of accelerations were compared at an equal forward speed. The capacity to reduce the speed before impact proved to be an important component to reduce the vertical acceleration level. This minimum attainable speed at impact depends on the initial forward speed, the specific power of the ship and the length of the prediction window. A significant reduction of the vertical accelerations can be expected if sufficient time to decelerate to a sufficiently low speed before impact is available. This is provided that the vertical accelerations are predicted accurately.

Confirming the findings with the conceptual model presented in Chapter 3, the idealised model also showed that the vertical acceleration level can be reduced if sufficient time to decelerate is available. In the idealised model the elementary response model has been replaced by a more adequate computational model to describe the nonlinear seakeeping behaviour. If the time to decelerate is limited the reduction of the vertical accelerations still may be realised, compared to simulations carried out using an equal but constant forward speed. The reduction, however, becomes less. It is directly related to the available time to decelerate and consequently to the minimum attainable speed at impact.

The uncertainty of the predictions of the vertical peak accelerations, using the computational model developed by Zarnick (1978) and Keuning (1994), affected the level of reduction but does not violate the feasibility of proactive control. Inaccurate predicted peaks yield incorrect control of the thrust. This has an effect on the final average forward speed and distribution of the vertical accelerations. In case of overestimated peaks, the thrust reductions are chosen conservatively, resulting in a low average forward speed compared to the ideal situation (peaks were estimated accurately). In case of underestimated peaks, the thrust reductions are chosen optimistically, resulting in a limited reduction of the vertical accelerations compared to the ideal situation. The time step has an influence on the accuracy of the response predictions. In case of a large time step, using the present computational model, peaks will be 'missed' (they are not anticipated), resulting in a limited reduction of the acceleration level.

The model tests carried out in regular and bichromatic waves have shown that it is possible to control the vertical acceleration level by means of proactive control for one variable (the forward speed). Control is based on predicted vertical peak accelerations. The predictions were carried out real-time during the runs. The vertical accelerations can be kept within a predefined bandwidth, if the vertical peak accelerations are predicted accurately. In case of bichromatic waves the speed was reduced in time for gradual increases of the wave amplitude.

Overall, it can be concluded that using automated proactive control of the thrust on board of a planing monohull sailing in head seas a reduction of the vertical acceleration level can be realised. Automated proactive thrust control was the first step towards a proactive control system for more than one control variable. The results presented in this dissertation have shown that proactive control, based on predicted vertical peak

accelerations, is a promising way to reduce the vertical accelerations and therewith improve the operability of planing monohulls sailing in head seas.

The order of magnitude of the independent variables ship, sea state and desired forward speed in relation to the minimum attainable forward speed at impact (the possible minimum value of the control variable) determine to what extent the vertical accelerations can be reduced or increased using thrust control on board of a planing monohull. In this study the SAR boat of the Arie Visser class has been used as a benchmark vessel. This ship has a high specific power and a low gradient of the resistance curve and is therefore able to decelerate quickly. Two combinations of sea state and desired forward speed, resulting in sufficiently frequent thrust reductions during the simulation time, were elected for the simulations in Chapter 4. Larger planing monohulls most likely have a smaller specific power than the Arie Visser. The gradients of the resistance curve is often steeper for larger planing monohulls. More time to decelerate is required. For ships above a certain length thrust control is probably not useful. It is not expected that thrust control is required (often) in calm sea states. The ship can sail safely at a high forward speed. In very rough sea states it is not expected that temporary speed reductions have a large effect on the vertical accelerations. The hydrodynamic lift is small, so temporary speed reduction have a limited effect on the vertical accelerations. The largest reduction of the vertical accelerations may be expected in moderate to rough sea states where the ship is able to sail in the middle to high speed range of its design speed. In that speed range a significant hydrodynamic lift exists. A temporary speed reduction has more effect on the next vertical peak acceleration. The last variable, the desired forward speed, influences the frequency of the thrust reductions during a trip, the average forward speed and the final level of accelerations. The magnitude of the desired forward speed, however, can be considered an input parameter when automated proactive thrust control is applied in reality.

The results presented in this dissertation have shown that automated proactive thrust control opens the possibility to sail at higher forward speeds in seaway, particularly useful for patrol, search and rescue or military operations. Ship-owners of (small) planing boats can improve the operability of their ships using automated proactive control of the thrust. Shipyards that are able to deliver ships including automated proactive thrust control may obtain a significant advantage in the market of fast ships (depending on the total costs of such a system).

6.2 Recommendations

A model of the dynamics of the bridge handle, engines, gearboxes, shafts, propellers or waterjets and ultimately the thrust force is desired. This model could be used to determine the time lag for a propulsive system. This provides more insight in the dependency of the time lag on the inertia of the engines, shafts and propellers/waterjets.

When the time lag becomes too large it may jeopardise the feasibility of automated proactive thrust control.

Automated proactive thrust control as it should function in reality could be setup in a towing tank. These model tests should be carried out in irregular head waves. Similar results could be generated as presented in Chapter 4 in this dissertation, with the difference that these results are not generated using a computational model. The measured distributions of the vertical peak accelerations obtained from a number of runs using automated proactive thrust control can be compared to the measured distributions obtained from a number of runs at a constant speed equal to the average forward speed when thrust control was applied.

The following aspects with respect to the experimental setup are required:

- An accurate wave measurement system and a reliable wave prediction method for long-crested irregular waves;
- Sufficient deceleration, yielding the possibility to realise a sufficiently large speed reduction before impact;
- A significant reduction of the calculation time to create the possibility to predict the response for a number of control settings;

To improve the accuracy of the response predictions the computational should be tuned for the ship under consideration and the desired wave conditions.

Research into possible on board wave measurement systems, such as laser, radar, lidar, that can provide the wave input for the next few seconds sufficiently accurate, is desired. If automated proactive thrust control functions on model scale in irregular waves, the next step would be to perform full scale trials in head seas. For this a reliable on board wave measurement system is required.

The approach followed in this study can be used to analyse the reduction of the vertical acceleration level possible with proactive control of another variable than the forward speed, eg. interceptors or stern flaps, or a combination of the two. A preliminary study into the hydrodynamics of interceptors or stern flaps and their interaction with the ship is required (this study has already commenced at the department of ship hydromechanics and structures at the Delft University of Technology in January 2011 Rijkens et al. (2011), Rijkens (2013a;b))

Appendices

Appendix A

Coefficients in elementary response model

The mass, mass moment of inertia, the steady-state values (sinkage and trim) and the calm water resistance used in the equations of motion (Equation 3.6) are based on the 19° deadrise parent model of the DSDS with a length of 15 *m* (Keuning et al. 1993).

Main dimensions ship

$$\begin{aligned}m &= 23400 && [kg] \\k &= 3.75 && [m] \\I &= 3.2906 \cdot 10^5 && [kgm^2]\end{aligned}$$

Steady-state values

$$\begin{aligned}\gamma_o &= 1.0 \\d\gamma/dt &= 1 && [1/s] \\x_o &= 12 && [m/s] \\z_o &= 1.0 && [m] \\\theta_o &= 5^\circ\end{aligned}$$

A steady-state forward speed \dot{x}_o of 12 *m/s* has been chosen (see Figure A.1).

Calm water resistance

$$f_x(\dot{x}) = 0.05 \cdot \dot{x}^3 - 0.05 \cdot \dot{x}^2 + 0.15 \cdot \dot{x}$$

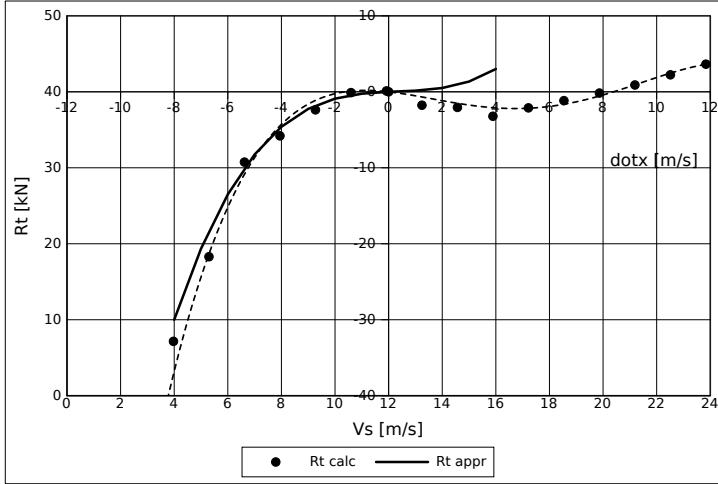


Figure A.1: Calm water resistance ($Rt_o = 40 \text{ kN}$)

Added mass

$$\begin{aligned}
 a_{zz} &= 5850 && [\text{kg}] \\
 a_{\theta\theta} &= 5.4844 \cdot 10^4 && [\text{kgm}^2] \\
 a_{z\theta} &= 2.1938 \cdot 10^4 && [\text{kgm}] \\
 a_{\theta z} &= 2.1938 \cdot 10^4 && [\text{kgm}] \\
 a_{zx} &= 585 && [\text{kg}] \\
 a_{\theta x} &= 2.1938 \cdot 10^3 && [\text{kgm}]
 \end{aligned}$$

Damping

$$\begin{aligned}
 b_{zz} &= 275 \cdot 10^3 && [\text{Ns/m}] \\
 b_{\theta\theta} &= 1700 \cdot 10^3 && [\text{Nm s/rad}] \\
 b_{z\theta} &= 0 && [\text{Ns/rad}] \\
 b_{\theta z} &= 0 && [\text{Nm s/m}] \\
 b_{zx} &= 32 \cdot 10^3 && [\text{Ns/m}] \\
 b_{\theta x} &= -10 \cdot 10^3 && [\text{Nm s/m}]
 \end{aligned}$$

Nonlinear damping force pitch

$$\begin{aligned}
 \dot{\theta} \geq 0 : & \quad f_{\theta\dot{\theta}}(\dot{\theta}) = b_{\theta\theta} \cdot \dot{\theta} && [\text{Nm}] \\
 \dot{\theta} < 0 : & \quad f_{\theta\dot{\theta}}(\dot{\theta}) = b_{\theta\theta} \cdot \dot{\theta} - b_{\theta\theta} \cdot \dot{\theta}^2 && [\text{Nm}]
 \end{aligned}$$

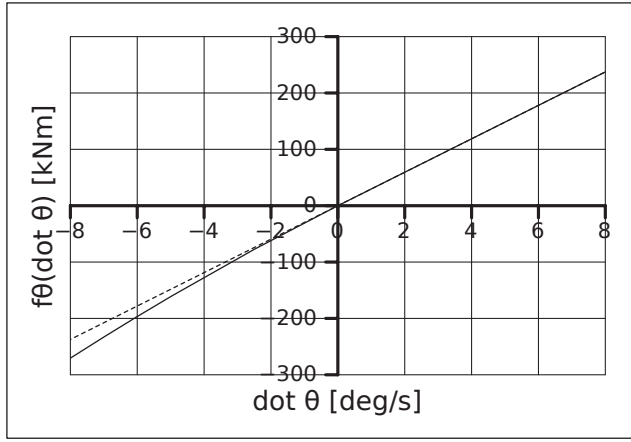


Figure A.2: Assumed nonlinear damping force pitch

Spring terms

$$c_{zz} = 750 \cdot 10^3 \quad [N/m]$$

$$c_{\theta\theta} = 2000 \cdot 10^3 \quad [Nm/rad]$$

$$c_{z\theta} = 1000 \cdot 10^3 \quad [N/rad]$$

$$c_{\theta z} = -50 \cdot 10^3 \quad [Nm/m]$$

Nonlinear restoring force heave

$$\begin{aligned} z \geq 0 : \quad & f_{zz}(z) = c_{zz} \cdot z + c_{zz} \cdot z^2 \quad [N] \\ -1.5 < z < 0 : \quad & f_{zz}(z) = c_{zz} \cdot z + c_{zz}/3 \cdot z^2 \quad [N] \\ z \leq -1.5 : \quad & f_{zz}(z) = -562500 \quad [N] \end{aligned}$$

Assumed nonlinear restoring force pitch

$$\theta \geq 0 : \quad f_{\theta\theta}(\theta) = c_{\theta\theta} \cdot \theta + c_{\theta\theta} \cdot \theta^2 \quad [Nm]$$

$$\theta < 0 : \quad f_{\theta\theta}(\theta) = c_{\theta\theta} \cdot \theta - c_{\theta\theta} \cdot \theta^2 \quad [Nm]$$

Nonlinear coupling terms

$$f_{z\dot{x}}(\dot{x}) = b_{zx} \cdot \dot{x} - b_{zx}/8 \cdot \dot{x}^2 \quad [N]$$

$$f_{\theta\dot{x}}(\dot{x}) = b_{\theta x} \cdot \dot{x} - b_{\theta x}/6 \cdot \dot{x}^2 \quad [Nm]$$

Excitation

$$F_{w_z}(x, t) = \sum F_{w_{z a_j}} \cdot \sin(\omega_j \cdot t + k_j \cdot x + \phi_j) \quad [N]$$

$$M_{w_\theta}(x, t) = - \sum M_{w_{z a_j}} \cdot \cos(\omega_j \cdot t + k_j \cdot x + \phi_j) \quad [Nm]$$

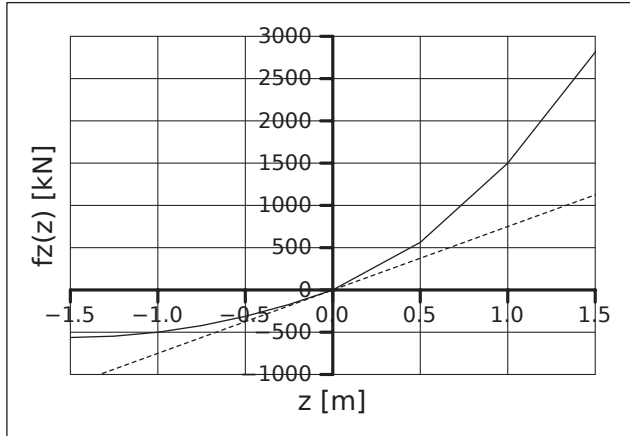


Figure A.3: Assumed nonlinear restoring force heave

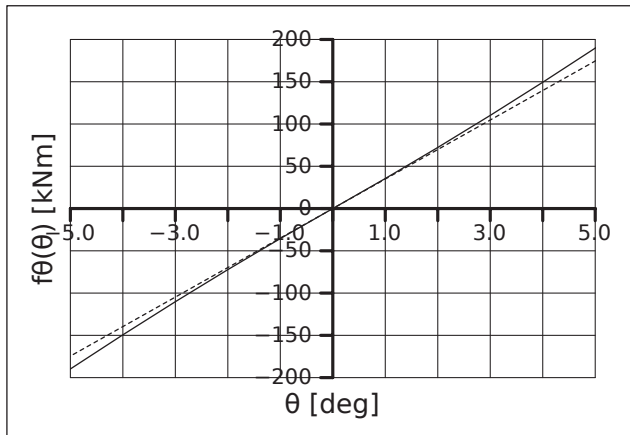


Figure A.4: Assumed nonlinear restoring force pitch

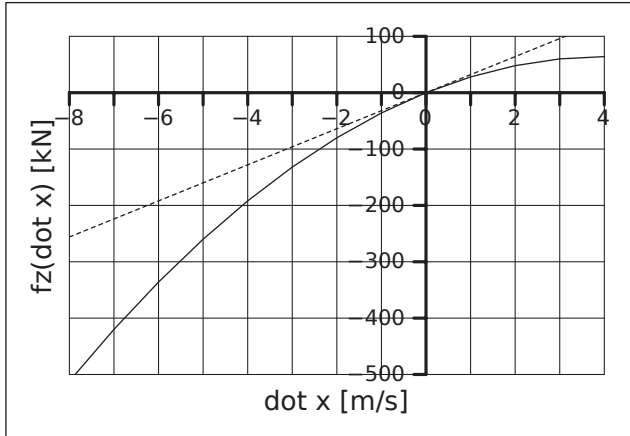


Figure A.5: Assumed nonlinear coupling term between forward speed and heave motion

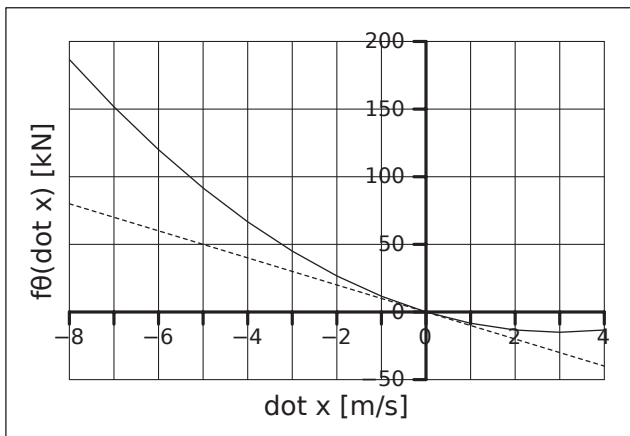


Figure A.6: Assumed nonlinear coupling term between forward speed and pitch motion

Appendix B

Repetition intervals

An irregular wave pattern (or as in Chapter 3 an irregular pattern of the excitation), built up out of a number of sines using an equally spaced frequency step, repeats itself. At a certain location, it takes t_r s before the time traces repeats itself; at a certain time instant the snapshot repeats itself after x_r m (see Figure B.1). The values for t_r and x_r for a discretization of a certain wave spectrum using equally spaced frequency steps can be determined using the following approach.

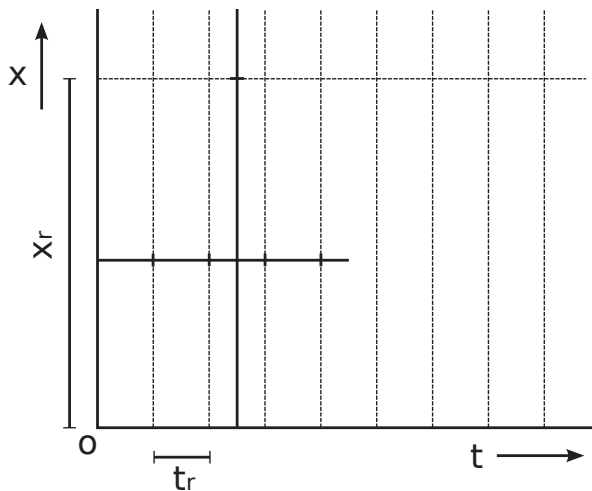


Figure B.1: *Repetition intervals for an irregular wave pattern*

If we consider two components, $i = 1$ and $i = 2$, the time these components repeat

themselves is for both components respectively:

$$\begin{aligned}\omega_1 \cdot t_r &= n \cdot 2\pi \vee \omega_2 \cdot t_r = m \cdot 2\pi \\ t_r &= n \cdot \frac{2\pi}{\omega_1} = m \cdot \frac{2\pi}{\omega_2} \Rightarrow \frac{\omega_1}{\omega_2} = \frac{n}{m}\end{aligned}$$

in which n and m are positive integers. The distance over which these components repeat themselves is equal to:

$$\begin{aligned}k_1 \cdot x_r &= p \cdot 2\pi \vee k_2 \cdot x_r = q \cdot 2\pi \\ x_r &= p \cdot \frac{2\pi}{k_1} = q \cdot \frac{2\pi}{k_2} \Rightarrow \frac{k_1}{k_2} = \frac{p}{q}\end{aligned}$$

in which p and q are positive integers. If the repetition distance is rewritten in the following manner:

$$\frac{p}{q} = \frac{k_1}{k_2} = \frac{\omega_1^2/g}{\omega_2^2/g} = \left(\frac{\omega_1}{\omega_2}\right)^2 = \frac{n^2}{m^2} \Rightarrow p = n^2 \vee q = m^2$$

the relation between the repetition time and distance becomes apparant:

$$\begin{aligned}t_r &= n \cdot \frac{2\pi}{\omega_1} = m \cdot \frac{2\pi}{\omega_2} = o \cdot \frac{2\pi}{\omega_3} = \dots \\ x_r &= n^2 \cdot \frac{2\pi}{k_1} = m^2 \cdot \frac{2\pi}{k_2} = o^2 \cdot \frac{2\pi}{k_3} = \dots\end{aligned}$$

The spectrum of the excitation used in Chapter 3 was built up out of 40 components ($d\omega = 0.05 \text{ rad/s}$). If we consider $\omega_1 = 0.95 \text{ rad/s}$, $\omega_2 = 1.00 \text{ rad/s}$ and $\omega_3 = 1.05 \text{ rad/s}$, we find that the repetition time is equal to:

$$\begin{aligned}t_r &= n \cdot \frac{2\pi}{0.95} = m \cdot \frac{2\pi}{1.00} = o \cdot \frac{2\pi}{1.05} \\ t_r &= 19 \cdot 2\pi \cdot \frac{20}{19} = 20 \cdot 2\pi \cdot \frac{20}{20} = 21 \cdot 2\pi \cdot \frac{20}{21} = 125.66 \quad [\text{s}]\end{aligned}$$

and the distance equal to:

$$x_r = 20^2 \cdot \frac{2\pi}{1.00^2/g} = 24.655 \quad [\text{km}]$$

The Jonswap wave spectrum used in Chapter 4 was built up out of 100 components ($d\omega = 0.025 \text{ rad/s}$). If we consider $\omega_1 = 0.975 \text{ rad/s}$, $\omega_2 = 1.00 \text{ rad/s}$ and $\omega_3 = 1.025 \text{ rad/s}$, we find that the repetition time is equal to:

$$\begin{aligned}t_r &= n \cdot \frac{2\pi}{0.975} = m \cdot \frac{2\pi}{1.00} = o \cdot \frac{2\pi}{1.025} \\ t_r &= 39 \cdot 2\pi \cdot \frac{40}{39} = 40 \cdot 2\pi \cdot \frac{40}{40} = 41 \cdot 2\pi \cdot \frac{40}{41} = 251.33 \quad [\text{s}]\end{aligned}$$

and the distance equal to:

$$x_r = 40^2 \cdot \frac{2\pi}{1.00^2/g} = 98.621 \quad [km]$$

For a ship having zero forward speed the wave (or excitation) pattern will repeat itself already after $2\pi/d\omega$ s, where $d\omega$ is an equally spaced frequency step. For a ship sailing in head seas at a constant speed the wave pattern repeats itself if the ship crosses (more or less) an intersection point $(a \cdot t_r, b \cdot x_r)$, where a and b are positive integers. See Figure B.2 for a clarification. This implies that the repetition time is speed dependent:

$$b \cdot x_r = \bar{V}_s \cdot a \cdot t_r \Rightarrow \bar{V}_s = \frac{b \cdot x_r}{a \cdot t_r}$$

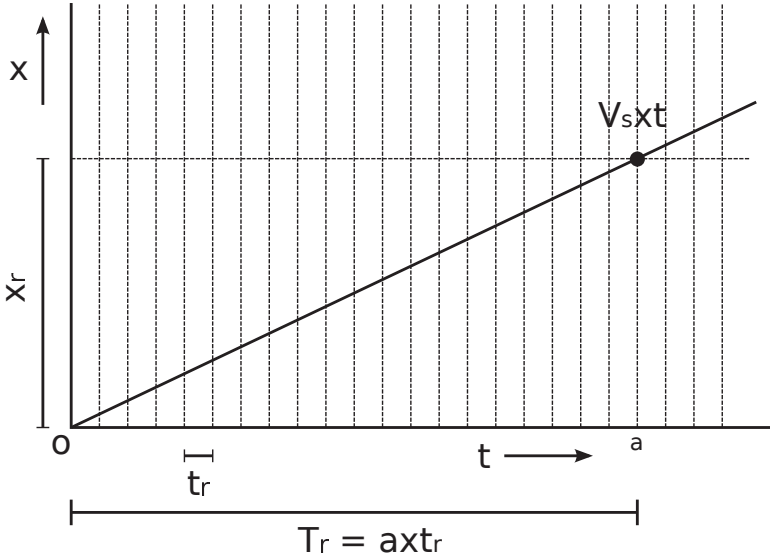


Figure B.2: Repetition intervals for an irregular wave pattern including forward speed

Table B.1 presents the average forward speeds for which the ship would cross intersection points $(a \cdot t_r, 1 \cdot x_r)$ and the corresponding repetition time $T_r = a \cdot t_r$ for a ship sailing in head seas if the equally spaced frequency step is equal to 0.05 rad/s ; Table B.2 if the frequency step is equal to 0.025 rad/s . Having an average forward speed where the ship would cross the $1 \cdot x_r$ line halfway $a \cdot t_r$ and $(a + 1) \cdot t_r$ the total repetition time and distance would be doubled. The most conservative repetition time for a ship sailing in head seas is found if we assume a constant forward speed and if we assume that the ship crosses an intersection point lying on the line $1 \cdot x_r$. The repetition times for a number of constant speeds are given in Tables B.1 or B.2.

Table B.1: Total repetition time if $d\omega = 0.05$ [rad/s]

a	T_r	\bar{V}_s
[-]	[s]	[m/s]
15	1885	13.08
16	2011	12.26
17	2136	11.54
18	2262	10.90
19	2388	10.33
20	2513	9.81
21	2639	9.34
22	2765	8.92
23	2890	8.53
24	3016	8.18
25	3142	7.85

Table B.2: Total repetition time if $d\omega = 0.025$ [rad/s]

a	T_r	\bar{V}_s
[-]	[s]	[m/s]
20	5027	19.62
21	5278	18.69
22	5529	17.84
23	5781	17.06
24	6032	16.35
25	6283	15.70
26	6535	15.09
27	6786	14.53
28	7037	14.01
29	7288	13.53
30	7540	13.08
31	7791	12.66
32	8042	12.26
33	8294	11.89
34	8545	11.54
35	8796	11.21
36	9048	10.90
37	9299	10.61
38	9550	10.33
39	9802	10.06
40	10053	9.81

Bibliography

- J. J. Blok and H. W. Roeloffs. De invloed van voorschip vlaktiling op het zeegangsgedrag. Technical Report 49207-1-HT, Maritime Research Institute Netherlands, 1989.
- E. P. Clement and D. L. Blount. Resistance tests of a systematic series of planing hull forms. *Society of Naval Architects and Marine Engineers Transactions*, 1963.
- P. De Jong. *Seakeeping behaviour of high speed ships - An experimental and numerical study*. PhD thesis, Delft University of Technology, Ship Hydromechanics Laboratory, 2011.
- G. Fridsma. A systematic study of the rough-water performance of planing boats. Technical Report R1275, Stevens Institute of Technology, Davidson Laboratory, Nov 1969.
- G. Fridsma. A systematic study of the rough-water performance of planing boats (irregular waves-part ii). Technical Report 1495, Stevens Institute of Technology, Davidson Laboratory, March 1971.
- T. C. Fu, E. E. Hackett, A.M. Fullerton, and C. Merrill. Shipboard measurement of ocean waves. In *Proceedings of the ASME 2011 30th International Conference on Ocean, Offshore and Arctic Engineering*, June 2011.
- K. Garne. *Modeling of planing craft in waves*. PhD thesis, Royal Institute of Technology KTH, Department of Aeronautical and Vehicle Engineering, Stockholm, Sweden, Sept 2004.
- S. T. Grilli, C. A. Guerin, and B. Goldstein. Ocean wave reconstruction algorithms based on spatio-temporal data acquired by a flash lidar camera. In *Proceedings of the 21st International Offshore (Ocean) and Polar Engineering Conference*, June 2011.
- H. Grimmelius, E. Meshabi, P. Schulten, and D. Stapersma. The use of diesel engine simulation models in ship propulsion plant design and operation. In *CIMAC Congress*, 2007.

- N. Hogben and F. E. Lumb. *Ocean wave statistics*. London, Her Majesty's stationary office, 1967.
- J. A. Keuning. *The nonlinear behaviour of fast monohulls in head waves*. PhD thesis, Delft University of Technology, Ship Hydromechanics Laboratory, 1994.
- J. A. Keuning. Grinding the bow or how to improve the operability of fast monohulls. *International Shipbuilding Progress*, 53:281–310, 2006.
- J. A. Keuning and J. Gerritsma. Resistance tests of a series of planing hull forms with a 25 degrees deadrise angle. *International Shipbuilding Progress*, 29(337): 222–249, Sept 1982.
- J. A. Keuning and J. Pinkster. Optimisation of the seakeeping behaviour of a fast monohull. In *Proceedings of the 3rd International Conference on Fast Sea Transportation*, Sept 1995.
- J. A. Keuning and J. Pinkster. Further design and seakeeping investigations into the "enlarged ship concept". In *Proceedings of the 4th International Conference on Fast Sea Transportation*, March 1997.
- J. A. Keuning and F. van Walree. The comparison of the hydrodynamic behaviour of three fast patrol boats with special hull geometries. In *Proceedings of the 5th International Conference on High Performance Marine Vehicles (HIPER'06)*, pages 137–152, 2006.
- J. A. Keuning, J. Gerritsma, and P. F. van Terwisga. Resistance tests of a series of planing hull forms with a 30 degrees deadrise angle, and calculation model based on this similar systematic series. Technical Report MEMT 25, Delft University of Technology, Ship Hydromechanics Laboratory, June 1993.
- J. A. Keuning, S. Toxopeus, and F. van Walree. The effect of bow shape on the seakeeping performance of a fast monohull. In *Proceedings of the 6th International Conference on Fast Sea Transportation*, Sept 2001.
- J. A. Keuning, J. Pinkster, and F. van Walree. Further investigation into the hydrodynamic performance of the axe bow. In *Proceedings of the WEGEMT Conference on High Performance Marine Vehicles*, Sept 2002.
- M. Martin. Theoretical predictions of motions of high-speed planing boats in waves. *Journal of Ship Research*, 22(3):140–169, 1978.
- M. R. A. Nieuwenhuis. The ultimate performance of fast ribs - an experimental investigation into the influence of the helmsman. In *International Conference Rigid Inflatables*, pages 51–58. The Royal Institution of Naval Architects, June 2005.

- A. A. K. Rijkens. Improving the sea keeping behaviour of fast ships using a proactive ride control system. In *Proceedings of the 12th International Conference on Fast Sea Transportation*, 2013a.
- A. A. K. Rijkens. On the hydrodynamic performance. In *Proceedings of the 12th International Conference on Fast Sea Transportation*, 2013b.
- A. A. K. Rijkens, J. A. Keuning, and R. H. M. Huijsmans. A computational tool for the design of ride control systems for fast planing vessels. *International Shipbuilding Progress*, 58(4):165–190, 2011.
- D. Savitsky. Hydrodynamic design of planing hulls. *Marine Technology*, 1(1):71–95, 1964.
- D. Savitsky. On the seakeeping of planing monohulls. *Marine Technology*, 5(2): 164–174, April 1968.
- W. R. Story, E. E. Hackett, and T. C. Fu. Radar measurement of ocean waves. In *Proceedings of the ASME 2011 30th International Conference on Ocean, Offshore and Arctic Engineering*, June 2011.
- N. C. Townsend, T. E. Coe, P. A. Wilson, and R. A. Sheno. High speed marine craft motion mitigation using flexible hull design. *Ocean Engineering*, 42:126–134, 2012.
- A. W. Troesch. On the hydrodynamics of vertically oscillating planing hulls. *Journal of Ship Research*, 36:317–331, 1992.
- A. W. Troesch. Recent advances in the analysis of high speed planing hydrodynamics and dynamics. In *Proceedings 16th Congresso Nacional de Transportes Maritimos e Construcao Naval, SEBENA*, Rio de Janeiro, Oct 1996.
- J. J. Van den Bosch. Tests with two planing boat models in waves. Technical Report 266, Delft University of Technology, Ship Hydromechanics Laboratory, Feb 1970.
- A. F. J. Van Deyzen. A nonlinear mathematical model of motions of a planing monohull in head seas. In C. Bertorello, editor, *Proceedings of the 6th International Conference on High-Performance Marine Vehicles (HIPER'08)*, pages 187–199, Sept 2008.
- F. Van Walree. *Development, validation and application of a time domain seakeeping method for high speed craft with a ride control system*. PhD thesis, Delft University of Technology, Ship Hydromechanics Laboratory, 1999.
- K. J. Vermeulen. Model tests with three fast mono-hulls - in calm water and head waves. Technical Report 1418-M, Delft University of Technology, Ship Hydromechanics Laboratory, March 2005.

- G. L. Visch. Damen axehull and double chine hull test series in calm water and head waves. Technical Report 1552-O, Delft University of Technology, Ship Hydromechanics Laboratory, Nov 2007.
- G. L. Visch and J. A. Keuning. Knrm 1816 project: Comparison of the resistance in calm water and the seakeeping behavior of the arie visser, concept 1 and concept 2. Technical Report 1702-O, Delft University of Technology, Ship Hydromechanics Laboratory, Feb 2011.
- L. W. Wang. A study on motions of high speed planing boats with controllable flaps in regular waves. *International Shipbuilding Progress*, 32(365):6–23, 1985.
- E. E. Zarnick. A nonlinear mathematical model of motions of a planing boat in regular head waves. Technical report, David W. Taylor Ship R&D Center, USA, March 1978.
- E. E. Zarnick. A nonlinear mathematical model of motions of a planing boat in irregular head waves. Technical report, David W. Taylor Ship R&D Center, USA, 1979.

Summary

Improving the operability of planing monohulls using proactive control

From idea to proof of concept

The demand to sail at high forward speeds in both calm water and in a seaway remains high. For various patrol, search and rescue or military operations attaining high forward speeds is essential. In head and bow quartering seas, the main factor for voluntary speed reduction is the occurrence of large vertical peak accelerations. The occurrence of large vertical peak accelerations imposes limits to the operability of planing monohulls sailing in head seas.

A challenge for designers of fast monohulls is to explore different possibilities to increase the operability of planing monohulls sailing in head seas. To achieve this a reduction of the vertical accelerations is required. The operability can be considered improved if the level of accelerations can be reduced compared to a trip at an equal but constant forward speed. This implies that it is possible to sail at a higher speed without increasing the discomfort on board.

A solution for increasing the operability of planing monohulls sailing in head seas has been found in proactive control. Vertical peak accelerations have a very short duration. Unacceptably large vertical peak accelerations have a low frequency of occurrence. These two aspects are the incentive for a proactive control system. What makes proactive control unique is the fact that the control is based on predicted vertical peak accelerations. The response of the ship for the next few seconds needs to be simulated real-time while sailing. These predictions should be carried much faster than real-time, since there is little to effectuate control because of the high relative velocity between ship and incoming waves.

In this dissertation proactive control of the forward speed, also termed automated proactive thrust control, has been presented. The purpose of this study is to show the level of reduction of the vertical accelerations possible with automated proactive thrust control.

Full scale trials, carried out on board of Dutch Search and Rescue vessels, indicated that using thrust control more or less a 20% higher average forward speed could be attained, compared to a trial where the operator had to choose a constant thrust beforehand. The operators typically choose a desired forward speed that they want to maintain during the trial. They reduce the thrust if they anticipate that the next occurring vertical peak acceleration might be unacceptable. The operator observes the incoming wave, roughly estimates the magnitude of the next vertical peak acceleration and acts as a controller.

Based on the knowledge obtained from the full scale trials a setup for automated proactive thrust control is proposed. The following three components are essential:

1. A shipboard wave measurement system that provides a sufficiently accurate description of the incoming wave(s) over the next few seconds;
2. A computational model that predicts the response (the vertical peak accelerations) of the ship based on the measured incoming wave faster than real-time;
3. A stable control system that determines the thrust force continuously;

Throughout this study it has been assumed that it will be possible to measure the waves used for predicting the response (eg. laser, radar, lidar) in the near future. The wave are therefore assumed to be known.

To show the level of reduction of the vertical accelerations possible with automated proactive thrust control in an early stage of the study a conceptual simulation model has been setup. The response of a planing monohull sailing in head seas has been mimicked by an elementary model. A control system continuously determines the desired thrust. The results show that the vertical acceleration level may be reduced significantly when automated proactive thrust control is applied on board of a planing monohull, if sufficient time to decelerate to a sufficiently low speed before impact is available. This provided that the vertical accelerations are estimated accurately.

Automated proactive thrust control in more realistic conditions on board has also been modelled. This has been termed the idealised model of automated proactive thrust control. The response of the Dutch SAR boat of the Arie Visser class has been generated using an adequate computational model for calculating the seakeeping behaviour of a planing monohull sailing in head seas (Zarnick 1978, Keuning 1994). The distributions of the vertical peak accelerations for the situation where thrust control was applied have been compared with the distributions found at an equal and constant forward speed. Confirming the findings with the conceptual model, these calculated results show that a significant reduction of the vertical acceleration level can be realised, if sufficient time to decelerate is available. The capacity to reduce the speed before impact proved to be an important component to reduce the vertical acceleration level. If the time to decelerate is limited the reduction of the vertical accelerations still may be realised, compared to simulations carried out at an equal but constant forward

speed. The reduction, however, becomes less. It is directly related to the available time to decelerate and consequently to the minimum attainable speed at impact.

The uncertainty of the predictions of the vertical peak accelerations, using the computational model developed by Zarnick (1978) and Keuning (1994), affect the level of reduction but does not violate the feasibility of proactive control. Inaccurate predicted peaks yield incorrect control of the thrust. In case of overestimated peaks, the thrust reductions are chosen conservatively, resulting in a lower average forward speed than what was found when the peaks were estimated accurately. In case of underestimated peaks, the thrust reductions are chosen optimistically, resulting in a limited reduction of the vertical accelerations. The time step has an influence on the accuracy of the response predictions. In case of a large time step, using the present computational model, peaks will be 'missed' (they are not anticipated), resulting in a limited reduction of the acceleration level.

Model tests have been carried out in regular and bichromatic waves to proof that it is possible to control the vertical acceleration level by means of proactive control of the forward speed. During the model tests, the actual speed of the towing carriage was constantly determined by the outcome of real-time response predictions. The water elevation in front of the carriage and the instantaneous heave and pitch motion were measured real-time. This provided the input for the computational model used for response predictions. The results show that if the vertical peak accelerations were predicted accurately the vertical peak accelerations could be kept within the predefined bandwidth. For gradual increases of the wave amplitude in case of bichromatic waves the speed was adjusted in time as well.

It can be concluded that it is possible to reduce the vertical acceleration level using automated proactive thrust control. The results presented in this dissertation have shown that proactive control, based on predicted vertical peak accelerations, is a promising way to reduce the vertical acceleration level and therewith improve the operability of planing monohulls sailing in head seas.

It is desired to simulate automated proactive thrust control as it should function in reality in a towing tank. Model tests should be carried out in irregular head waves. Measured distributions of the vertical accelerations using thrust control could be compared with measured distributions obtained at a constant forward speed. The reduction of the vertical accelerations using automated proactive thrust control could be determined in a more realistic setting.

This study can be followed up by a study where the effectiveness of proactive control of two control variables, e.g. the thrust in combination with stern flaps or interceptors, for a planing monohull sailing in head seas is analysed.

Samenvatting

Het verbeteren van de inzetbaarheid van planerende schepen middels proactief regelen

Van idee tot bewijs van het concept

De vraag om op hoge snelheid te kunnen varen zal altijd blijven, niet alleen op vlak water, maar ook in golven. Voor patrouille, reddings- en militaire operaties het kunnen varen op hoge snelheid is essentieel. De belangrijkste factor waarom de bemanning snelheid terugneemt varend in kopgolven is het optreden van verticale piekversnellingen. Het optreden van deze verticale versnellingen beperken de inzetbaarheid van planerende schepen (monohulls).

De uitdaging voor ontwerpers van snelle schepen is om een oplossing te vinden voor het verbeteren van de inzetbaarheid in kopgolven. Voor het verbeteren van de inzetbaarheid dienen de verticale versnellingen gereduceerd te worden. De inzetbaarheid is verbeterd als het versnellingsniveau gereduceerd kan worden vergeleken met een vaart bij een gelijke, maar wel een constante snelheid. Dit impliceert dat het mogelijk is om sneller te varen zonder dat het comfort aan boord verslechtert.

Een oplossing voor het verbeteren van de inzetbaarheid van planerende schepen in kopgolven is gevonden in een proactieve regelaar. Verticale piekversnellingen hebben een zeer korte duur. Unacceptabel hoge versnellingen hebben een lage frequentie van voorkomen (niet elke ontmoeting met de inkomende golf levert een unacceptabel hoge piekversnelling). Deze twee aspecten zorgen ervoor dat proactief regelen een mogelijk oplossing zou kunnen zijn. Proactief regelen is uniek, omdat er geregeld wordt op voorspelde verticale piekversnellingen. De responsie van het schip moet voorspeld worden voor de volgende paar seconden tijdens het varen. De voorspellingen dienen snel berekend te worden; er is maar weinig tijd om de regeling uit te voeren, vanwege de hoge relative snelheid tussen schip en inkomende golf.

In dit proefschrift wordt proactieve regelen van de voorwaartse snelheid (ook gedefinieerd als automatische proactieve regeling van de voortstuwing) gepresenteerd. Het doel van deze studie is om te laten zien in hoeverre het mogelijk is om

het versnellingsniveau te verminderen middels automatische proactieve regeling van de voortstuwing.

De uitkomst van ware grootte metingen, uitgevoerd aan boord van Nederlandse reddingsboten, hebben aangegeven dat het mogelijk is om ongeveer 20% sneller te varen wanneer de stuurman gebruik mocht maken van thrust control. De stuurmannen kiezen vaak een gewenste voorwaartse snelheid welke ze ongeveer zouden willen handhaven. Ze verminderen de voortstuwing als zij denken dat de volgende verticale piekversnelling onacceptabel zou kunnen zijn. De stuurman neemt de golf waar, op basis van zijn gevoel voorspelt hij de grootte van de volgende piekversnelling en hij treedt op als een regelaar.

Gebaseerd op de waarnemingen en metingen gedurende de ware grootte metingen, is opzet voor automatische proactieve regeling van de voortstuwing voorgesteld. De volgende drie onderdelen zijn hierin essentieel:

1. Een golfmeetsysteem aan boord, welke een voldoende nauwkeurige beschrijving geeft van de inkomende golven voor de volgende paar seconden;
2. Een rekenmodel, dat de responsie van het schip (met name de verticale piekversnellingen) kan voorspellen gebaseerd op de gemeten inkomende golf; dit dient sneller dan de werkelijke tijd te gebeuren;
3. Een stabiel regelsysteem, welke continu de juiste voortstuwingskracht bepaalt;

Het is aangenomen dat het binnenkort mogelijk is om de golven te kunnen meten vanaf planerend schip in golven (bijvoorbeeld met een laser, radar of lidar). In dit proefschrift zijn de golven daarom bekend verondersteld.

Een conceptueel simulatiemodel van automatische proactieve regeling van de voortstuwing is opgezet om in een vroeg stadium de mogelijke vermindering van het versnellingsniveau te kunnen laten zien. De responsie van een planerend schip in kopgolven is nagebootst middels een elementair model. Een regelsysteem bepaalt de voortstuwingskracht gebaseerd op de voorspelde piekversnellingen. De resultaten hebben laten zien dat het verticale versnellingsniveau aanzienlijk verminderd kan worden wanneer automatische proactieve regeling van de voortstuwing toegepast wordt, mits er voldoende tijd beschikbaar is om te vertragen tot een voldoende lage snelheid op het moment van de klap. Dit is onder voorbehoud dat de verticale piekversnellingen nauwkeurig voorspeld zijn.

Automatische proactieve regeling van de voortstuwing is ook gemodelleerd voor meer realistische condities. De responsie van de reddingboot van het type Arie Visser (KNRM) is berekend gebruikmakend van een toepasselijker rekenmodel. Het rekenmodel ontwikkeld door Zarnick (1978) en Keuning (1994) beschrijft het niet-lineaire zeegangsgedrag van een planerende boot (monohull) vrij goed. De verdelingen van de verticale piekversnellingen waar thrust control wel was toegepast is vergeleken met de verdelingen gevonden bij een gelijke, maar constante voorwaartse snelheid.

De resultaten laten zien dat de het verticale versnellingsniveau aanzienlijk vermindert kan worden mits er voldoende tijd beschikbaar is om te vertragen (gelijk aan wat was gevonden met het conceptuele simulatiemodel). De capaciteit om in korte tijd snelheid te kunnen verminderen is een belangrijke component voor het verlagen van het versnellingsniveau. Een vermindering van het versnellingsniveau kan nog steeds gerealiseerd worden wanneer er minder tijd is om te vertragen, vergeleken met een simulatie bij een gelijke, maar constante snelheid. De reductie wordt wel minder. Het is direct gerelateerd aan de beschikbare tijd om te vertragen en daardoor aan de minimale snelheid welke gerealiseerd kan worden op het moment van impact.

De onzekerheid in de voorspellingen van de piekversnellingen, berekend met het simulatiemodel ontwikkeld door Zarnick (1978) en Keuning (1994), beïnvloedt wel de mate van reductie van het versnellingsniveau, maar doet geen geweld aan de haalbaarheid van het proactieve regelsysteem. Onnauwkeurig voorspelde pieken leiden tot onjuiste reducties van de voortstuwing. In geval dat de pieken overschat zijn, worden de verminderingen van voortstuwing te conservatief gekozen. Dit leidt tot een lagere gemiddelde snelheid dan wanneer de pieken wel nauwkeurig voorspeld zijn. In geval dat de pieken onderschat zijn, worden de verminderingen van voortstuwing te optimistisch gekozen. Dit leidt tot een beperkte afname van het versnellingsniveau. De reketijdstap heeft ook effect op de nauwkeurigheid van de voorspellingen. In geval van een grote tijdstap, gebruikendmakend van het simulatiemodel ontwikkeld door Zarnick (1978) en Keuning (1994), pieken zullen 'gemist' worden. Zij worden niet geanticipeerd. Dit leidt tot eveneens tot een beperkte afname van het versnellingsniveau.

Modelproeven zijn uitgevoerd in regelmatige en bichromatische golven om aan te tonen dat het mogelijk is om het verticale versnellingsniveau te kunnen controleren middels het proactief regelen van de voorwaartse snelheid. Gedurende de modeltesten werd de responsie van het schip continu bepaald. De uitkomst van deze voorspellingen bepaalde de actuele snelheid van de sleepwagen. De gemeten waterhoogte voor de wagen en de momentane domp- en stampbeweging dienden als invoer voor de berekeningen. Deze modelproeven hebben laten zien dat, als de verticale piekversnellingen nauwkeurig bepaald zijn, ze binnen een bepaalde bandbreedte gehouden konden worden middels proactief regelen van de snelheid. De snelheid was op tijd aangepast voor geleidelijke verhoging van de golfamplitude in geval bichromatische golven.

Het mogelijk is om het verticale versnellingsniveau te reduceren middels automatische proactieve regeling van de voortstuwing. De resultaten gepresenteerd in dit proefschrift hebben laten zien dat proactief regelen, gebaseerd op voorspelde verticale piekversnellingen, een veelbelovende manier is om het versnellingsniveau aan boord van een planerend schip te verminderen. Dit betekent automatisch een verbetering van de inzetbaarheid.

Het is gewenst om automatische proactieve regeling van de voortstuwing te modelleren in een laboratorium zoals het zou werken in de werkelijkheid. De proeven zouden daarom in onregelmatige golven moeten worden uitgevoerd. Gemeten verdelingen van de verticale piekversnellingen, voor het geval dat thrust control toegepast is, kunnen vergeleken worden met gemeten verdelingen bij een gelijke, maar constante snelheid. De mate van reductie van het verticale versnellingsniveau zou dan bepaald kunnen worden in een meer realistische omgeving.

Deze studie zou kunnen worden opgevolgd door een studie waar het effect van proactief regelen van twee variabelen, bijvoorbeeld de voortstuwing in combinatie met trimflappen of interceptoren, op het verticale versnellingsniveau voor een planerend schip in kogolven wordt geanalyseerd.

Dankwoord

Promoveren. Ik heb het ervaren als een lange zit, waar buiten je intelligentie vooral je uithoudingsvermogen op de proef gesteld wordt. Ik denk dat het te vergelijken is met een marathon, hoewel ik er nog nooit één gelopen heb. Je hebt conditie nodig, maar meer dan dat moet je doorzetten, vooral wanneer het even niet mee zit.

Alhoewel je een marathon toch echt alleen loopt en men dat ook vaak denkt van promoveren, doe je het laatste eigenlijk niet alleen. Voor het tot een succesvol einde brengen van mijn promotieonderzoek zou ik graag de volgende mensen willen bedanken.

Allereerst wil ik graag mijn promotor Rene Huijsmans en co-promotor Lex Keuning bedanken voor de supervisie en begeleiding tijdens het gehele proces. Tevens wil ik de gehele promotiecommissie bedanken voor de tijd die ze vrijgemaakt hebben voor het doorlezen van mijn proefschrift en voor het deelnemen aan de promotiezitting.

Ik wil ook het personeel van de sleeptank, Hans van 't Hek, Frits Sterk, Peter Poot, Jasper den Ouden, Michiel Katgert en Guido Visch, bedanken voor het helpen realiseren en uitvoeren van de modelproeven. Verder wil ik graag Michiel ook bedanken voor de mooie omslag van dit proefschrift en Guido voor het voorzien van de data van de ware grootte metingen. Piet de Heer voor de assistentie bij de administratieve zaken en Rina van Moesbergen voor de gezelligheid tijdens mijn korte pauzes in de werkplaats.

Ik zou ook graag Rene Hiemstra en Volkert Oosterlaak willen bedanken voor respectievelijk hun stage- en afstudeerwerk gedurende mijn promotie. Doordat zij met aanverwante onderwerpen bezig zijn geweest, heb ik meer afwisseling gedurende mijn promotie ervaren, iets wat het gehele proces voor mij aangenamer heeft gemaakt. Hetzelfde geldt voor Ivor Cleine met wie ik samen een onderzoeksproject naast mijn promotie gedaan heb, namelijk het voorspellen van het dwarskrachten en momentelijn voor een planerend schip in koggolven. Verder wil ik Peter Wellens voor de mooie discussies in de sleeptank, en nog meer op de fiets tussen Delft en Rotterdam. Peter Naaijen voor de discussies over golfvoorspellingen en hoe je dat nu het beste kunt aanpakken. Aan het eind van de rit hebben Marcel Cleijnsen en Ties van Bruinissen delen van proefschrift gelezen en herzien, iets waarvoor ik ze graag wil bedanken.

Ik wil graag mijn ouders en zusje bedanken voor hun mentale ondersteuning. En in het bijzonder Monique, die mij altijd ondersteund heeft tijdens dit lange proces en die op de juiste momenten mij altijd heeft kunnen motiveren om door te zetten.

En last but not least: Pepijn de Jong en Albert Rijkens, mijn paranimfen en my partners in crime. Ik denk simpelweg niet dat ik het zonder hen tot een goed einde had kunnen brengen. Toen mijn onderzoek zich langzamerhand begon te vormen kwamen de discussies over het niet-lineair gedrag van planerende schepen, bewegingsvergelijkingen, piekversnellingen, Rayleigh plots, Fastship, bijlboegen, proactive control, proeven, en nog veel meer van dit lekker op gang. Ik heb veel aan hun als sparringspartners gehad. Hun hulp bij het voorbereiden van de verdediging, door tijd vrij te maken voor een mini-defense, heeft mij zeer veel geholpen. En zelfs tot en met het einde stonden ze mij bij, als de beschermende paranimfen. Mocht de discussie oververhit raken dan zullen zij in de bres gesprongen zijn (denk ik...).

En natuurlijk wil ik nogmaals iedereen uit de sleeptank bedanken voor de mooie tijd, de koffiepauzes, vis op donderdag, lunches in de bieb, met ieder zo z'n eigen lunchritueel en met de mooiste discussies, voor de boottochtjes op de Schie en op het Hollandsch Diep, de verschillende dineetjes en alles wat ik nog vergeten ben.

Curriculum Vitae

Alex van Deyzen was born on the 24th of December 1979 in Roosendaal en Nispen. He started secondary school in 1992 at the Johannes Calvijn Scholen Gemeenschap in Rotterdam. He received his gymnasium diploma in June 1998. He studied Marine Technology from September 1998 to January 2006 at the Delft University of Technology. During this period he studied one year abroad at the Norwegian University of Technology in Trondheim (from August 2003 to July 2004). After studying abroad, he did his internship at Marine Structure Consultants b.v. in Schiedam and subsequently his master thesis at the Department of Ship Hydromechanics and Structures at the Delft University of Technology. During his thesis he studied the roll behaviour of planing monohulls sailing in waves. He included the roll motion in an existing nonlinear mathematical model of motions of a planing monohull sailing in waves.

During his studies he was a student assistant at the Department of Ship Hydromechanics and Structures for three years. He also was the chairman of a student committee who organised a three-week study-tour to South Korea and Japan.

After his graduation he started working for the Council for Scientific and Industrial Research (CSIR) at the Coastal Engineering Department in Stellenbosch, South Africa. He worked as a maritime engineer in a hydraulic laboratory. He was part of the team performing and analysing 3D physical model tests. He was responsible for the ship motion tests of moored ships in harbours.

In September 2007 he commenced with his PhD research at the Department of Ship Hydromechanics and Structures of the Delft University of Technology, under the supervision of promotor prof.dr.ir. R.H.M. Huijsmans and co-promotor dr.ir. J.A. Keuning. The research project was aimed at improving the operability of planing monohulls sailing in head seas using automated proactive control of the thrust. The results of this study are presented in this dissertation.

When his contract at the university ended in October 2012 he started working for Royal HaskoningDHV for the division Maritime and Waterways in Rotterdam. He mostly works on projects involving the behaviour of moored ships in harbours and nearshore areas. His education in ship hydromechanics and his experience in a hydraulic laboratory make him an expert in this field of work.



Improving the operability of planing monohulls using proactive control

From idea to proof of concept

A.F.J. van Deyzen

The demand to sail at high forward speeds in both calm water and in a seaway remains high. For various patrol, search and rescue or military operations attaining high forward speeds is essential. Ships used for such mission purposes are often planing monohulls. In head and bow quartering seas, the main factor for voluntary speed reduction is the occurrence of large vertical peak accelerations. The motion and acceleration levels increase with decreasing ship size.

Operators on board of small, planing boats temporarily reduce the forward speed before impact (proactive control) if they anticipate that the next vertical peak acceleration might be unacceptably large. By doing so, they try to avoid unacceptably large vertical peak accelerations during a trip, while they strive at the highest possible forward speed. It is believed that this so-called thrust control may be a very effective way of increasing the operability of planing monohulls.

Inspired by the operator's actions, a solution for improving the operability of planing monohulls sailing in head seas may be found in proactive control. As a first step, proactive control of the forward speed, called automated proactive thrust control, is presented in this dissertation. Advantages of automated proactive thrust control are that experience of the operator, misjudgements, fatigue or loss of concentration do not play a role. It is also possible to apply automated proactive thrust control having poor visibility (e.g. at night or in case of excessive spray). On unmanned fast ships automation of the thrust is required to limit the acceleration level on board. Moreover, the outcome of this study is used for a follow-up study, in which the effectiveness of a combination of proactive controlled thrust and stern flaps or interceptors for a planing monohull sailing in head seas is analysed (this study has already commenced at the department of ship hydromechanics and structures at the Delft University of Technology in January 2011).